

Diss. ETH No. 18007

**Thermodynamic and kinetic characterization  
of the interactions between  
 $\beta_2$ -adrenoceptor agonists and lipid membranes**

A dissertation submitted to the  
ETH ZURICH  
for the degree of  
Doctor of Science

presented by  
*Dario Lombardi*

Dipl. Chemist, University of Pisa, Italy  
born 09.04.79  
citizen of Italy

accepted under the recommendation of

Prof. Dr. Heidi Wunderli-Allenspach, examiner  
Prof. Dr. Karl-Heinz Altmann, co-examiner  
PD. Dr. Stefanie D. Krämer, co-examiner  
Dr. Bernard Cuenoud, co-examiner

Zurich, 2008



# Contents

<b>1</b>	<b>Introduction</b>	<b>1</b>
1.1	$\beta_2$ -Adrenoceptor agonists in asthma therapy and chronic obstructive pulmonary diseases (COPD) . . . . .	1
1.2	Pharmacological profiles and membrane interactions of the $\beta_2$ -adrenoceptor agonists . . . . .	2
1.3	Mechanisms and characteristics of drug/membrane interactions . . . . .	9
1.4	Liposomes as model membranes . . . . .	17
1.5	Techniques to study drug-membrane interactions with liposomes . . . . .	17
1.6	Aim of the thesis . . . . .	21
<b>2</b>	<b>Materials and Methods</b>	<b>23</b>
2.1	Chemicals and buffers . . . . .	23
2.2	Preparation and characterization of liposomes . . . . .	25
2.3	Octanol/buffer partitioning . . . . .	28
2.4	Determination of drug-membrane affinity by equilibrium dialysis . . . . .	28
2.5	Determination of drug-membrane affinity by surface plasmon resonance (SPR)	31
2.6	Kinetic studies by SPR . . . . .	32
2.7	Determination of equilibrium constants by spectrofluorimetric titrations . . .	33
2.8	Kinetics of complex formation . . . . .	35
2.9	Permeation Kinetics . . . . .	35
<b>3</b>	<b>Results</b>	<b>37</b>
3.1	Characterization of the model membranes . . . . .	37
3.1.1	Lipid composition and membrane fluidity . . . . .	37
3.1.2	Zetapotentials of liposomes . . . . .	39
3.2	Octanol partitioning . . . . .	40
3.3	Drug/membrane affinities by equilibrium dialysis . . . . .	41
3.4	Investigation of the drug/membrane interactions by SPR . . . . .	51

3.4.1	Determination of drug/membrane affinity by SPR . . . . .	51
3.4.2	Kinetic studies by SPR . . . . .	52
3.4.3	Concentration-dependence of salmeterol and indacaterol partitioning in the PhC liposome system . . . . .	56
3.5	Permeation of lipid bilayers by Tb-permeation assay . . . . .	59
3.5.1	Complex formation between Tb(III) and 2-hydroxynicotinic acid (OHNA)	59
3.5.2	Kinetics of the 1:1 complex formation between OHNA and Tb(III) . .	62
3.5.3	Permeation kinetics of OHNA . . . . .	63
<b>4</b>	<b>Discussion</b>	<b>69</b>
4.1	Permeation kinetics . . . . .	77
<b>5</b>	<b>Conclusions and Outlook</b>	<b>81</b>
	Bibliography	94
	List of Publications	95
	Curriculumvitae	97



# List of Tables

1.1	Dissociation constants for the $\beta_2$ -adrenoceptor agonists at the human adrenoceptors. . . . .	3
1.2	Functional properties for the $\beta_2$ -adrenoceptor agonists at the human $\beta$ adrenoceptors. . . . .	3
1.3	Physico-chemical parameters for the $\beta_2$ -adrenoceptor agonists. . . . .	5
1.4	Investigated liposome compositions. . . . .	6
1.5	Molecular structure of phospholipids and cholesterol. . . . .	8
3.1	Membrane fluidity. . . . .	38
3.2	Zetapotentials of the investigated liposomes. . . . .	39
3.3	Membrane affinity parameters of indacaterol and salmeterol in different liposomal systems. . . . .	48
3.4	$D$ and $\log D$ values of indacaterol and salmeterol with diverse liposomal systems, rafts and octanol at pH 7.4. . . . .	49
3.5	Overall equilibrium constants and thermodynamic parameters of the complex formation between OHNA and Tb(III) at 25°C. . . . .	61
3.6	Activation parameters of the permeation kinetics $Perm_{1app}$ and $Perm_{2app}$ of OHNA into Tb(III) $\beta$ and EDTA/Tb(III)-containing liposomes at 298K. . . . .	67



# List of Figures

1.1	Chemical structures of indacaterol, formoterol, salmeterol and salbutamol. . . . .	2
1.2	Model of lipid bilayer permeation of an amphiphilic molecule . . . . .	11
1.3	Phase diagram of DMPC/cholesterol membranes. . . . .	15
1.4	Equilibrium dialysis . . . . .	18
1.5	Diagram of the biosensor assay. . . . .	19
2.1	Excitation and emission spectra of the OHNA/Tb(III) complex. . . . .	33
3.1	Membrane fluidity. . . . .	37
3.2	Lipid quantification by HPLC . . . . .	39
3.3	Distribution profiles of indacaterol, salmeterol and propranolol in the octanol/buffer system. . . . .	40
3.4	Distribution profiles of indacaterol, salmeterol and propranolol in PhC liposomes. . . . .	41
3.5	Distribution profiles of indacaterol and salmeterol in DPPC liposomes. . . . .	42
3.6	Distribution profiles of indacaterol and salmeterol in DMPC and DMPC/Chol liposomes. . . . .	43
3.7	Distribution profiles of indacaterol and salmeterol in negatively charged liposomes. . . . .	44
3.8	Distribution profiles of indacaterol and salmeterol in DOPC and DOPC/Chol liposomes. . . . .	46
3.9	Distribution profiles of indacaterol and salmeterol in SM and SM/Chol liposomes. . . . .	46
3.10	Distribution profiles of indacaterol and salmeterol in BLES and raft-like liposomes. . . . .	47
3.11	SPR sensograms of the PhC liposomes adsorption on the L1 chip and of the interactions of indacaterol, salmeterol and propranolol with PhC liposomes at pH 7.2. . . . .	51

3.12	Binding isotherms of propranolol, salmeterol and indacaterol to PhC liposomes at pH 7.2. . . . .	53
3.13	Association and dissociation kinetics of indacaterol and salmeterol with PhC liposomes. . . . .	54
3.14	pH-Dependence of the fitted apparent rate constants $k_2$ and $k$ of the liposome association and dissociation phases of indacaterol and salmeterol. . . . .	55
3.15	Comparison between the ratios of the fitted apparent rate constants of the association and the dissociation phases and the plateau values of the association phases. . . . .	57
3.16	Concentration-dependent partitioning of salmeterol in PhC liposomes. . . . .	58
3.17	Binding isotherms for the 1:1 complex formation between Tb(III) and OHNA in various buffers at pH 6.5 and at 25°C. . . . .	59
3.18	Influence of liposomes on the binding isotherms of the OHNA/Tb(III) complex formation. . . . .	60
3.19	Van't Hoff Plots for the OHNA/Tb(III) complex formation. . . . .	61
3.20	Stopped flow trace of the OHNA/Tb(III) complex formation in TRIS 0.2M, pH 6.5 at 25°C. . . . .	62
3.21	Kinetics of OHNA entry into Tb(III)-containing egg PhC liposomes at pH 6.5, 25°C. . . . .	64
3.22	Apparent permeation coefficients of the entry of OHNA into Tb(III)-containing liposomes. . . . .	65
3.23	Eyring's plot of the permeation kinetics of OHNA into Tb(III) and EDTA/Tb(III)-containing liposomes at pH 6.5 and 2.5. . . . .	66
4.1	Sterical arrangements of salmeterol with phospholipid membranes. . . . .	70
4.2	Model to explain pharmacology differences between beta-2 adrenoceptor agonists. . . . .	73
4.3	Apparent partition and translocation rate constants as a function of the partition coefficient and the volume ratios between the aqueous phases and the lipid leaflets. . . . .	76



# Abbreviations

A	Anion
ACA	Aromatic carboxylic acid
BLES	Bovine lipid extract surfactant
C	Cation
Chol	Cholesterol
COPD	Chronic obstructive pulmonary disease
D	Apparent distribution coefficient
DMPC	Dimyristoyl-phosphatidyl-choline
DMPG	Dimyristoyl-phospho-glycerol
DOPC	Dioleoyl-phosphatidyl-choline
DOPS	Dioleoyl-phosphatidyl-serine
DPH	1,6-Diphenyl-1,3,5-hexatriene
DPPC	Dipalmitoyl-phosphatidyl-choline
DPPE	Dipalmitoyl-phospho-ethanolamine
DPPG	Dipalmitoyl-phospho-glycerol
EDTA	Ethylenediaminetetraacetic acid
FEV1	Forced expiratory volume in one second
L	Luminescence
LABA	Long acting $\beta_2$ -adrenoceptor agonist
<i>ld</i>	Liquid disordered
<i>lo</i>	Liquid ordered
LSC	Liquid scintillation counting
LUV	Large unilamellar vesicles
MLV	Multilamellar vesicles
MOPS	3-(N-morpholino) propane sulfonic acid
MW	Molecular weight
N	Neutral
OHNA	2-Hydroxynicotinic acid
P	Partition coefficient
$Perm_{app}$	Permeation coefficient
P-gp	P-Glycoprotein
PhC	Egg phosphatidylcholine

PhC	Phosphatidyl-inositol
PhS	Spinal cord phosphatidyl-serine
POPC	Palmitoyl-oleoyl-phosphatidyl-choline
RT	Room temperature
RU	Resonance unit
SM	Egg sphingomyelin
<i>so</i>	Solid ordered
SPR	Surface plasmon resonance
SUBS	Standardized universal buffer solution
Tb(III)	TbCl <sub>3</sub> hexahydrate
TRIS	Tris(hydroxymethyl)aminomethan
Z	Zwitterion





# Abstract

The results of a series of clinical studies show that indacaterol (formerly known as QAB149) could become the first compound of a new class of "once-daily  $\beta_2$ -adrenoceptor agonists", offering full 24 hour symptoms control with a single administration, in contrast to currently available long acting  $\beta_2$ -agonists (LABAs) such as salmeterol and formoterol which have to be taken twice daily. Furthermore indacaterol is the first  $\beta_2$ -adrenoceptor agonist that combines a sustained duration of action with a rapid onset of its therapeutic effects.

The current study concentrates on the analysis of the interactions of indacaterol and salmeterol with lipid membranes in order to shed light on the mechanism leading to differences in the *in vivo* behaviour of the  $\beta_2$  agonists.

Two key aspects of the  $\beta_2$ -adrenoceptor agonists/membrane interactions are investigated:

- the pH-dependent affinity to lipid membranes;
- the pH-dependent kinetics of the interaction with immobilized liposomes.

Particular attention was paid to the influence of pH, temperature and lipid composition of the model membranes: these parameters were varied in order to investigate the relationship between the physico-chemical properties of the drugs and the mechanism of the drug-membrane interactions.

Equilibrium dialysis experiments with lipid membranes revealed that the cationic species of indacaterol and salmeterol had the highest membrane affinity in most liposomal systems while partition profiles obtained with the octanol partition system were characterized by a maximal lipophilicity of the net neutral species. Interestingly we found that when raft vesicles prepared by the cold TritonX-100 method were used as the partition phase, the membrane affinity of indacaterol was two fold greater than that of salmeterol. The pH-dependent kinetics of the interactions between indacaterol and salmeterol and immobilized liposomes were investigated by surface plasmon resonance technology (SPR). In this work we compare the rate constants defining the interactions of indacaterol and salmeterol with PhC lipid bilayers. The data are in agreement with a model including drug translocation at physiological pH. The observed rate constant was two times higher, at pH values  $< 8.8$ , for indacaterol than for salmeterol.

A third aspect, i.e. membrane permeation kinetics, was investigated with a model compound (2-hydroxynicotinic acid, OHNA) with the goal to establish the experimental conditions to study membrane permeation with  $\beta_2$ -adrenoceptor agonists. The permeation kinetics were

investigated by the Terbium(III)-permeation assay. The temperature variation allowed the analysis of the thermodynamics of OHNA permeation. The permeation of anionic and neutral OHNA mainly differed in  $-T \cdot \Delta S^\ddagger$  rather than in  $\Delta H^\ddagger$ . We concluded that the rate-limiting step for ion permeation was probably the dehydration. This study provides the basis for further developing the Tb(III)-permeation assay as a method for studying membrane permeation of  $\beta_2$ -agonists. The drugs may be covalently linked to an aromatic carboxylic acids (ACA) to shed light on their permeation behavior.

The results of this work revealed that the fast onset and long duration of effect of indacaterol are likely related to multiple factors. This study suggests a new possible model to explain the relationships between the drug/membrane interactions and drug's biological effect, supporting the view that the membrane affinity plays a key role for the long duration of action of the  $\beta_2$ -adrenoceptor agonists.

# Riassunto

I risultati di una serie di prove cliniche dimostrano che l' indacaterolo (conosciuto come QAB149) potrebbe diventare il primo composto di una nuova classe di farmaci agonisti dei recettori adrenergici  $\beta_2$  a singola assunzione giornaliera, offrendo totale controllo dei sintomi nell'arco di 24 ore, differenziandosi dai farmaci attualmente in commercio che necessitano una assunzione due volte al giorno. Inoltre indacaterolo è il primo  $\beta_2$  agonista che combina la prolungata efficacia nel tempo con un rapido effetto broncodilatativo al momento dell'assunzione.

Questo studio si concentra sull'interazione di indacaterolo e salmeterolo con membrane biologiche allo scopo di mettere in luce il meccanismo responsabile delle differenze degli effetti biologici tra i diversi  $\beta_2$  agonisti.

Due aspetti chiave delle interazioni agonista/membrana sono state investigate:

- la dipendenza dal pH della affinità per membrane lipidiche;
- la dipendenza dal pH delle cinetiche di interazione con liposomi immobilizzati.

Un terzo aspetto, che è la cinetica di permeazione di membrane lipidiche, è stato investigato mediante un composto di prova al fine di stabilire le condizioni sperimentali per studiare successivamente la permeazione di membrana con i farmaci agonisti.

Particolare attenzione è stata posta sulle condizioni sperimentali di pH, temperatura e composizione lipidica delle membrane utilizzate: questi parametri sono stati variati al fine di studiare le relazioni tra le proprietà chimico-fisiche dei farmaci e il meccanismo di interazione tra farmaco e membrana.

Dialisi di equilibrio con membrane lipidiche hanno evidenziato che le specie cationiche dell' indacaterolo e del salmeterolo hanno la più alta affinità per le membrane con la maggior parte delle composizioni lipidiche utilizzate, mentre la ripartizione nel sistema acqua/ottanolo è stata caratterizzata da una lipofilia massima delle specie a carica totale neutra. In ogni caso gli esperimenti presentati in questo lavoro non hanno mostrato differenze significative nella affinità dei composti per le membrane tali da giustificare le diverse proprietà biologiche.

La dipendenza dal pH delle cinetiche di interazione di indacaterolo e salmeterolo con membrane immobilizzate è stata studiata per mezzo della risonanza plasmonica di superficie (SPR). In questo studio sono state confrontate le costanti di tempo che definiscono le in-

terazioni di indacaterolo e salmeterolo con doppi strati lipidici costituiti di fosfatidilcolina. I dati generati sono in accordo con un modello che prevede la traslocazione del farmaco in membrana (flip-flop) a pH fisiologici. La costante cinetica dell'indacaterolo e' risultata essere due volte maggiore rispetto a quella del salmeterolo.

Le cinetiche di permeazione del composto di prova, l'acido 2-idrossinicotinico (OHNA) sono state investigate con il saggio "Terbium(III)-permeation". La variazione controllata della temperatura ha permesso una analisi termodinamica del processo di permeazione del OHNA. I risultati dimostrano che la permeazione di anioni e specie neutre differisce principalmente in  $-T \cdot \Delta S^\ddagger$  anziche in  $\Delta H^\ddagger$ . Se ne conclude che il processo cineticamente limitante per il processo di permeazione degli ioni e' probabilmente la loro deidratazione. Questo studio fornisce le basi per sviluppare ulteriormente il saggio "Tb(III)-permeation" come strumento per misurare la permeazione dei  $\beta_2$  agonisti. I farmaci potrebbero essere legati covalentemente ad un acido carbossilico aromatico per investigarne la loro permeazione.

I dati ottenuti in questo lavoro rivelano che la velocita' e la lunga durata dell'effetto terapeutico dell'indacaterolo sono probabilmente da attribuire a molteplici fattori. Questo lavoro suggerisce un possibile meccanismo responsabile per le differenze di tempo di azione e durata dell'effetto terapeutico dei  $\beta_2$  agonisti, e conferma che l'affinita' di membrana sembra giocare un ruolo chiave per la lunga durata di azione dei  $\beta_2$  agonisti.

# 1 Introduction

Many pharmacokinetic and several pharmacodynamic processes are determined by the interaction of a drug with lipid membranes. Examples are the passage through cell membranes and the interaction with membrane proteins. A better understanding of the relationships between physicochemical characteristics of drugs and their membrane interactions would help to shed light on the mechanisms that lead to the biological activity of a drug. This work investigates the thermodynamics and the kinetics of the interactions between  $\beta_2$ -adrenoceptor agonists and lipid membranes in order to rationalize the role of the membranes for the mechanisms that determine the biological effects of the agonists.

## 1.1 $\beta_2$ -Adrenoceptor agonists in asthma therapy and chronic obstructive pulmonary diseases (COPD)

$\beta_2$ -Adrenoceptor agonist drugs are effective in the management of asthma and chronic obstructive pulmonary disease (COPD). They induce bronchodilatation via direct relaxation of airway smooth muscles, and give rapid relief of asthma symptoms [Barnes, 1977, Waldeck, 2002]. The  $\beta_2$ -adrenoceptor agonists are characterized by a basic amine group and an acidic phenol group as shown in Fig. 1.1. In solution they can exist in four different ionization forms: the cation (C), the net neutral species (N) including the uncharged species as well as the zwitterionic species, and the anion (A). The acid-base equilibria are defined in terms of the macroscopic constants  $K_{a1}$  and  $K_{a2}$  that refer to the stoichiometric ionization [Bouchard et al., 2002] where the two globally neutral species are treated collectively as being two tautomers of a single form (N).

Salmeterol is an inhaled  $\beta_2$ -adrenoceptor agonist that has been widely used in the past 30 years. It is a long-acting  $\beta_2$ -adrenoceptor agonist (LABA) that, in humans, provides an extended bronchodilating effect lasting 12h after a single inhalation [Anderson et al., 1994]. The major drawback of salmeterol is its slow onset of action ( $\sim 15$  min) compared to other

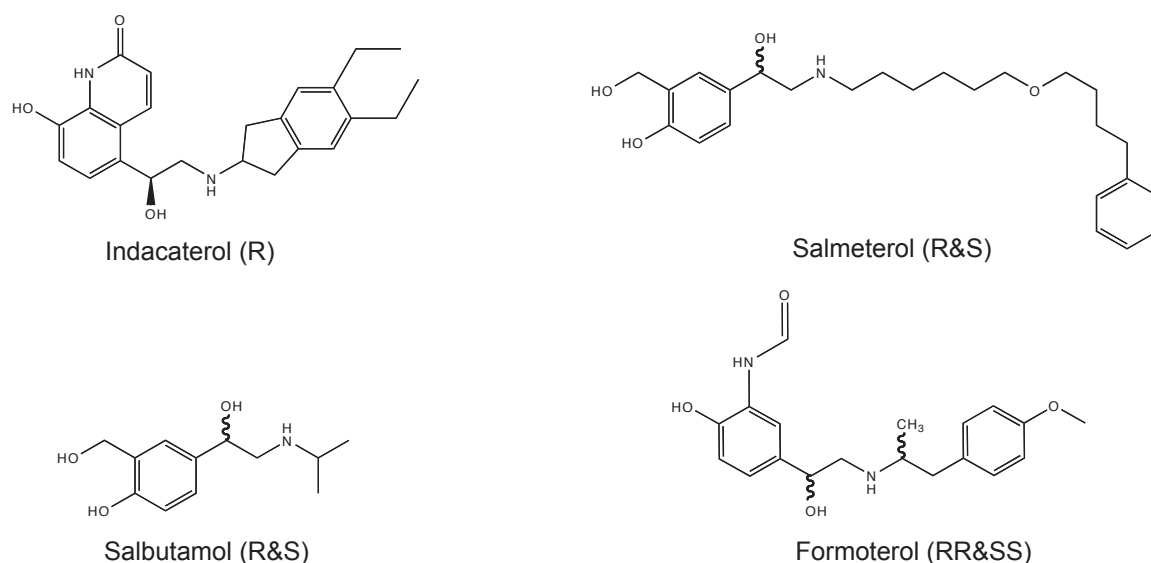


Fig. 1.1: Chemical structures of indacaterol, formoterol, salmeterol and salbutamol.

available  $\beta_2$ -adrenoceptor agonists such as formoterol and salbutamol (onset of action  $\sim 3$  min) [Lindberg et al., 2007, Palmqvist et al., 1997] which, however, show a shorter duration of action [Anderson et al., 1994]. Indacaterol, previously known as QAB149, is a novel, chirally pure inhaled  $\beta_2$ -adrenoceptor agonist that provides a bronchodilating effect of 24h after inhalation, combined with a fast onset of action and an increased therapeutic index compared with the marketed inhaled  $\beta_2$ -adrenoceptor agonists [Beeh et al., 2007]. The extended duration of action of indacaterol which greatly exceeds that of salmeterol and the fast onset of action comparable with other available  $\beta_2$ -adrenoceptor agonists such as salbutamol and formoterol is prompting considerable interest on the relationship between interactions with biological membranes and pharmacological activity as shown in the following paragraphs.

## 1.2 Pharmacological profiles and membrane interactions of the $\beta_2$ -adrenoceptor agonists

The basic pharmacological properties of indacaterol and other marketed  $\beta_2$ -adrenoceptor agonists such as salmeterol, salbutamol and formoterol are similar. The drugs are highly potent relaxants of human bronchial smooth muscles and they display a high degree of binding selectivity for the  $\beta_2$ -receptor subtype as shown in Tab. 1.1.

<i>Agonist</i>	$pK_D$		
	$\beta_1$	$\beta_2$	$\beta_3$
Indacaterol	6.21	7.36	5.48
Formoterol	6.12	7.84	5.49
Salmeterol	6.11	9.19	5.58
Salbutamol	5.39	6.12	4.62

Table 1.1: **Dissociation constants for the  $\beta_2$ -adrenoceptor agonists at the human adrenoceptors.**

Data adapted from [Battram et al., 2006].  $pK_D$ ,  $-\log K_D$  [M].

The functional potency and intrinsic efficacy of the compounds were studied by Battram et al. [2006] measuring cAMP production in cells stably transfected with human  $\beta$  adrenoceptors. The order of functional potency for the compounds was the same as their binding affinity for the  $\beta_2$ -adrenoceptor (Tab. 1.2). Significant differences were found for the onset of action measured *in vitro* with pig tracheal strips; it was ( $30 \pm 4$  min) for indacaterol, ( $32 \pm 1$  min) for formoterol, and ( $28 \pm 3$  min) for salbutamol, whereas it was much slower for salmeterol ( $169 \pm 32$  min). The durations of action of indacaterol ( $529 \pm 99$  min) and salmeterol ( $475 \pm 130$  min) were greater than those estimated for formoterol ( $158 \pm 30$  min) or salbutamol ( $22 \pm 9$  min). In the clinical situation, it is recognized that indacaterol, salbutamol and formoterol have a fast onset of action, whereas salmeterol has a slower onset. The duration of action of indacaterol and salmeterol exceeds those of formoterol and salbutamol [Beeh et al., 2007, Beier et al., 2007, Chuchalin et al., 2007, Kanniss et al., 2005, van Noord et al., 1996, Wegener et al., 1992].

<i>Agonist</i>	$\beta_1$		$\beta_2$		$\beta_3$	
	pEC <sub>50</sub>	$E_{max}$	pEC <sub>50</sub>	$E_{max}$	pEC <sub>50</sub>	$E_{max}$
Isoprenaline	7.46	99	7.22	98	7.91	99
Indacaterol	6.60	16	8.06	73	6.72	113
Formoterol	6.96	29	8.58	90	7.56	103
Salmeterol	7.17	-11	9.15	38	6.03	59
Salbutamol	5.93	-3	6.60	47	5.74	99

Table 1.2: **Functional properties for the  $\beta_2$ -adrenoceptor agonists at the human  $\beta$  adrenoceptors.**

$E_{max}$  data are presented as percentage of maximal isoprenaline-induced cAMP increase. Data adapted from [Battram et al., 2006]. pEC<sub>50</sub>,  $-\log EC_{50}$  [M]

Receptor affinity could be a contributory factor influencing persistence of agonists action, as it might be hypothesised, that agonists with high affinity would have longer receptor activation than those with lower affinity following washout of the tissue where receptors are located. It is clear that both salmeterol and formoterol have a higher affinity for the  $\beta_2$ -adrenoceptor than salbutamol and isoprenaline [Green et al., 2001, Johnson, 1995], but the affinity of salmeterol has been shown to be similar to that of formoterol [Anderson et al., 1994, Alikhani et al., 2004, Johnson, 1995], yet salmeterol is more resistant to washout. In addition, in the presence of GTP, the affinity of indacaterol has been shown to be similar to that of formoterol [Battram et al., 2006] but indacaterol is far more resistant to washout than formoterol. These studies suggest that the reason for the persistent receptor activation of salmeterol as compared to molecules like formoterol following washout is unlikely to be due to differences in affinity for the  $\beta_2$  adrenoceptor.

The mechanism of the persistent receptor activation is not fully understood. Two models have been proposed to account for the differences of action. The exo-site hypothesis is based on the concept that the large lipophilic N-substituent of long acting  $\beta_2$ -adrenoceptor agonists, interacts with a distinct non-polar region in the cell membrane in the vicinity of  $\beta_2$ -adrenoceptor, the exo-site region [Anderson et al., 1994, Brittain, 1990, Clark et al., 1996, Johnson, 1998]. This model consistently explains the long-lasting bronchodilating effect of salmeterol by suggesting that the long aliphatic tail remains anchored at the hydrophobic exo-site domain, while the saligenin head activates the  $\beta_2$ -adrenoceptor in a continuous manner. However, the idea of a specific exo-site binding region is not optimal to rationalize the long duration of action of indacaterol, since its lipophilic side chain is much too short to allow anchorage on the membrane and at the same time let the polar side to interact with the  $\beta_2$ -adrenoceptor glycoprotein [Linden et al., 1996]. It has therefore been proposed that accumulation and retention of  $\beta_2$ -stimulating bronchodilators in the plasma membrane account for the pharmacodynamic effects observed and result in a long-lasting stimulation of  $\beta_2$ -adrenoceptor being embedded in the plasma membrane of airway smooth muscle [Lofdahl, 1990, Jeppsson et al., 1989, Mason et al., 1991, Anderson et al., 1994]. Bergendal et al. [1996] demonstrated that structural mimics of the side chain of salmeterol failed to block the relaxation and extended duration of action in the guinea pig isolated trachea. The work of Ochsner et al. [1999] supports the concept that transitory retention of the agonists in plasma membranes of smooth muscle determines the long duration of bronchodilating effect after inhalation *in vivo*. With this model they expanded the traditional picture of a ligand approaching the receptor exclusively via the aqueous bio-phase and attributed the long-acting relaxant effect of these drugs to their high lipophilicity. Teschemacher and Lemoine [1999] demonstrated that in a cell membrane cAMP assay the duration of action of salmeterol following washout was dependent on the concentration of salmeterol studied.



It still remains to be elucidated, to what extent the prolonged relaxation observed *in vivo* results from an enhanced accumulation and/or retention of lipophilic  $\beta_2$ -adrenoceptor agonists in plasmalemma lipid bilayers of smooth muscles, or the hindered permeation of lipophilic drugs across the bronchial epithelium towards airway smooth muscle [Ochsner et al., 1999]. The transport of bronchodilator drugs through the tracheal epithelium of the guinea-pig studied by Jeppsson et al. [1989b] revealed that hydrophilic compounds slowly cross the epithelium and are not retained in the tissue, whereas lipophilic compounds rapidly cross the epithelium and are retained by the tissue. Ullman et al. [1992] found that the washability and the onset of action for salbutamol, salmeterol and formoterol were independent of the presence of epithelium in isolated guinea pig trachea. These data on one hand support the findings of Ochsner but on the other hand generate inconsistencies for explaining the slow onset of action of salmeterol. The high lipophilicity of the drugs may prove to be a required, but not a sufficient condition for induction of a sustained relaxation. In addition, as far as the delayed therapeutic response of salmeterol is concerned, it is also likely that diverse mechanisms operate in parallel. The highly lipophilic salmeterol is thought to approach the receptor mainly via migration in the lipid bilayer, hence the slow onset of action. Salbutamol with a low lipophilicity may approach the receptor only from the aqueous phase, hence rapid onset. The fast onset of action of indacaterol and its relatively high lipophilicity generates a notable inconsistency of the model. Studies on how physico-chemical properties of indacaterol might influence its biological properties have identified a unique feature: at physiological pH 7.4, indacaterol is present as a mixture of 4 ionization species, predominantly the zwitterion (54.1%) and the neutral one (21.5%), while salmeterol is mainly in its cationic form (95.6%) Tab. 1.3.

<i>Agonist</i>	pKa <sub>1</sub> <i>alcohol</i>	pKa <sub>2</sub> <i>amine</i>	C pH 7.4	Z pH 7.4	N pH 7.4	A pH 7.4	<i>logD</i> pH 7.4
Indacaterol	6.7	8.3	13.6	54.1	21.5	10.8	4.9
Formoterol	8.0	9.1	80.4	6.4	12.8	0.4	2.8
Salmeterol	8.8	9.8	95.6	3.8	0.6	0	4.2-5.3
Salbutamol	9.3	10.1	98.5	1.2	0.3	0	1.9

Table 1.3: **physico-chemical parameters for the  $\beta_2$ -adrenoceptor agonists.**

C, Z, N and A are the molar fractions of the ionization species at pH 7.4 for cation zwitterion neutral and anion, respectively. *logD* was measured by equilibrium dialysis with POPC/DOPS 9:1 liposomes. Unpublished data from Novartis.

The fact that zwitterion/neutral species and cations may have different tissue interactions might explain, in part, why indacaterol has a significantly faster onset of action. The current study concentrates on an extensive analysis of the kinetics and steady state interactions

## 1 Introduction

of indacaterol and salmeterol with lipid membranes. Due to the complexity of the cell membrane, we used the liposome system as an easy model for reproducing in a flexible manner the membrane properties. Several liposome compositions were chosen in order to investigate a wide range of membrane properties that could influence the drug/membrane interactions. The liposome compositions and the chemical structure of the lipids used in this work are summarized in Tab. 1.4 and Tab. 1.5, respectively.

<i>Liposome composition</i>	<i>molar ratios</i>	<i>carbons:insaturations of acyl chains</i>
PhC	100	18:1/16:0 <sup>a)</sup>
PhC/Chol	60/40	18:1/16:0 <sup>a)</sup>
DMPC	100	14:0/14:0
DPPC	100	16:0/16:0
DOPC	100	18:1/18:1
SM	100	16:0 <sup>b)</sup>
DMPC/Chol	60/40	14:0/14:0
SM/Chol	60/40	16:0 <sup>b)</sup>
DOPC/Chol	60/40	18:1/18:1
PhC/PhS	70/30	18:1/16:0 18:1/16:0
DPPC/DPPG	80/20	16:0/16:0 16:0/16:0
PhC/DPPG	70/30	18:1/16:0 16:0/16:0
DMPC/Chol/DMPG	30/40/30	16:0/16:0 16:0/16:0
<i>Raft-like liposomes: <sup>c)</sup></i>		
SM/Chol/DPPE/PhI/PhS/DPPC	16/32.2/25.8/6.5/6.5/13	
BLES	100	16:0/16:0 <sup>d)</sup>

Table 1.4: **Investigated liposome compositions.** <sup>a,b)</sup> Indicated are the most abundant fatty acid chains. The egg PhC composition from Avanti polar lipids (Alabaster, USA) is 18:1(32%) 16:0(34%) 18:2(18%) 18:0(11%) 16:1(2%) 20:4(3%). The egg SM composition is 16:0 (84%) 18:0(6%) 20:0(2%) 22:0(4%) 24:0(4%). <sup>c)</sup> Raft-like liposomes were prepared according to the composition of the raft-extract analyzed by Kamau et al. [2005]. <sup>d)</sup> Lipid extract of bovine surfactant contains 3% cholesterol, 79% PhC (53% is saturated) 11% phosphatidylglycerol (23% is saturated), phosphatidylethanolamine, phosphatidylinositol, lyso-bis-phosphatidic acid and sphingomyelin. BLES also contains the two highly hydrophobic surfactant associated proteins "B" and "C".

Particular attention was given to negatively charged lipids since they are abundant in the lung [Rodgers et al., 2005]. We investigated the effect of cholesterol on the membrane affinities of the drugs as well as the affinity to extracted rafts since it has recently been suggested that highly ordered membrane micro-domains are in the vicinity of the  $\beta_2$ -adrenoceptors and could be of physiological relevance for their function [Cherezov et al., 2007, Rosenbaum et al., 2007]. Liposomes made of bovine lipid extract surfactant (BLES) were used as a model to investigate the affinity of the agonists for the lung surfactant. The pH and the temperature were varied in order to shed light on the mechanism of drug/membrane interactions that could lead to differences in the biological effect.

## 1 Introduction

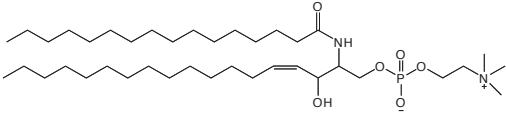
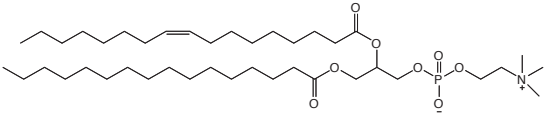
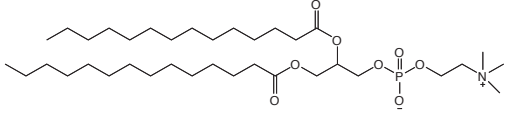
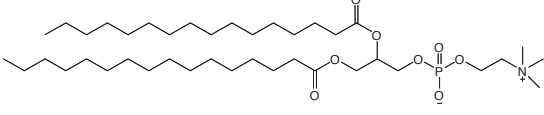
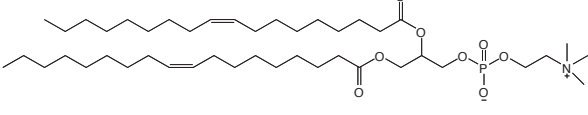
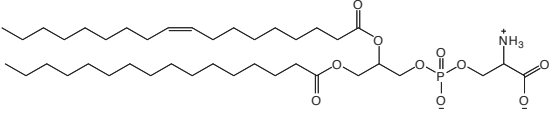
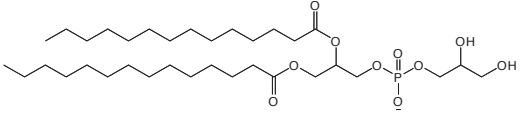
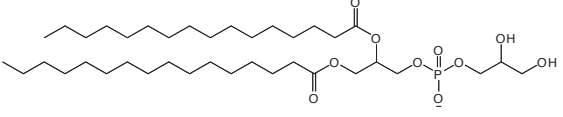
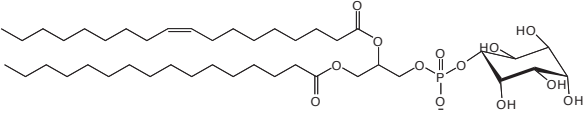
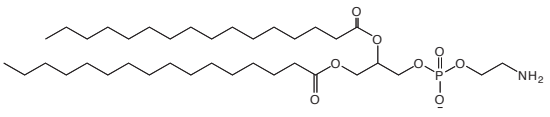
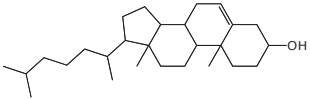
<i>Phospholipids</i>	<i>Molecular structure</i>	<i>Relative content of phospholipid-class in rat lung</i>
SM		11.6%
PhC		42.9%
DMPC		
DPPC		
DOPC		
PhS		12.5%
DMPG		5.7%
DPPG		
PhI		3.8%
DPPE		22.7%
Chol		~3% <sup>a)</sup>

Table 1.5: **Molecular structure of phospholipids and cholesterol.** Data adapted from [Rodgers et al., 2005]. <sup>a)</sup> Relative amount in guinea-pig lung [Yamanaka and Ostwald, 1968].

## 1.3 Mechanisms and characteristics of drug/membrane interactions

### Membrane structure

Biological membranes consist primarily of a thin double layer of amphipathic phospholipids, cholesterol and proteins. The phospholipids arrange in aqueous environments as bimolecular sheets, or *lipid bilayers*, with the hydrophobic "tail" regions sandwiched by the polar "head" groups. Lipid bilayers form a continuous and spherical coat with a thickness of  $\sim 7$  nm. They are fundamental for the life of a cell. The "fluid mosaic model" of the cell membrane proposed by Singer and Nicolson [1972], considers the biological membranes as a two-dimensional fluid matrix where lipids and proteins are partially free to diffuse within a space scale of 10 nm.

### Partition in to lipid bilayers

The lipophilicity of a drug is by far the most often used parameter to estimate its ability to interact with the lipid bilayers and permeate them [Camenisch et al., 1998, Testa et al., 1996]. The partition coefficient  $P$  is the concentration ratio of a solute species (e.g. an ionization species) between a hydrophobic and an aqueous phase at equilibrium according to eq. 1.1, where  $[A]$  equals the molar concentration of a single solute species in either phase, respectively. It is usually expressed in its logarithmic form,  $\log P$  and used to express the lipophilicity of a drug [Camenisch et al., 1998, Testa et al., 1996].

$$P = \frac{[A]_{hydrophobic}}{[A]_{aqueous}} \quad (1.1)$$

The larger the partition coefficient, the higher the tendency of the solute species to distribute into the lipid phase. When considering all ionization species of a compound the partition coefficient is referred to as distribution coefficient  $D$ , which is pH-dependent for ionizable compounds. Although the lipophilicity is usually assigned to a drug, it is rather an interplay of the properties of the drug and the lipid and aqueous phases and thus dependent on the composition of the lipid phase.

The octanol/buffer partition system is widely used for the characterization of the lipophilicity, however, it is only a crude predictor of the true extent of drug interaction with biological

membranes. Electrostatic interactions between the lipophilic phase and the solute play a minor role, since octanol carries no charge. In contrast, lipid membranes, the major lipophilic phase in vivo, contain various amounts of charged lipids providing a polar environment at the membrane surface with predominantly negative net charges [Kramer et al., 1998].

Besides membrane partition coefficients, the single rate constants determining partitioning and permeation are crucial for the membrane interaction of a solute. The pharmacokinetic and pharmacodynamic properties of drugs are often regulated by their interactions with membranes: a better understanding of the relationships between physicochemical characteristics of drugs and their membrane interactions would help to shed light on the mechanisms that lead to the biological activity of a drug. Despite its significance as most important transport mechanism for drugs, lipid bilayer diffusion is poorly understood [Kerns, 2001, Malkia et al., 2004].

### Permeation through lipid bilayers

The passive diffusion of a solute across the lipid bilayer is described by two theories: The solubility-diffusion model and the flip-flop model.

The solubility-diffusion model approximates the biological membrane as a homogeneous barrier [Diamond and Katz, 1974, Stein, 1997, Zwolinski et al., 1949]. Lipid bilayer permeation is assumed to follow eq. 1.2, a modification of Fick's first law,

$$Perm = \frac{D_m \cdot P}{h} \quad (1.2)$$

where  $Perm$  [ $cm \cdot s^{-1}$ ] is the permeation coefficient,  $P$  the partition coefficient of the solute,  $D_m$  [ $cm^2 \cdot s^{-1}$ ] the diffusion coefficient in the membrane and  $h$  [ $cm$ ] the membrane thickness. Higher partition coefficients lead to higher concentration gradients within the membrane and thus to an increased permeability. Most drugs, however, hold amphiphilic properties and their permeation behaviour is better described by the flip-flop model [Eytan and Kuchel, 1999, Eytan, 2005, Kleinfeld and Storch, 1993, Kleinfeld et al., 1997, Thomae et al., 2005, 2007, Zwolinski et al., 1949] as depicted in Fig. 1.2.

After association of the solute to the outer lipid leaflet of the membrane, the translocation from the outer to the inner lipid leaflet is, in contrast to the solubility-diffusion model, considered as distinct flip-flop event and not as diffusion down a gradient. From the inner lipid leaflet the drugs can dissociate to the inner aqueous phase or flop backwards to the outer leaflet. The permeation can be described by three reversible consecutive reactions as suggested by [Lauger et al., 1981, Kleinfeld and Storch, 1993, Kleinfeld et al., 1997, Thomae

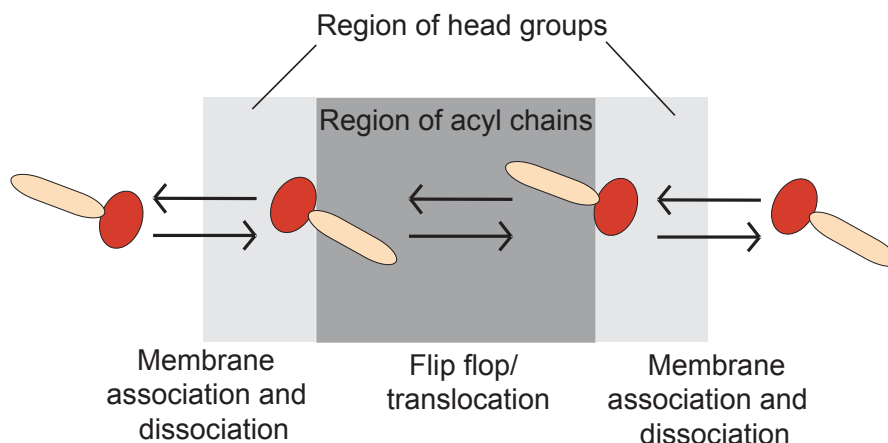
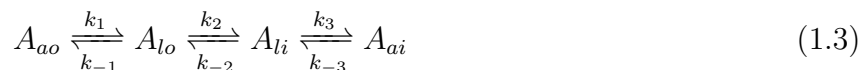


Fig. 1.2: **Model of lipid bilayer partitioning and permeation of an amphiphilic molecule.** The polar headgroup and the hydrophobic acyl chain regions of a lipid bilayer are indicated in dark and light grey, respectively. Four favored positions of an amphiphilic molecule are shown. In the membrane, its hydrophilic moiety (dark grey) locates towards the lipid headgroup region and the hydrophobic part (light grey) orients towards the hydrophobic acyl chains. The molecule partitions between the aqueous phase and the two lipid leaflets and translocates between the two lipid leaflets. The corresponding equilibria are indicated. Adapted from [Kramer, 2005].

et al., 2005, 2007, Zwolinski et al., 1949] with  $A_{ao}$ , the amount of solute  $A$  in the outer aqueous phase,  $A_{lo}$  and  $A_{li}$  the amount of solute in the outer and inner lipid leaflet, respectively, and  $A_{ai}$  the amount of solute in the inner aqueous phase (eq. 1.3).



The flip-flop model is more appropriate to describe permeation of drugs than the solubility-diffusion model, since it considers also the anisotropic properties of the lipid bilayer, rather than simplifying it to a lipophilic bulk.

## Factors influencing drug/lipid bilayer interactions

Drug/membrane interactions are influenced by several factors, which will be discussed in this section. Among the solute properties, the solute charge, the hydrogen bonding capacities, the molecular size and flexibility are the most important variables determining membrane affinities and transmembrane permeation. The electrostatic and fluidity properties of the lipid barrier affect its dynamic properties as well as the affinity and the permeation process of solutes [Malkia et al., 2004].

### *Solute charge*

Most of the marketable drugs are weak acids or weak bases with  $pK_a$  values between 1 and 13. Thus, at the physiological pH 7.4 a considerable fraction of them may be ionized. From early gastric secretion studies, Brodie and coworkers concluded that only the neutral species of an ionizable solute is able to cross biological membranes [Brodie and Hogben, 1957, Shore et al., 1957]. Based on this widely accepted pH-partition hypothesis the transmembrane permeation of charged solutes is assumed to be negligible [Dordas and Brown, 2000, Gutknecht and Tosteson, 1973, Saparov et al., 2006, Takanaga et al., 1994].

The reason for the poor partitioning and permeation through lipid bilayers towards ions is desolvation. Before entering the hydrocarbon core, ions will give up some of their hydration water. This is energetically unfavourable and represents the main reason for the low diffusive permeation of ions in lipid bilayers [Cevc, 1990]. The loss of energy is usually estimated from the Born equation taking into account the dielectric constants of the membrane interior and water, the ion charge and the ion radius [Disalvo and Simon, 1995]. This estimation, however, simplifies the lipid bilayer to a bulk phase with a very low dielectric constant and considers neither the anisotropic properties of the bilayer nor its flexibility.

Deviations from the pH-partition hypothesis have been observed [Males and Herring, 1999, Mashru et al., 2005, Thomae et al., 2005]. The Born energy concept does not distinguish between cations and anions. In reality, however, anions with the exception of large multivalent ions, such as phosphate or sulfate, are 20-1000 times more permeable than cations [Lasic, 1993] moreover lipophilic ions have been shown to partition into membrane phases on their own account [Kramer et al., 1998, Kurschner et al., 2000, Pauletti and Wunderli-Allenspach, 1994]. To explain the deviations Neubert [1989] and Takacs-Novak and Szasz [1999] suggested the formation of neutral ion pairs of the ionic solutes with lipophilic counterions present in the solution.

Other studies revealing higher permeation of the ionized species than predicted from the pH-partition hypothesis suggest the presence of an acidic microclimate at the membrane surface leading to a shift of the inflection point in the pH/permeation profile of the permeants, if the pH is measured in the bulk phase [Hogben et al., 1959]. Until today, it is not sufficiently elucidated whether and if so to which extent the ionized species contribute to lipid bilayer permeation.

### *Hydrogen bonding*

Lipid bilayers provide a considerable amount of hydrogen bonding groups. They are located exclusively in the head group region of the lipids. The membrane affinity of a solute



can be increased by H-bond interactions [Kramer et al., 1998], however, in order to translocate across the hydrocarbon region of the bilayer the solute must be hydrophobic enough to overcome the energy losses due to the breaking of the hydrogen bonds with water or the lipid head groups. Depending on the hydrogen bonding capacities of a solute this step can present a considerable energy barrier. The hydrogen bonding is also taken into account by Lipinski, stating that drug absorption is less likely if the number of H-bond donor (expressed as the sum of all OHs and NHs) exceeds 5 and/or the number of H-bond acceptors (expressed as the sum of all Os and Ns) exceeds 10 [Lipinski et al., 2001].

#### *Solute size*

The impact of the solute's size on membrane affinity and permeation is difficult to analyze, since changes in size are usually combined with changes of other properties, e.g. solubility, charge distribution, hydrogen bond capacity etc., which have an impact on the partitioning and permeation process on their own. The well-known and widely-applied "Lipinski Rules" deduced from a drug library with  $\sim 2000$  compounds indicate that among other factors such as hydrogen bonding capacities and lipophilicity of the molecules, drug absorption is unlikely if the molecular weight is  $>500$  Da [Lipinski et al., 2001]. The molecular volume is taken into account as an important factor determining the lipophilicity and permeation properties also in the solvation equation derived by Abraham [Abraham M. H., 1996]. In agreement with the Lipinski rules, Pardridge [1995] showed a correlation between  $\log P$  and molecular size up to a molecular size threshold of 400-600 Da for the permeability through the blood-brain barrier.

#### *Molecular flexibility*

A high molecular flexibility can, however, also be of advantage for the drug partition and permeation, e.g. by a facilitation of internal hydrogen bond formation resulting in the reduction of the hydrogen-bond capacities [Pagliara et al., 1999]. However Veber et al. [2002] studied structural properties that increase oral bioavailability in rats. They concluded that for good oral bioavailability the molecular flexibility (expressed as the number of rotatable bounds) must not exceed 10.

#### *Electrostatics of lipid bilayer*

Biological membranes are typically negatively charged, since the headgroups of the natural lipids are either zwitterionic or anionic. In the lung there is a considerable amount of phosphatidylserine (PhS) [Rodgers et al., 2005], an anionic phospholipid. The charge is,

however, nonuniformly distributed throughout the bilayer. The charged groups are located on the membrane surface while the membrane core is usually free of charge. Negatively charged phospholipids are generally situated on the cytoplasmic leaflet while glycosylated and sialic acid carrying lipids are in the exoplasmic leaflet [Allan, 1996]. A complex electric profile is generated over the membrane which is composed of the surface potential and the dipole potential [Cevc, 1990]. The surface potential originates from the negative surface charges, which attract counterions from the membrane surrounding leading to the formation of an electrical double layer at the bilayer/bulk interface. The surface potential is dependent on the charge density as well as on the bulk ionic strength. For natural membranes it is usually several tens of mV and results in an increased local concentration of cations, including protons, as well as a decreased local anion concentration as compared to the bulk aqueous phase [McLaughlin, 1989].

### *Fluidity and order of lipid bilayer*

Lipids show thermotropic polymorphism. The chain melting temperature (transition temperature  $T_m$ ), which is characteristic for each lipid, separates the solid-ordered state from the liquid-disordered state. The liquid crystal (liquid-disordered, *ld*) state, which exists at temperatures above the transition temperature  $T_m$ , is characterized by a higher fluidity as well as a lower thickness and translational order of the bilayer as compared to the gel (solid-ordered, *so*) state, which is formed at temperatures below the  $T_m$ . Higher fluidity of the membrane has been shown to correspond to enhanced partitioning and permeation rates [Frezard and Garnier-Suillerot, 1998, Hashizaki et al., 2003]. Membrane fluidity is commonly investigated by NMR [Brown and Williams, 1985] and fluorescence spectroscopy [Lentz, 1993]. Measurements are achieved by observing the motion of spin or fluorescent probes incorporated in synthetic bilayers. Lipid composition, lipid package, hydrostatic pressure, temperature, amount of cholesterol in the bilayer and several other parameters have a great impact on membrane fluidity [Lasic, 1993]. The lipid composition affects various characteristics of the lipid bilayer such as the phase transition behaviour, the fluidity, the physical stability and its electrostatic properties and therefore is one of the major factor influencing drug/membrane interactions [Pokorny et al., 2000].

In mixtures of different lipids the phase behaviour can be characterized by phase diagrams as shown for a binary mixture of phosphatidylcholine/cholesterol in Fig. 1.3. The phase boundaries are not only a function of temperature, but also of the lipid ratio. The phase diagram of binary mixtures of DMPC/cholesterol (Fig. 1.3) is of special interest since it shows the appearance of a new phase, the liquid-ordered phase (*lo*). The presence of cholesterol in a range between 7 and 30 % generates a coexistence region of *so* or *ld* and *lo* state. With

higher amounts of Chol only the *lo* state is formed [Lasic, 1993]. This phase is characterized by the high acyl chain order of the *so* state and the freedom of lateral diffusion present in the *ld* state [Ipsen et al., 1987]. The fluidity of the bilayer decreases with increasing lipid chain saturation and total chain length.

Cholesterol has diverse effects on membrane fluidity, it typically decreases fluidity for the *ld* phases at the level of the chain ends but lowers the average chain order near the headgroups. Apart from the bilayer fluidity, the bilayer composition will obviously affect the surface potential as described above, which is dependent on the electrostatic properties of the lipid headgroups. Changes of the headgroup could also influence the interactions between the headgroups based on hydrogen bonds or electronic interactions. Interestingly, the different lipid species are not randomly distributed but are laterally ordered in dynamic domains [Kahya et al., 2004, Mouritsen and Jorgensen, 1997].

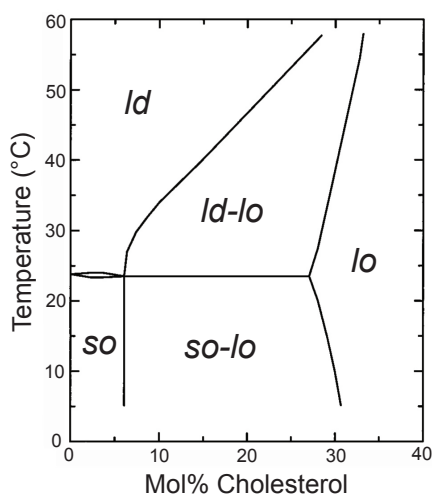


Fig. 1.3: **Phase diagram of DMPC/cholesterol membranes.** *so*, solid ordered phase; *ld*, liquid-disordered phase; *lo*, liquid-ordered phase. Data from Pokorny et al. [2000].

A synthetic membrane consisting of a binary (or more components) mixture of lipids, as shown in Figure 1.3 is not an homogeneous fluid but a dynamic system with phase-separations and differing physico-chemical properties within its structure. In this case, the probes used for fluidity measurements may assume different locations, orientations, axis of rotations and constrained-motions within the bilayers, according to the nature of the lipid surrounding [Kaiser and London, 1998]. The observed membrane fluidity results from the combination of the different factors influencing the spin or the fluorescence properties of the probe. A rigorous quantification of membrane fluidity involves four parameters, that can be derived from the spectroscopic properties of the probes. These include (i) the rotational correlation time; (ii) the order parameter of the spin or fluorescent probe; (iii) the steady-state *anisotropy* (or *polarization*) of the fluorescent probe, and (iv) the partition coefficient of the probe into

the bilayers [Gennis, 1989]. The use of only one of the cited parameters is, therefore, not sufficient to characterize the state of the bilayer. However, anisotropy measurements with the hydrophobic probe 1,6-diphenyl-1,3,5-hexatriene (DPH) have been useful for monitoring *changes* in membrane state in function of temperature, cholesterol content and lipid composition [Halling et al., 2008, Simonin et al., 2007]. It has to be noted that, when DPH is excited by polarized light, the resulting fluorescence is also polarized. The rotational speed of the probe in the membrane is lower in a rigid state (giving high values of anisotropy) than in a fluid state (low values of anisotropy) [Lentz, 1993, Seo et al., 2006].

### *Lipid rafts*

Cell membranes contain "detergent-insoluble" microdomains, i.e. *lipid rafts*, which are specialized areas where sphingolipids, cholesterol and several proteins are accumulated [Brown and Rose, 1992, Munro, 2003, Simons and Ikonen, 1997]. As lipid rafts have different physico-chemical properties than the rest of the plasma membrane, they can be isolated from the bilayers. The extraction is based on the resistance of rafts to non-ionic detergents, such as Triton X-100 at low temperatures (4 °C). When the detergent is added, the "fluid" membrane dissolves while the "rigid" lipid rafts remain intact and can be isolated by sucrose density centrifugation [Brown and Rose, 1992] [Bucher et al., 2005]. It is still controversial whether raft domains as extracted with detergents exist in the cell membrane or are an artifact of the extraction method. It is supposed that the raft domains have higher rigidity and thickness than the rest of the membrane [Sengupta et al., 2007]. Such microenvironments can accommodate certain proteins, including  $\beta_2$ -adrenoceptors [Allen et al., 2005].

## 1.4 Liposomes as model membranes

### Liposomes

Liposomes are vesicles consisting of one or several concentric bilayers. After the first description of the phenomenon that lipids spontaneously form closed bilayer membranes in aqueous surroundings [Bangham et al., 1965], liposomes gained quickly in importance as models for cellular membranes. The abundance of available lipids and preparation techniques has resulted in the possibility to produce liposomes custom-tailored to specific needs. Concerning their biomimetic qualities liposomes are superior to any other artificial membrane or bulk lipids and thus the ideal tool to model biological membranes wherever biomembranes are too complex. Liposomes are also a valuable alternative to octanol in partition studies. A standard method to determine affinities to liposomal membranes has been established by Pauletti and Wunderli-Allenspach [1994] and has been applied since then [Kramer et al., 1998, Kramer, 2001, Marenchino et al., 2004, Thomae et al., 2007]. Liposomes have also been used for membrane permeation studies [Kramer and Wunderli-Allenspach, 2003, Thomae et al., 2005] or to study the binding kinetics of solutes with membranes [Clarke, 1991].

## 1.5 Techniques to study drug-membrane interactions with liposomes

From the many techniques that are used to study drug-membrane interactions with liposomes, those applied in this work are shortly introduced here.

### Equilibrium dialysis to study drug-membrane affinities

Several methods such as microcalorimetry, fluorescence spectrometry, electron paramagnetic resonance spectroscopy (EPR), NMR and other spectroscopic techniques can be used to determine the partition coefficients of neutral and charged solutes between liposomal membranes and an aqueous phase [Testa et al., 2001]. Equilibrium-dialysis is a standard technique because it allows the determination of partition coefficients under equilibrium conditions and guarantees a sufficiently high lipid/solute ratio within the membrane so that partitioning is not affected by the solute concentration [Testa et al., 2001]. The principle of the equilibrium-dialysis technique is shown in Fig. 1.4. A dialysis cell consists of two half-cells which are

separated by a semipermeable membrane. A liposome suspension containing the solute is added into one half and buffer into the other half. After the equilibration of the solute between the two compartments separated with a cellulose membrane usually with a molecular weight cutoff of 10000, the partition coefficient is derived from the solute concentrations in the two chambers.

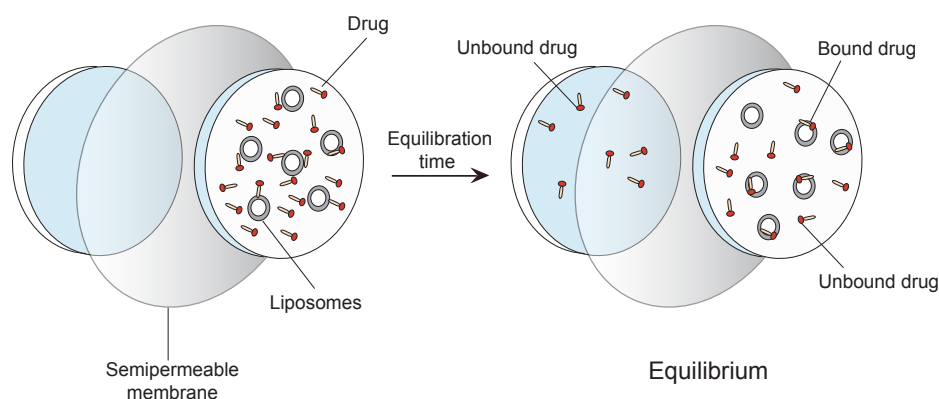


Fig. 1.4: **Equilibrium dialysis.** One side of the dialysis cell contains the buffer, the other side the liposomes. The drug is added in the liposomes side. After the equilibration of the system, usually 5 - 7 h, the concentrations of unbound drug is equal on both sides. The partition coefficient is calculated from the respective drug concentration of the two half cells.

## Surface plasmon resonance (SPR) to analyze drug-membrane interactions

Surface Plasmon Resonance (SPR) is a technique that is frequently applied to measure binding rate constants between two interacting entities, generally proteins [Salamon et al., 1997a,b]. Several studies have demonstrated that the technique is sensitive enough to monitor interactions of solutes with lipid bilayers in the form of liposomes [Abdiche and Myszka, 2004, Danelian et al., 2000, Frostell-Karlsson et al., 2005]. These authors illustrated how liposomes could be captured on a specially designed sensor chip (referred to as L1) consisting of a carboxymethyl dextran hydrogel derivatized with lipophilic alkanes Fig. 1.5.

Surface plasmon resonance (SPR) biosensors have the potential to further the liposome-based in vitro systems for predicting partitioning and permeation. Liposomes captured on a sensor chip provide a lipid barrier representative of the cell membrane. As a drug in solution is flown over the surface, interactions with lipids as they occur in real time can be monitored by SPR without the need for intrinsic or extrinsic labels. In this thesis we show how to

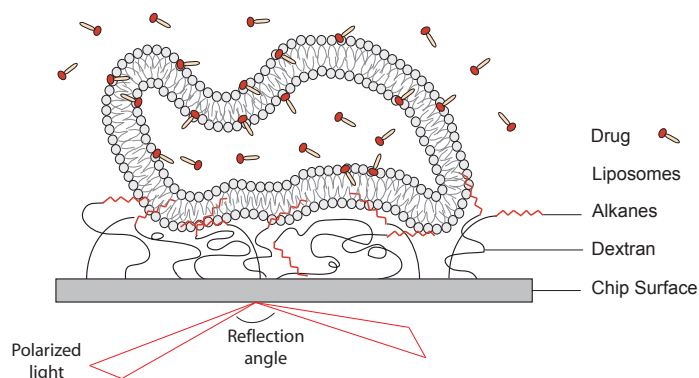


Fig. 1.5: **Diagram of the biosensor assay.** Liposomes are captured on a Biacore L1 sensor chip through interactions with alkane groups attached to the dextran matrix. As drug in solution is flown over the surface, interactions with the lipid are detected by changes in the reflection angle. Figure modified from [Baird et al., 2002]

use SPR for the estimation of the rate constants defining partitioning and translocation of a drug compound into and across lipid bilayers.

## The Terbium(III)-permeation assay to study membrane permeation kinetics

Tb(III)-containing liposomes were first used in membrane fusion studies by Wilschut et al. [1980]. Two liposome populations loaded with Tb(III) and dipicolinic acid, respectively, are mixed in the presence of e.g. fusion-inducing agents. Upon fusion of the vesicles and mixing of the aqueous contents Tb(III) and dipicolinic acid form a luminescent complex, and thus, vesicle fusion is registered as fluorescence increase. The idea of Tb(III)-containing liposomes was exploited by Kramer and Wunderli-Allenspach [2003] to design a novel permeation assay. It is based on the chelation of Tb(III) by aromatic carboxylic acids (ACA) resulting in a characteristic luminescence signal. The permeation of ACA into the interior of the Tb(III)-containing liposomes can thus directly be monitored by luminescence stopped-flow measurements. The assay has originally been developed to investigate the ability of the cell-penetrating peptide TAT(44-57) to permeate lipid bilayers [Kramer and Wunderli-Allenspach, 2003]. For this purpose two TAT peptide sequences were coupled to N-(4-carboxy-3-hydroxyphenyl)maleimide via a cystein residue. The carboxy-hydroxyphenyl-succinimide group functioned as probe interacting with Tb(III). Hydroxylation of entrapped Tb(III), however, limits the stability of Tb(III)-loaded liposomes to 24 h. Since Tb(III) interacts with a wide range of ACAs, the Tb(III)-permeation assay presents an ideal tool to

## ***1 Introduction***

---

study the permeation not only of ACA-labeled peptides but also of ACAs which exhibit drug-like properties and to investigate different aspects of lipid bilayer permeation [Thomae et al., 2005, 2007].



## 1.6 Aim of the thesis

The aim of this thesis is to investigate the interactions occurring between lipophilic  $\beta_2$ -adrenoceptor agonists (indacaterol and salmeterol) and lipid membranes. A better understanding of these interactions may disclose some of the mechanism at the basis of the differences in the *in vivo* behaviour of  $\beta_2$  agonists.

The focus is particularly at the differences in the time to onset and duration of effect between indacaterol and salmeterol. Knowledge of the principles behind the advantageous characteristic of indacaterol, i.e. fast onset and long duration, would allow to develop further compounds of this kind, possibly even for other targets.

To explore the interactions between agonists and lipid membranes we chose equilibrium dialysis, that allows the investigation of the drug affinity to membranes, and surface plasmon resonance, a method dealing with the kinetics of the interactions. Moreover the Tb(III)-permeation assay was adopted to investigate the thermodynamic and kinetic features of permeation across lipid membranes.

Particular attention was given to the conditions such as liposome composition, pH and temperature: these parameters were varied to further differentiate the relationship between the physico-chemical properties of the agonists and the membrane interactions. We investigated the effect of cholesterol on the membrane affinities since it is responsible for the geometry and rigidity of the membranes whereas negatively charged lipids were of particular interest because they are abundant in the lung. Liposomes made of bovine lipid extract surfactant (BLES) were used as a model to investigate the affinity of the agonists for the lung surfactant. The affinity to rafts was of special interest since it has recently been suggested that highly ordered membrane micro-domains are in the vicinity of the  $\beta_2$ -adrenoceptors and could be of physiological relevance for their function. The temperature was varied in order to change the membrane properties such as fluidity and phase state. A broad pH range allowed the investigation of the relationships between the ionization species of the agonists and the mechanism of drug-membrane interactions. The thermodynamics of permeation were investigated by varying the temperature in the Tb(III)-permeation assay.



## 2 Materials and Methods

### 2.1 Chemicals and buffers

#### Chemicals

Salmeterol (1660) was obtained from Tocris bioscientific (Ellisville, USA), indacaterol from Novartis (Basel, CH).  $^3\text{H}$ -indacaterol and  $^3\text{H}$ -salmeterol were from Novartis (Basel, CH).  $\pm$ -Propranolol hydrochloride (P0884), 1,6-diphenyl-1,3,5-hexatriene (DPH) and valinomycin were purchased from Sigma (Buchs, CH). 2-Hydroxynicotinic acid (OHNA) (55966) and ethylenediaminetetraacetic acid (EDTA) (03610) were purchased from Fluka (Buchs, CH).  $\text{TbCl}_3$  hexahydrate (Tb(III)) (21290-3) was from Aldrich (Buchs, CH) and zwittergent 3-14<sup>®</sup> from Calbiochem (San Diego, USA). TritonX-100 was purchased from Fluka (Buchs, CH). Complete<sup>®</sup>, methanol, chloroform, trifluoro-acetic acid and acetonitrile (HPLC grade) for lipid extraction and HPLC investigations were from Merck (Darmstadt, DE). All other chemicals were of analytical grade.

*Lipids:* Egg phosphatidylcholine (PhC), spinal cord phosphatidylserine (PhS), phosphatidylinositol (PhI) and sphingomyelin (SM) all grade 1, were purchased from Lipid Products (Nutfield, UK). Dipalmitoylphosphoglycerol (DPPG) (840455) dipalmitoylphosphatidylcholine (DPPC) (850355), dioleoylphosphatidylcholine (DOPC) (850375), dimyristoylphosphatidylcholine (DMPC) (850345), dimyristoylphosphoglycerol (DMPG) (840445) and dipalmitoylphosphoethanolamine (DPPE) (850705) were from Avanti polar lipids (Alabaster, USA). Cholesterol (Chol) (C8667) was from Sigma (Buchs, CH). Bovine lipid extract surfactant (BLES) (BPAI-51) was purchased from BLES Biochemical (London, ON).

### Buffers

- **MOPS buffer**

(0.2 M Mops, pH 7.4)

To prepare 1 l buffer, 46.25 g 3-(N-morpholino)propanesulfonic acid sodium salt (MW 231.2 g mol<sup>-1</sup>) (69947) from Fluka (Buchs, CH) were dissolved in 800 ml water, adjusted to pH 7.4 with 0.1 M HCl NaCl 50 mM was added and diluted to 1 l. The buffer was stored at 4°C.

- **SUBS (Standardized Universal Buffer Solution)**

To prepare 1 l solution A, 7 g citric acid monohydrate, 3.54 g boric acid, 3.5 ml phosphoric acid 85% and 343 ml 1 M NaOH were dissolved in 1 l water, transferred in a plastic bottle and stored under nitrogen at 4 °C. The solution B was HCl 0.1 M and the solution C was sodium chloride 3.2 M. To prepare 100 ml buffer of a specific pH value (between pH 4 and 13), 20 ml of solution A were mixed with the required amount of B, while the ionic strength of the buffer was adjusted with C to a constant value of 0.23 M (buffer ratios according to Pauletti and Wunderli-Allenspach [1994]). The solutions were stored at 4°C.

- **TNE buffer**

(25 mM Tris, 150 mM NaCl, 5 mM EDTA, pH 7.4)

To prepare 1 l buffer, 1.46 g EDTA, 8.76 g sodium chloride, 3.03 g tris-(hydroxymethyl)-amminomethane (93352) from Fluka (Buchs, CH) were dissolved in 800 ml water. The pH was adjusted to 7.4 with concentrated HCl and the solution was diluted to 1 l. The buffer was stored at 4°C.

- **TRIS buffer**

(0.2 M Tris, pH 7.4)

To prepare 1 l buffer, 31.52 g tris-(hydroxymethyl)-amminomethane (MW 157.60 g mol<sup>-1</sup>) (93352) from Fluka (Buchs, CH) were dissolved in 800 ml water. After adjusting the pH to 7.4 with concentrated HCl, the buffer was diluted to 1 l, filtered through a PES membrane filter (0.2 μm) and stored at 4°C.

## 2.2 Preparation and characterization of liposomes

### Preparation

Liposomes with various lipid compositions (PhC, DMPC, DPPC, DOPC, SM, DMPC/Chol 60/40 mol/mol, SM/Chol 60/40 mol/mol, DOPC/Chol 60/40 mol/mol, PhC/PhS 70/30 mol/mol, DPPC/DPPG 80/20 mol/mol, PhC/DPPG 70/30 mol/mol, DMPC/Chol/DMPG 30/40/30 mol/mol, SM/Chol/DPPE/PhI/PhS/DPPC 16/32.2/25.8/6.5/6.5/13 mol/mol (raft-like) [Kamau et al., 2005] and BLES, were prepared by extrusion [Mayer et al., 1986, Kramer et al., 1998]. The lipids were dried from a chloroform/methanol solution to a thin layer in a round flask. For the preparation of Tb(III)-containing liposomes a methanol solution containing 0.2 mmol TbCl<sub>3</sub> hexahydrate was added to the lipid solution. The lipid film was subsequently resuspended with buffer (SUBS, pH 7.4 for Tb(III)-free liposomes, MOPS or TRIS for Tb(III)-containing liposomes) to form multilamellar vesicles (MLV) containing 20 mg lipid per ml. The MLV were submitted to 5 cycles of freeze and thaw. Large unilamellar vesicles (LUV) were prepared at 50°C by extrusion of the MLV preparation through polycarbonate filters (0.1, 0.2 or 0.4 μm pore size, Nucleopore<sup>®</sup>, Whatman) using the 10 ml Lipex extruder from Northern Lipids (Burnaby, Canada). Liposome preparations were equilibrated overnight before being used. Tb(III)-containing liposomes were used immediately and non-incorporated Tb(III) was removed by size exclusion chromatography on a Sephadex G-25 PD-10 desalting column (Amersham Biosciences, Freiburg, Germany) with 0.2 M NaCl. The collected liposome fraction contained 10 to 15 mg lipids per ml. The local concentration of Tb(III) in the liposomal lumen was between 3 and 7 mM [Kramer and Wunderli-Allenspach, 2003]. Tb(III)-containing liposomes were used within a day. Liposomes without Tb(III) were stored at 4°C and used within five days. Liposomes containing EDTA and Tb(III) were prepared as described above with 3 ml 0.2 M EDTA pH 6.5 instead of MOPS, SUBS or TRIS and with an average pore diameter of 200 nm for extrusion. In this case, the local concentration of Tb(III) in the liposomal lumen was around 4 mM. These liposomes were used within five days after preparation.

### Size distribution and zeta potential measurements

Liposome size distributions and zeta potentials were analysed by dynamic light scattering and micro electrophoresis using a Zetasizer 3000 HAS (Malvern Instruments, UK). The hydrodynamic average mean diameters of all preparations for dialysis were between 80 and 120 nm (intensity distribution). The polydispersity index was usually below 0.1, indicat-

ing a narrow size distribution with a standard deviation of  $< 32\%$  assuming a Gaussian distribution function. The size distribution was unchanged during equilibrium dialysis or permeation experiments within the investigated pH range.

### Lipid quantification

The lipid content in liposome preparations was characterized via HPLC by injecting 50  $\mu\text{l}$  of sample in a BDS Hypersil C<sub>8</sub> column (150 mm x 4.6 mm I.D., 5  $\mu\text{m}$  particle size, Thermo, Bellefonte, PA, USA) kept at 50°C. The mobile phase was an isocratic mixture of acetonitrile:trifluoroacetic acid:water (89.9:0.1:13 v/v) for DPPC and DPPG containing liposomes or acetonitrile:water (86.9:0.1:13 v/v) for the other lipid compositions. The flow rate was 2 ml/min. The wavelength of the detector was 215 nm. Samples were diluted in chloroform/methanol 1:1 v/v before injection. Lipid concentrations were obtained via an appropriate calibration curve ( $n = 5$ ). Since egg PhC is a mixture of differently unsaturated phospholipids, the quantification was performed using the total peak areas.

### Determination of membrane fluidity

To study the fluidity of the lipid bilayers, liposomes were labeled with the probe DPH and subjected to anisotropy measurement with an LS50B Luminescence Spectrometer (Perkin Elmer) [Lentz, 1993] [Seo et al., 2006]. The wavelengths of excitation and emission were 355 and 430 nm, respectively, with a bandwidth of 5 nm. For the DPH labeling, a liposome suspension (0.15 mg/ml) in SUBS pH 7.4 (Sec. 2.1) was incubated for 30 min at 37 °C with 10  $\mu\text{M}$  DPH that was added as a 100-fold concentrated stock solution in tetrahydrofuran. The fluorescence intensity values of the vertical and the horizontal polarizers were converted in anisotropy according to eq. 2.1:

$$Anisotropy = \frac{VV - (G \cdot VH)}{VV + (2G \cdot VH)} \quad (2.1)$$

where  $VV$  is the fluorescence intensity of the probe measured with vertical excitation and vertical emission polarizers,  $VH$  is the fluorescence intensity with vertical excitation and horizontal emission polarizers, and  $G$  is the instrument correction factor ( $G = HV/HH$ ).

## Preparation of rafts

Rafts were prepared as previously described by Bucher et al. [2005]. In brief, about  $4 \times 10^8$  P388/ADR or P388 cells [Belli et al., 2008], were incubated on ice with 2 ml of TNE buffer (Sec. 2.1) containing Complete<sup>®</sup> (1 tablet per 50 ml of solution) and 1% (v/v) Triton X-100. The cell lysate was homogenized at 4°C with 50 strokes at 1000 rpm using a Dounce homogenizer (2 ml glass tube, B.Braun, Biotech International). The homogenate was mixed with an equal volume of 80% sucrose in TNE, transferred into a centrifuge tube and overlaid with 2 ml each of 30%, 20%, 10% sucrose and 1.5 ml of 5% sucrose in TNE. All sucrose solutions contained Complete<sup>®</sup>. After centrifugation at 200'000 g for 19 hours at 4 °C in an SW41Ti rotor (Beckman Instruments) the rafts were visible as a turbid band in the upper part of the centrifuge tube (density range between 1.04 and 1.09 g/cm<sup>3</sup>) and were pooled in a 2.5 ml fraction. Protein concentrations of different raft preparations were typically between 75 and 120  $\mu\text{g}/\text{ml}$ . Raft fractions showed an average mean diameter between 240 and 280 nm with polydispersity indices between 0.4 and 0.5, indicating a broad size distribution. The quantification of the total protein amount was performed with the DC protein assay kit from Bio-Rad (Hercules, CA, USA) the lipid content was estimated from the concentration of proteins assuming a ratio protein/lipid 1:3 [Brown and Rose, 1992]. The lipid concentration was typically around 0.1 mg/ml. Aliquots of 400  $\mu\text{l}$  were stored at -20°C and used within 4 weeks.

### 2.3 Octanol/buffer partitioning

The distribution profile in the octanol/buffer system of indacaterol and salmeterol was determined in the pH range of 4 to 13 with the shake flask method. For each investigated pH, 5, 10 or 20  $\mu\text{l}$  of a 2 mM methanolic stock solution of indacaterol and salmeterol, respectively, were dried in a reaction tube. The compounds were re-dissolved in 1 ml water-saturated 1-octanol and 5 ml of standardized universal buffer solution (SUBS) at the desired pH, containing phosphate, citrate, borate and sodium chloride adjusted to a physiological osmolality and a constant ionic strength of 0.23 M [Pauletti and Wunderli-Allenspach, 1994] were added. The tubes were shaken for 1 h at room temperature and centrifuged for 10 min at 9000 g. Shaking for 3 hours revealed the same results, indicating that equilibrium was reached after 1 h. At the end of the experiments no significant pH shifts were observed in the buffer phases. From both phases of 200  $\mu\text{l}$  were diluted with 800  $\mu\text{l}$  methanol and the concentrations were determined by LC/MS/MS with a Waters 2759 HPLC equipped with an Xterra column (C8, 3.5 $\mu\text{m}$ , 1x50mm) and an MS Quattro Micro Mass detector. The drugs were eluted with a linear gradient of H<sub>2</sub>O/acetonitrile 95%/5% to 100% acetonitrile. The partition coefficients were calculated as the ratios of the concentrations in the respective 1-octanol and aqueous phases.

### 2.4 Determination of drug-membrane affinity by equilibrium dialysis

The membrane partitioning of indacaterol and salmeterol were characterized by equilibrium dialysis with liposomes of various lipid compositions (Tab. 1.4). For each investigated pH, 1  $\mu\text{l}$  of a methanolic 2 mM indacaterol or salmeterol stock solution was dried in a reaction tube and 100  $\mu\text{l}$  liposomes were added. The pH was adjusted to values between 6 and 10.5 by dilution with SUBS. The final lipid and drug concentrations were 1 mg/ml (1.3 mM) and 1  $\mu\text{M}$ , respectively, if not stated otherwise. For experiments with rafts, 1  $\mu\text{l}$  of stock solution was dried in a reaction tube and 1 ml of raft extract was added, TNE buffer pH 7.4 was used for the dialysis instead of SUBS. Equilibrium dialysis experiments (Macro 1 cells, 1.0 ml; cellulose membrane, MW cut-off 10,000, (10.16) Dianorm, Germany) were performed for 5h at 25 °C or 7h at 4 and 37 °C against SUBS buffer of the respective pH, as shown in control experiments the equilibrium was reached at all pH values (between 6.0 and 10.5). At the end of the experiment, the pH was measured in the buffer phase. No significant pH shift was observed during the dialysis. The content of the chamber containing the liposomes was diluted 1:5 in methanol in order to solubilize the liposomes and the concentrations of drugs in



both chambers were determined as described above for the octanol partitioning experiments. Some experiments for the pH-distribution profiles were performed with up to three different compounds simultaneously and quantified by LC/MS/MS. Control experiments showed that this had no influence on the results under the applied experimental conditions. The lipid concentration was determined at the end of the dialysis by HPLC with a Hitachi L2130 pump equipped with a Thermo C8 column (5 $\mu$ m, 150x4.6mm) and a Hitachi L2480 UV detector. Lipids were eluted with H<sub>2</sub>O/acetonitrile 87/13 (vol%) and detected at 215 nm. Control experiments performed with radio-labelled indacaterol and salmeterol and quantification by liquid scintillation counting revealed the same results as partition experiments with non-labelled compounds and quantification by LC/MS/MS. No lipid hydrolysis products, i.e. free fatty acids or lysophosphatidylcholine were detectable by HPLC in PhC liposomes after equilibrium dialysis. The pH-dependent partitioning of indacaterol and salmeterol was in addition analysed after an overnight incubation of PhC liposomes with the drug. No significant differences were observed with or without overnight incubation.

*Data analysis of the partitioning experiments by equilibrium dialysis*

Partition coefficients (D) of indacaterol and salmeterol between lipid bilayers and buffer were calculated from the drug concentrations in the two dialysis chambers as previously described Pauletti and Wunderli-Allenspach [1994] and shown in eq. 2.2,

$$D = \frac{C_{LB} - C_B}{C_B} \cdot \frac{V_{LB}}{V_L} + 1 \quad (2.2)$$

where  $C_{LB}$  denotes the molar drug concentration in the liposome-containing chamber and  $C_B$  the molar drug concentration in the buffer chamber.  $V_{LB}$  is the volume of the liposome suspension,  $V_L$  the volume of the lipophilic phase, i.e. the lipid bilayer (calculated with a density of 1.0 g/ml [Huang and Mason, 1978]), within  $V_{LB}$ . The partition coefficients (P) of the single ionization species, i.e. the cation (C), the net neutral species (N) including the uncharged species as well as the zwitterionic species, and the anion (A) were estimated by nonlinear curve fitting of the D/pH diagrams with the function described in eq. 2.3 [Kramer, 2001],

$$D = \sum_{n=1}^i (\alpha_i \cdot P_i) \quad (2.3)$$

where  $\alpha_i$  denotes the molar fraction of the ionization species  $i$  of the drug and  $P_i$  is the partition coefficient of the species  $i$ .  $P_C$ ,  $P_N$  and  $P_A$  are defined for the cationic, net neutral and

## 2 Materials and Methods

---

anionic species, respectively. For the analysis, the  $pK_a$  values of salmeterol and indacaterol were kept variable. Data were fitted with the Systat software TableCurve2D. For the curve fitting residuals were weighted by their reciprocal squares.

In order to compare the membrane affinities determined by equilibrium dialysis and SPR,  $D$  values were transformed to dissociation constants  $K_D$  by eq. 2.4 according to Kramer [2001],

$$K_D = \frac{L^*}{(D - 1)} \quad (2.4)$$

where  $K_D$  has the dimension [M] and  $L^*$  denotes the local lipid concentration within the membrane, i.e. 1.3 M (calculated from the bilayer density of 1.0 g/ml and the average MW of PhC). This is a rough estimate as it assumes a 1:1 interaction between drug and lipid in solution and may therefore not reflect the real situation.  $K_D$  is a relative measure here for  $D$  under concentration-independent conditions. Molar lipid/drug ratios within the lipid bilayers in equilibrium dialysis were calculated from  $L^*$  and the local drug concentration  $CL^*$ . The latter was estimated from the start concentration in the liposome-containing chamber  $C_{start}$  according to eq. 2.5

$$CL^* = D \cdot C_B \approx \frac{D \cdot C_{start}}{\frac{(D-1) \cdot V_L}{V_{LB}} + 2} \quad (2.5)$$

## 2.5 Determination of drug-membrane affinity by surface plasmon resonance (SPR)

The interactions of propranolol, salmeterol and indacaterol with PhC bilayers were investigated at 25°C in a pH range between 5 and 9.7 with a Biacore 3000 instrument equipped with an L1 chip. Sensor chips were pre-conditioned with two consecutive 30 s pulses of 20 mM zwittergent<sup>®</sup> detergent followed by 50 mM HCl in (1/1) v/v isopropanol at a flow rate of 0.1 ml/min before their first use [Abdiche and Myszkka, 2004]. Liposomes were typically diluted in SUBS pH 7.4 to 5 mg lipids per ml and captured to saturation across isolated flow cells at 0.005 ml/min for 2 min. The flow rate was increased to 0.075 ml/min and the liposome surface was washed with running buffer at the respective pH (SUBS containing 0.2% or 5% DMSO) for 1000 s. According to Anderluh et al. [2005], 1000 *RU* correspond to ~1.2 ng lipids. Considering the volume of the flow cell, i.e. 6 nl, and the increase of 5000 to 6000 *RU* upon liposome capture, the lipid content of the cell is equivalent to a concentration of 1 to 1.2 mg/ml (1.3 to 1.5 mM, calculated with an average *MW* for PhC of 780 g/mol). To estimate the membrane affinity of propranolol and salmeterol, their association to liposome-covered sensor chip surfaces was analyzed at different concentrations between 97.6 and 3125  $\mu$ M and between 9.38 and 150  $\mu$ M, respectively. The adsorption experiments were performed at 25°C with SUBS pH 7.2 containing 5 % DMSO. As the drug-binding response ( $RU_{Drug}$ ) is linearly related to the lipid capture level ( $RU_{Lipid}$ ) and to the *MW* of the binding solute ( $MW_{Drug}$ ), the resulting  $RU_{Drug}$  values were normalized for the respective  $RU_{Lipid}$  levels and for  $MW_{Drug}$  as described in eq. 2.6 [Abdiche and Myszkka, 2004].

$$RU_{scaled} = 10^6 \cdot \frac{RU_{Drug}}{MW_{Drug} \cdot RU_{Lipid}} \quad (2.6)$$

The apparent dissociation constants  $K_D$  between the drug and the lipid bilayer were estimated from the  $RU_{scaled}$  values of the absorption phase at equilibrium and the salmeterol concentrations in the buffer ( $c$ ) by fitting a single site binding isotherm to the experimental data as shown in eq. 2.7,

$$RU_{scaled} = \frac{RU_{Max}}{1 + \frac{K_D}{c}} \quad (2.7)$$

where  $RU_{max}$  is the maximum scaled surface-binding capacity [Abdiche and Myszkka, 2004], i.e. the fitted  $RU_{scaled}$  at infinite  $c$ . The  $RU_{Drug}$  values were not corrected for the corresponding  $RU$  values of the reference chip, i.e. in the absence of liposomes, assuming that the sensor chip surface was completely covered by liposomes.

## 2.6 Kinetic studies by SPR

To study the pH-dependent kinetics of the interactions between the drugs and the lipid bilayers, 0.25 ml of salmeterol or indacaterol in running buffer containing 0.2% DMSO at pH values between 5 and 10 were injected at a flow rate of 0.05 ml/min. Control experiments with flow rates of 0.075 and 0.1 ml/min revealed the same kinetics. The injection type was “Kinject” and 400 s were chosen as dissociation time. After each binding cycle, the sensor surface was regenerated to the original matrix by injecting 50 mM HCl in 50% v/v isopropanol at 0.05 ml/min. As for the binding study, response data were not corrected for the binding to the reference surface (unmodified lipid-free flow cell). At an excess of lipids over solute, i.e. at drug concentration  $<100 \mu\text{M}$ , the kinetics were independent of the drug concentrations. Kinetic experiments were therefore performed with  $60 \mu\text{M}$  salmeterol or indacaterol if not stated otherwise. Most absorption and desorption phases followed bi-exponential functions according to eq. 2.8 (absorption) and eq. 2.9 (desorption),

$$RU(t) = RU(0) + RU_{Max1} \cdot e^{-k_1 \cdot t} + RU_{Max2} \cdot e^{-k_2 \cdot t} \quad (2.8)$$

$$RU(t) = RU(0) + RU_{Max1} + RU_{Max2} - (RU_{Max1} \cdot e^{-k_1 \cdot t} + RU_{Max2} \cdot e^{-k_2 \cdot t}) \quad (2.9)$$

where  $RU(t)$  and  $RU(0)$  are the  $RU_{Drug}$  at time  $t$  and the  $RU$  at time zero, i.e. before injection of the drug, respectively.  $RU_{max1}$  and  $RU_{max2}$  are the fitted plateau values of the two exponentials and  $k_1$  and  $k_2$  are the faster and the slower apparent rate constants, respectively. The faster apparent rate constants  $k_1$  were not reproducible and in some cases beyond the time resolution of the instrument and were therefore not further analyzed. For salmeterol, in the pH range between pH 8.6 and 10.0 the absorption and desorption phases followed either mono-exponential functions as shown in eq. 2.10 and eq. 2.11 or bi-exponential functions as shown above.

$$RU(t) = RU(0) + RU_{Max} \cdot e^{-k \cdot t} \quad (2.10)$$

$$RU(t) = RU(0) + RU_{Max} - RU_{Max} \cdot e^{-k \cdot t} \quad (2.11)$$

Data points recorded for 150 s after the injection of drug or buffer were fitted with the Systat software TableCurve 2D neglecting the data of the first 5 s [Rebolj et al., 2006]. The residuals were weighted by their reciprocal squares.

## 2.7 Determination of equilibrium constants by spectrofluorimetric titrations

Spectrofluorimetric titrations were carried out in order to determine the equilibrium affinity constants  $K_A$  for the 1:1 complex formation between OHNA and Tb(III) in MOPS, TRIS and 0.2 M EDTA pH 6.5 and at temperatures between 10 and 37°C. Beside pH 6.5, the complex formation was also characterized at pH 2.5. MOPS, TRIS and 0.2 M EDTA were therefore adjusted to pH 2.5 with hydrochloric acid. Note, that neither MOPS nor TRIS do buffer at this pH. Increasing volumes of 650  $\mu$ M Tb(III) were added to 0.8 ml 2  $\mu$ M OHNA in the measuring cell of a Perkin Elmer spectrofluorometer LS50B using a micro syringe equipped with a Mitutoyo micrometer head. Mixing was achieved with a magnetic stirrer. The temperature within the cell was controlled with a jacketed cell holder to  $\pm 0.1^\circ\text{C}$ . Titrations were carried out in the presence and absence of PhC liposomes (lipid concentrations were 1 or 10 mg/ml in the measuring cell as indicated). The liposomes were incubated with the OHNA solutions for  $\geq 2$  hours before the titrations to reach partitioning equilibria. The complex formation was followed by the increase in luminescence  $\Delta L$ . Excitation and emission wavelengths were  $\lambda_{ex}$  305 nm and  $\lambda_{em}$  545 nm, respectively. The luminescence was monitored with a time delay of 0.05 ms, a gate time of 1 ms, a cycle time of 20 ms, at 1 flash per cycle. Figure 2.1 shows representative excitation and emission spectra of the complex between Tb(III) and OHNA at an excess of Tb(III).

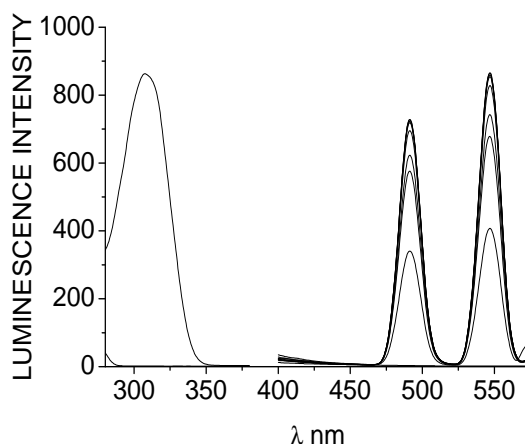


Fig. 2.1: **Excitation and emission spectra of the OHNA/Tb(III) complex.** The total OHNA concentration was  $2 \cdot 10^{-6}$  M in 0.2 M TRIS pH 6.5 at 25°C and total Tb(III) concentrations were  $3 \cdot 10^{-4}$  M for the excitation spectrum and  $2.5 \cdot 10^{-5}$ ,  $1.0 \cdot 10^{-4}$ ,  $1.5 \cdot 10^{-4}$ ,  $2.5 \cdot 10^{-4}$  and  $3 \cdot 10^{-4}$  M for the emission spectra.

As Tb(III) is known to form complexes with  $>1$  ligands, titrations were performed in excess of Tb(III) to allow 1:1 complexes only, assuming that the first ligand has a higher affinity than further ligands. Under these conditions the complex formation is described as follows:



and  $K_A$  of the 1:1 complex is defined

$$K_A = \frac{[Tb(III)/OHNA]}{[Tb(III)] \cdot [OHNA]} \quad (2.13)$$

The equilibrium constant  $K_A$  is related to  $\Delta L$  at the different Tb(III) concentrations as described below [Konnors, 1987],

$$\Delta L = \frac{\Delta L_\infty}{1 + 1/K_A \cdot 1/Tb(III)_{total}} \quad (2.14)$$

$$\Delta L = L - L_0 \quad (2.15)$$

where  $L_0$  and  $L$  are the luminescence signals before and later Tb(III) addition. The affinity constants  $K_A$  were determined by non-linear fitting of eq. 2.14 with TableCurve2D (Systat Software).

The Gibbs free energy variation ( $\Delta G^\circ$ ) was determined from  $K_A$  according to the following relationship:

$$\Delta G^\circ = -R \cdot T \cdot \ln(K_A) \quad (2.16)$$

where  $R$  and  $T$  are the gas constant and the absolute temperature, respectively. The enthalpy variation ( $\Delta H^\circ$ ) was estimated from the  $K_A$  values at different temperatures between 10 and 37°C according to the van't Hoff relationship shown in eq. 2.17.

$$\ln(K_A) = -\left(\frac{\Delta H^\circ}{R \cdot T}\right) + \left(\frac{\Delta S^\circ}{R}\right) \quad (2.17)$$

The  $\ln(K_A)$  values were therefore plotted against  $1/T$  and  $\Delta H^\circ$  was determined from the slope (eq. 2.17) by linear regression. To determine the entropy variation ( $\Delta S^\circ$ ), the respective value was back extrapolated for each  $\ln(K_A)$  with the determined  $\Delta H^\circ$  according to eq. 2.17 and the resulting values were averaged.

## 2.8 Kinetics of complex formation

The fast kinetics of the OHNA/Tb(III) complex formation were investigated with an Applied Photophysics SX.18MV stopped-flow instrument. Equal volumes of Tb(III) between 40 and 400  $\mu\text{M}$  and 2  $\mu\text{M}$  OHNA both in MOPS or TRIS pH 6.5 were mixed at 25 °C and the luminescence was monitored without time delay at  $\lambda_{ex}$  305 nm and  $\lambda_{em} \geq 400$  nm.

## 2.9 Permeation Kinetics

The kinetics of OHNA permeation into Tb(III)-containing liposomes were determined according to Thomae et al. [2005] on a Perkin Elmer spectrofluorimeter LS50B equipped with a Hi-tech Scientific SFA-20 Stopped Flow device. Tb(III)-containing liposomes were diluted in MOPS or TRIS at pH 2.5 or 6.5 at temperatures between 5 and 50°C. The final lipid concentration was  $\sim 1$  mg/ml, with a local Tb(III) concentration of  $\sim 4$  mM and a final OHNA concentration of 20  $\mu\text{M}$ . Under these conditions the kinetics were independent of the OHNA and lipid concentrations. Control experiments of OHNA permeation in TRIS 0.1 M/KCl 0.1M pH 6.5 were performed using Tb/(III)-containing liposomes including 0.1mg/ml of valinomycin. The liposomes were prepared adding 2  $\mu\text{l}$  of a methanol solution of valinomycin to reach a final concentration of 0.1mg/ml before the extrusion. The controls with and without valinomycin revealed similar results, excluding a kinetic limited permeation of OHNA due to the low proton concentration at pH 6.5. The luminescence of the Tb(III)/OHNA complex ( $\lambda_{ex}$  305 nm,  $\lambda_{em}$  545 nm) was monitored over time with a time delay of 0.05ms, a gate time of 1ms, a cycle time of 20 ms and at 1 flash per cycle. The resulting kinetic curves  $\Delta L = f(t)$  were fitted with a mono-exponential function eq. 2.18 or with a linear combination of two exponential functions to get the rate constants  $k_{p1}$  and  $k_{p2}$  eq. 2.19

$$\Delta L(t) = \Delta L(0) + \Delta L_{Max1} \cdot e^{-k_{p1} \cdot t} \quad (2.18)$$

$$\Delta L(t) = \Delta L(0) + \Delta L_{Max1} \cdot e^{-k_{p1} \cdot t} + \Delta L_{Max2} \cdot e^{-k_{p2} \cdot t} \quad (2.19)$$

The fitted values  $L_{max}$  correspond to the plateau values of the exponential functions. Most kinetics were determined with liposomes of 200 nm diameter. In the series with MOPS and TRIS pH 6.5, some experiments were performed with liposomes of 400 nm diameter. These experiments are equally distributed over the investigated temperature range. In order to generate size-independent kinetic parameters, apparent permeation coefficients  $Perm_{app}$

were calculated from the rate constants  $k_p$  and the liposomal radius  $r$  as follows (eq. 2.20 and eq. 2.21, [Thomae et al., 2005]):

$$Perm_{app1} = k_{p1} \cdot \frac{r}{3} \quad (2.20)$$

$$Perm_{app2} = k_{p2} \cdot \frac{r}{3} \quad (2.21)$$

were  $r/3$  is used as an approximation for the ratio between the total inner aqueous volume of the liposomes and the total membrane area [Paula et al., 1998]. The radius  $r$  was estimated from the hydrodynamic mean diameter of the liposomes. Replacing  $k_p$  by  $Perm_{app}$  reveals permeation kinetics which are independent of the liposome diameter.

The temperature dependence of the fast and slow  $Perm_{app}$  values were in good agreement with Eyring's equation (eq. 2.22).

$$\ln\left(\frac{Perm_{app1}}{T}\right) = \ln\left(\frac{k_b}{h}\right) + \ln\left(\frac{r}{3}\right) + \frac{\Delta S^\ddagger}{R} - \frac{\Delta H^\ddagger}{R \cdot T} \quad (2.22)$$

where  $R$ ,  $T$ ,  $k_b$  and  $h$  are the gas constant, temperature in Kelvin, Boltzmann constant and Planck's constant, respectively.  $\Delta H^\ddagger$  is the enthalpy of activation change and  $\Delta S^\ddagger$  is the entropy of activation change. The term  $\ln(r/3)$  is the correction term for the use of  $Perm_{app}$  instead of  $k$  in the Eyring equation.

According to the Eyring diagram  $\ln(Perm_{app}/T)$  was plotted vs.  $1/T$  resulting in a straight line with the slope  $-\Delta H^\ddagger/R$  (eq. 2.22). The term  $\Delta S^\ddagger/R$  was back extrapolated for each experimental  $Perm_{app}$  using the average of the received slope from the linear regression and calculating the term  $\ln(k_b/h) + \ln(r/3)$  setting a liposome radius of 100 nm.

The Gibbs free energy of activation,  $\Delta G^\ddagger$ , and the activation energy,  $E_a$ , were obtained from eq. 2.23 and eq. 2.24:

$$\Delta G^\ddagger = \Delta H^\ddagger - T \cdot \Delta S^\ddagger \quad (2.23)$$

$$E_a = \Delta H^\ddagger + R \cdot T \quad (2.24)$$



# 3 Results

## 3.1 Characterization of the model membranes

### 3.1.1 Lipid composition and membrane fluidity

The bilayer fluidity of liposome membranes was tested by fluorescence anisotropy measurements as described in Sec. 2.2. Liposomes of varying lipid composition were analyzed and anisotropy values were calculated according to eq. 2.1. Anisotropy values at 37°C are shown in Fig. 3.1. Table 3.1 summarizes the anisotropy values at different temperatures and the transition temperature ( $T_m$ ) for the membranes.

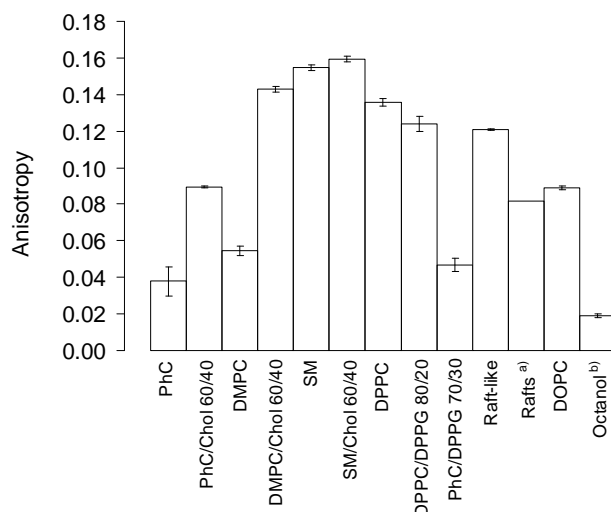


Fig. 3.1: **Membrane fluidity.** Anisotropy was calculated from DPH fluorescence polarization. Experiments were performed at 37°C, the bars represent the means of 3 experiments each with standard deviations. Lipid compositions according Tab. 1.4. <sup>a)</sup> Rafts preparation according to sec. 2.2. <sup>b)</sup> The anisotropy of octanol was measured at 22°C adding DPH to a water-saturated octanol solution.

### 3 Results

The anisotropy values at 37°C indicate higher fluidity for the lipid bilayers in their *ld* phase i.e. PhC, DMPC and DOPC than in *lo* or *so* phase. Increasing the acyl chain length of the phospholipids, e.g. from DMPC (14 carbons) to DPPC (16 carbons) (Fig. 1.5), the transition temperature increases, however, the fluidity of the bilayers below the  $T_m$  is not influenced. Increasing the number of insaturations, e.g. from DPPC (saturated chain) to DOPC (1 insaturation), the transition temperature substantially decreases. The fluidity of DOPC bilayers above the  $T_m$  appears to be lower than the *ld* phase of DMPC (shorter chain) and PhC liposomes which consist of a mixture of different phosphocholine lipids mainly constituted of 18:1 and 16:0 acyl chains. Cholesterol generally enhanced the anisotropy, indicating a reduction in fluidity of the lipid bilayers. Its influence is more significant for *ld* membranes suggesting the formation of the more geometrical ordered *lo* phase.

<i>Lipid composition</i>	$T_{exp}(^{\circ}C)$	$T_m(^{\circ}C)$	<i>Anisotropy</i>
PhC	37	-5 <sup>a)</sup>	0.038 ± 0.008
PhC	22	-5 <sup>a)</sup>	0.051 ± 0.002
PhC/Chol 60/40	37		0.089 ± 0.001
DMPC	37	23 <sup>b)</sup>	0.054 ± 0.003
DMPC	4	23 <sup>b)</sup>	0.153 ± 0.001
DMPC/Chol 60/40	37		0.142 ± 0.002
SM	37	41.4 <sup>b)</sup>	0.155 ± 0.002
SM	4	41.4 <sup>b)</sup>	0.156 ± 0.003
SM/Chol 60/40	37		0.159 ± 0.002
DPPC	37	41.5 <sup>b)</sup>	0.136 ± 0.004
DPPC/DPPG 80/20	37		0.124 ± 0.002
PhC/DPPG 70/30	37		0.047 ± 0.004
Raft-like	37		0.121 ± 0.001
Rafts <sup>c)</sup>	37		0.082 ± 0.003
DOPC	37	-21 <sup>b)</sup>	0.089 ± 0.001
Octanol	22		0.019 ± 0.001

Table 3.1: **Membrane fluidity.** The anisotropy values are the mean of 3 independent experiments with the standard deviation. Octanol anisotropy was measured at 22°C adding DPH to a water-saturated octanol solution. Lipid compositions according Tab. 1.4. <sup>a)</sup> [Huang and Mason, 1978]; <sup>b)</sup> [Marsh et al., 1990]. <sup>c)</sup> Rafts preparation according to sec. 2.2.  $T_{exp}$ , temperature in experiments.

The lipid content of liposome preparations was determined by HPLC (Sec.2.2). Figure 3.2 shows two typical chromatograms of a mixture of PhC/DPPC and PhC/cholesterol. The chromatogram of egg PhC shows several peaks indicating a variety of acyl chains.

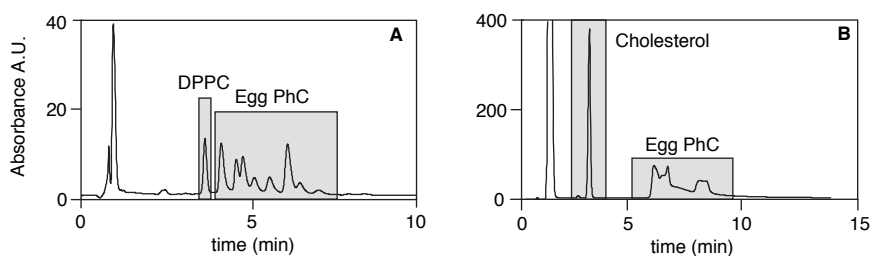


Fig. 3.2: **Lipid quantification by HPLC.** Chromatograms of (A) a mixture of PhC/DPPC and (B) PhC/cholesterol. The eluent was (A) acetonitrile:trifluoroacetic acid:water 86.9:0.1:13, (B) acetonitrile:water 87:13.

### 3.1.2 Zetapotentials of liposomes

The zetapotential measurements of the liposomes were performed as described in sec. 2.2. Negatively charged liposomes revealed increased absolute values with increasing pH. This was assigned to an increase in the surface charge density according to the pH-dependence of the protonation/deprotonation equilibria of PhS, PhI, PhE or DPPG [Kramer et al., 1997, 1998, Sacre and Tocanne, 1977]. Results are summarized in Tab. 3.2

<i>Lipid composition</i>	<i>Zetapotential (mV) in the pH range 4 to 10</i>
PhC	$3 \pm 4$ , pH independent
DMPC	$3 \pm 4$ , pH independent
DPPC	$3 \pm 4$ , pH independent
DOPC	$3 \pm 4$ , pH independent
SM	$3 \pm 4$ , pH independent
DMPC/Chol 60/40	$3 \pm 4$ , pH independent
SM/Chol 60/40	$3 \pm 4$ , pH independent
DOPC/Chol 60/40	$3 \pm 4$ , pH independent
PhC/PhS 70/30	-24 (pH 4) to -36 (pH 10)
DPPC/DPPG 80/20	-12 (pH 4) to -24 (pH 10)
PhC/DPPG 70/30	-14 (pH 4) to -26 (pH 10)
DMPC/Chol/DMPG 30/40/30	-14 (pH 4) to -26 (pH 10)
Raft-like	$-10 \pm 6$ (pH 6-9) to -32 (pH 10)
BLES	-16 (pH 4) to -26 (pH 10)

Table 3.2: **Zetapotentials of the investigated liposomes.** Lipid compositions according Tab. 1.4.

## 3.2 Octanol partitioning

The partitioning behaviour of indacaterol and salmeterol in the octanol/buffer system was examined between pH 4 and 13. The concentration was between 7.2 and 21.5  $\mu\text{M}$  for indacaterol and salmeterol and between 80 and 330  $\mu\text{M}$  for propranolol. The resulting  $D$ -pH diagrams are bell-shaped for indacaterol and salmeterol (Fig.3.3). For indacaterol,  $D$  was highest i.e. 6500 at pH 8.2, decreasing to around 10 at pH 13 and 100 at pH 4. For salmeterol  $D$  was highest, i.e. 1250, at pH 10, decreasing to around 100 at pH 4 and around 40 at pH 13. In order to describe the  $D$ -pH diagram quantitatively we used a combination of Henderson-Hasselbach equations (eq. 2.3). To fit the curves the inflection points (" $pK_a$ " in eq. 2.3) were kept variable resulting in the following inflection points:  $\text{pH}_1$  7.6,  $\text{pH}_2$  8.9 and  $\text{pH}_1$  8.6,  $\text{pH}_2$  11.4 for indacaterol and salmeterol, respectively. The results are summarized in Tab. 3.3. The net neutral species had the highest affinity for octanol, i.e.  $P_N$  7720 and  $P_N$  1692 for indacaterol and salmeterol, respectively. The partition coefficients for the cation and anion were  $P_C$  164 and  $P_A$  15 for indacaterol and  $P_C$  152, for salmeterol. Control experiments were performed with propranolol, results are shown in Fig. 3.3.

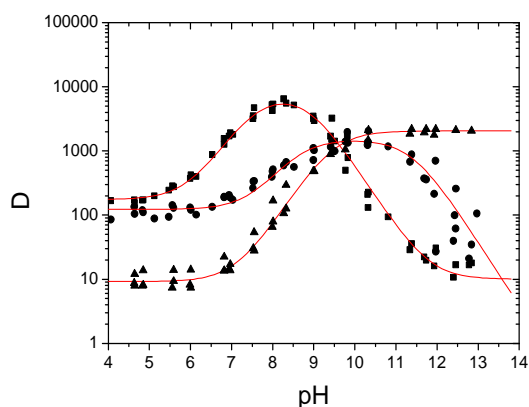


Fig. 3.3: **Distribution profiles of indacaterol, salmeterol and propranolol in the octanol/buffer system.** pH-Distribution profiles of indacaterol (■), salmeterol (●) and propranolol (▲). The experiments were fitted with eq. 2.3. The fitted partition coefficients  $P$  and the inflection points ( $\text{pH}_1$ ,  $\text{pH}_2$ ) are shown in Tab. 3.3.

### 3.3 Drug/membrane affinities by equilibrium dialysis

Equilibrium dialysis experiments were carried out with liposomes of different lipid compositions at 4°C, 25°C or 37°C as described under Materials and Methods. Liposomes of the compositions shown in Tab. 1.4 were prepared by extrusion as described in Sec. 2.2 and diluted in SUBS at pH values between 6.0 and 10.5.  $D$  was calculated according to eq. 2.2. In order to describe the  $D$ -pH diagram quantitatively we used a combination of Henderson-Hasselbach equations (eq. 2.3). To fit the liposomes partition data the inflection points (pH) of the drugs were kept variable. The fitted values of  $P$  and the inflection points are reported in Tab. 3.3.

Equilibrium dialysis experiments with PhC liposomes ( $T_m -5^\circ\text{C}$ ) at 22°C revealed a similar pH-partition profile for indacaterol and salmeterol characterized by the highest affinity for membranes of the cations (Fig. 3.4). Interestingly the pH partition profiles in liposomes substantially differed from the profiles in octanol (Fig. 3.3). The resulting  $D$ -pH diagrams in PhC liposomes are not bell-shaped neither for indacaterol nor for salmeterol. For indacaterol,  $D$  was highest i.e. around 4500 between pH 6.0 and 8.0, decreasing to around 1000 at pH 10.5 and 100 at pH 4.0. For salmeterol  $D$  was highest, i.e. 3500, between pH 6.0 and 7.5, decreasing to around 1700 at pH 10.5. Control experiments were performed with propranolol, results are shown in Fig. 3.4.

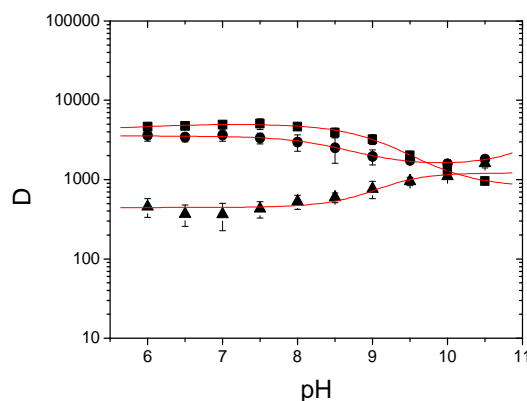


Fig. 3.4: **Distribution profiles of indacaterol, salmeterol and propranolol in PhC liposomes.** pH-Distribution profiles of indacaterol (■), salmeterol (●) and propranolol (▲) with PhC liposomes at 22°C. The experiments were fitted with eq. 2.3. The fitted values of  $P$  and the inflection points are reported in Tab. 3.3.

### 3 Results

#### *Influence of the order of lipid bilayer*

In order to better understand the differences between the pH-partitioning profiles in octanol and in PhC liposomes, experiments with more geometrically ordered membranes, i.e. DPPC, DMPC and DMPC/Chol 60/40 liposomes, were performed. Liposomes above and below the transition temperature ( $T_m$ ) were considered in the *ld* phase and in the *so* phase (sec. 1.3), respectively. Addition of cholesterol (>30 mol%) generated a more geometrical ordered phase, i.e. a *lo* phase [Lasic, 1993].

Equilibrium dialysis experiments with DPPC liposomes ( $T_m$  41.5°C ) at 37°C revealed a higher affinity (within a factor of 2) for the membrane of indacaterol, i.e. around 1700, than salmeterol, i.e. around 700. The partitioning was pH-independent for both agonists. Results are shown in Fig. 3.5.

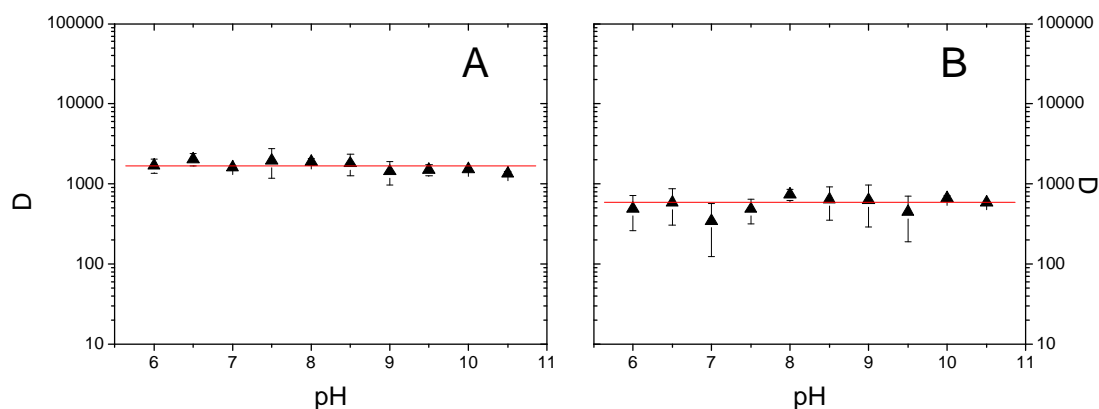


**Fig. 3.5: Distribution profiles of indacaterol and salmeterol in DPPC liposomes.** pH-Distribution profiles of indacaterol (A) and salmeterol (B) with DPPC liposomes at 37°C ( $\blacktriangle$ ). The experiments were fitted with eq. 2.3. The fitted values of  $P$  and the inflection points are reported in Tab. 3.3.

Equilibrium dialysis experiments performed with liposomes containing DMPC ( $T_m$  23°C) at 37°C, DMPC/Chol 60/40 at 37°C and DMPC at 4°C for the *ld*, *lo* and *so* membranes, respectively [Pokorny et al., 2000], showed similar behavior of the agonists (Fig. 3.6). The pH-partitioning profiles were characterized by highest affinity of their positively ionized species for the *ld* and *so* membranes. The experiments, between pH 6.0 and 8.0, revealed  $D$  values around 4000 and 2000 for indacaterol (Fig. 3.6 A) and around 5000 and 3000 for salmeterol (Fig. 3.6 B), for *ld* and *so* phases, respectively. The membrane affinity was lowest at pH 10.5,  $D$  was around 500 and 300 for indacaterol and around 1000 and 200 for salmeterol, for *ld* and *so* phases, respectively.

Interestingly the partitioning was pH-independent in the presence of high levels of cholesterol,

i.e. *lo* membranes rather than *so* membranes (Fig. 3.6), conversely the affinity was pH independent with DPPC liposomes in the *so* phase (Fig. 3.5).

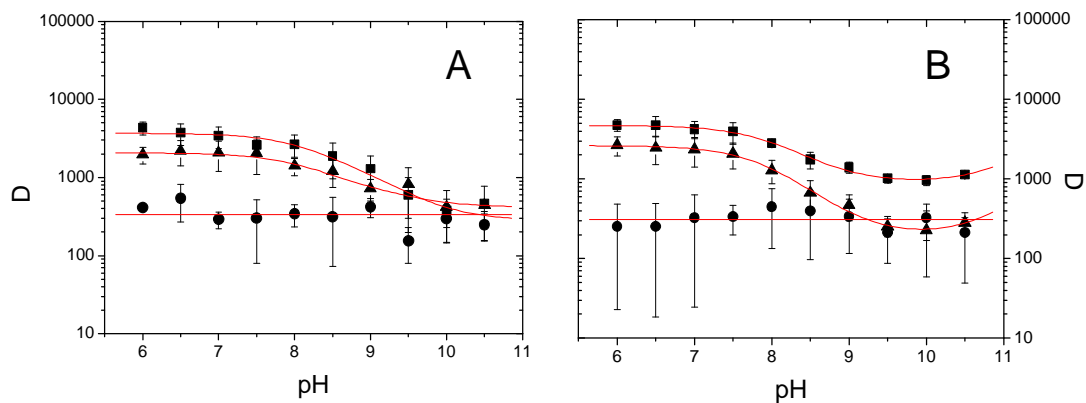


Fig. 3.6: **Distribution profiles of indacaterol and salmeterol in DMPC and DMPC/Chol liposomes.** pH-Distribution profiles of indacaterol (A) and salmeterol (B) with DMPC liposomes at 37°C (■) or 4°C (▲) and DMPC/Chol 60/40 liposomes at 37°C (●). The experiments were fitted with eq. 2.3. The fitted values of  $P$  and the inflection points are reported in Tab. 3.3.

### 3 Results

#### *Influence of the phospholipid charges*

In order to better differentiate the interactions of indacaterol and salmeterol with the lipid bilayers and to investigate the influence of negatively charged lipids several different lipid compositions were used: for the *ld* phase, liposomes containing PhC/PhS 70/30 and PhC/DPPG 70/30 at 25°C; for the *so* phase, DPPC/DPPG 80/20 liposomes at 22°C and for the *lo* phases, DMPC/Chol/DMPG 30/40/30 liposomes at 37°C. Results are shown in Fig. 3.7.

For both compounds the partition coefficients were highest with the negatively charged *ld* membranes between pH 6.0 and 7.5, i.e. around 40000 and 36000 with PhC/DPPG liposomes and around 17000 and 10000 with PhC/PhS liposomes, for indacaterol and salmeterol, respectively (Fig. 3.7). The membrane affinity decreased, at pH 10.5, to around 1000 and 3000 with PhC/DPPG and to around 300 and 2000 with PhC/PhS, for indacaterol and salmeterol, respectively (Fig. 3.7).

The presence of cholesterol dramatically reduced the affinity of the drugs for the membrane (Fig. 3.7). In contrast to the above described lipid compositions, the pH-partition profiles were bell-shaped in the *so* membrane containing DPPC/DPPG indicating highest affinity of the net neutral species. For indacaterol  $D$  was highest, i.e. around 4000, at pH 8.2, decreasing to around 1000 at pH 6.0 and pH 10.5. For salmeterol  $D$  was highest, i.e. around 2000, between pH 9.0 and 10, decreasing to around 1000 at pH 6.0.

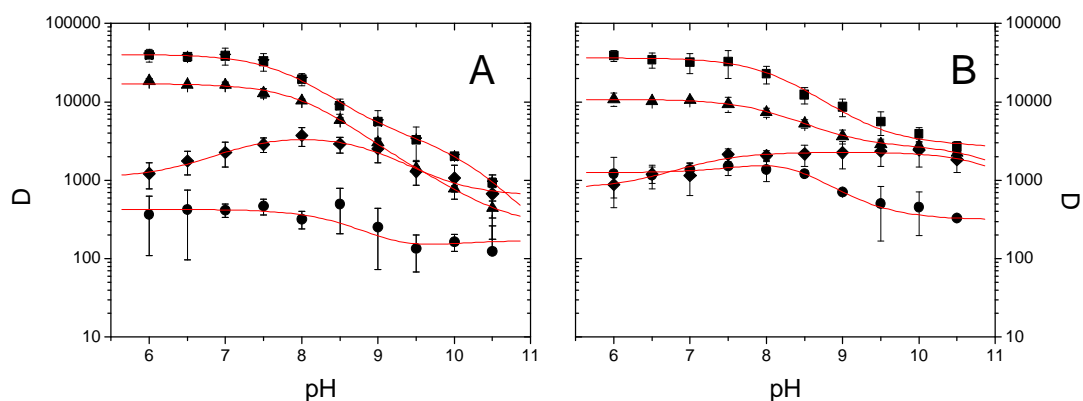


**Fig. 3.7: Distribution profiles of indacaterol and salmeterol in negatively charged liposomes.** pH-Distribution profiles of indacaterol (A) and salmeterol (B) with PhC/DPPG 70/30 liposomes at 25°C (■) PhC/PhS 70/30 liposomes at 37°C (▲), DPPC/DPPG 80/20 liposomes at 25°C (◆) and DMPC/Chol/DMPG 30/40/30 liposomes at 37°C (●). The experiments were fitted with eq. 2.3. The fitted values of  $P$  and the inflection points are reported in Tab. 3.3.



#### *Influence of the acyl-chain insaturations*

To further investigate the influence of the membrane properties on the partitioning, experiments with DOPC liposomes ( $T_m$   $-21^\circ\text{C}$ ), at  $37^\circ\text{C}$ , were performed (Fig. 3.8). The results revealed a considerable influence of the insaturations in the acyl-chain region of the phospholipids on the drug partitioning, largely increasing the affinity of the agonists as clearly shown by the comparison of the the pH-distribution profiles with DPPC (Fig. 3.5) and DMPC (Fig. 3.6). However, the  $D$ -pH-partition profiles in the DOPC liposome system were similar for indacaterol and salmeterol, as shown in Fig. 3.8.  $D$  values ranged from around 30000 at pH 6.0 to around 10000 at pH 10.5. The presence of cholesterol reduced the affinity (factor  $\leq 2$ ) of both agonists, however, the pH-dependence was not affected.

#### *Influence of the Hydrogen-bonding groups*

In order to shed light on the influence of H-bonding groups, investigations with SM liposomes ( $T_m$   $41.4^\circ\text{C}$ ) at  $37^\circ\text{C}$  were performed. The results revealed a bell-shaped pH-partition profile for indacaterol,  $D$  was highest, i.e. around 4000, at pH 8.2, decreasing to around 900 at pH 6.0 and pH 10.5. The affinity of salmeterol was highest, i.e. around 5000, between pH 8.0 and 10.5, decreasing to around 2000 at pH 6.0 (Fig. 3.9). The presence of cholesterol decreased the affinity of indacaterol and salmeterol to SM membranes, interestingly, the partitioning was not dependent on pH (Fig. 3.9).

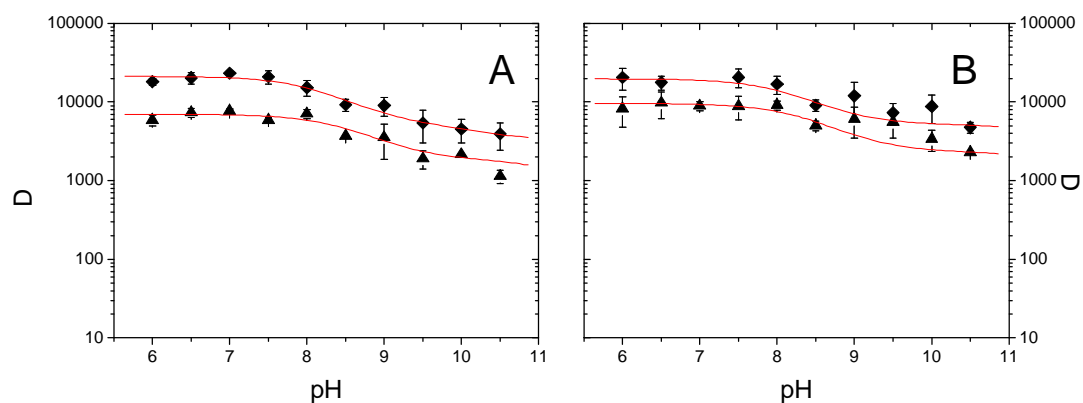


Fig. 3.8: **Distribution profiles of indacaterol and salmeterol in DOPC and DOPC/Chol liposomes.** pH-Distribution profiles of indacaterol (A) and salmeterol (B) with DOPC liposomes at 37°C (◆) and DOPC/Chol 60/40 liposomes at 37°C (▲). The experiments were fitted with eq. 2.3. The fitted values of  $P$  and the inflection points are reported in Tab. 3.3.

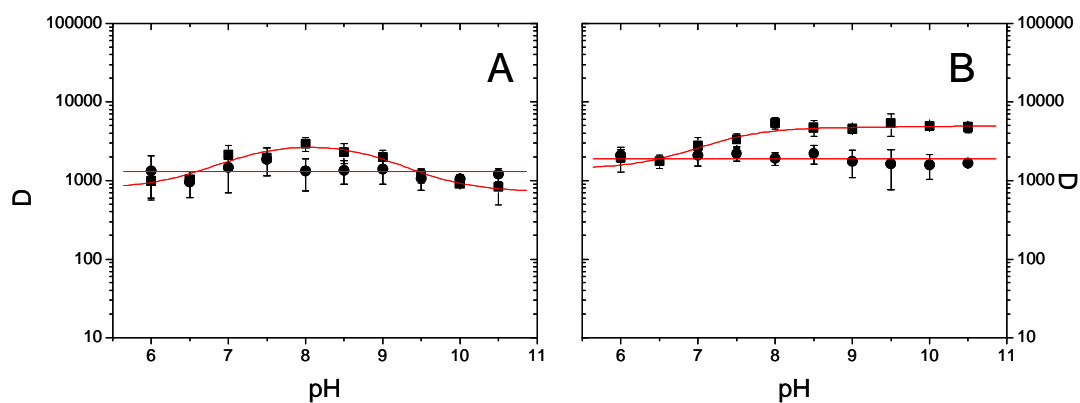


Fig. 3.9: **Distribution profiles of indacaterol and salmeterol in SM and SM/Chol liposomes.** pH-Distribution profiles of indacaterol (A) and salmeterol (B) with SM liposomes at 37°C (■) and SM/Chol 60/40 liposomes at 37°C (●). The experiments were fitted with eq. 2.3. The fitted partition coefficients  $P$  are shown in Tab. 3.3.

*Partitioning with BLES liposomes and rafts*

Additional equilibrium dialysis experiments were performed with lipid compositions reflecting the biological composition of the lung surfactant and of the raft domains of cellular membranes.

The experiments with BLES liposomes revealed similar pH-partition profiles for indacaterol and salmeterol. The affinity was highest, i.e. around 10000, between pH 6.0 and 7.5, decreasing to around 1700, at pH 10.5, for both agonists (Fig. 3.10).

Experiments with the raft-like liposomes (Tab. 1.4) are shown in Fig. 3.10. The affinity in the liposomal system was similar for the agonists, i.e. around 900. Interestingly, it was independent of the pH in the range under investigation.

The affinity of the agonists to rafts extracted from P388 or P388/ADR cells revealed a higher affinity of indacaterol, i.e.  $10473 \pm 731$ , than of salmeterol, i.e.  $4527 \pm 1426$ , at pH 7,4 and 37°C (results are given as means with standard deviation of three independent experiments).

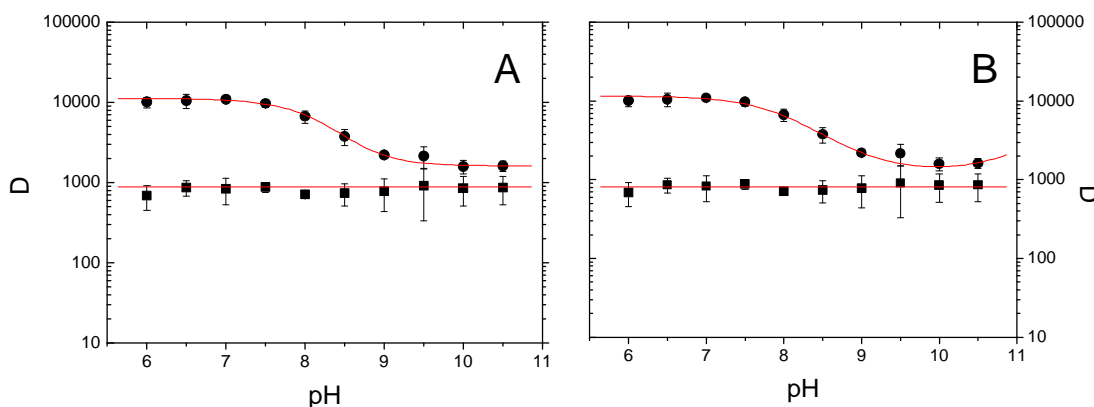


Fig. 3.10: **Distribution profiles of indacaterol and salmeterol in BLES and raft-like liposomes.** pH-Distribution profiles of indacaterol (A) and salmeterol (B) with raft-like liposomes (Tab. 1.4) at 37°C (■) and BLES liposomes at 37°C (●). The experiments were fitted with eq. 2.3. The fitted values of P and the inflection points are reported in Tab. 3.3.

Lipid composition	$T_{exp}$ (°C)	inflection points (pH)	indacaterol			salmeterol			
			$P_C$	$P_N$	$P_A$	inflection points (pH)	$P_C$	$P_N$	$P_A$
DMPC	37	8.2/9.2	3647±296	1183±1079	281±180	8.0/12.6	4710±213	880±64	<sup>c)</sup>
DMPC	4	8.2/9.4	2061±132	710±942	415±74	8.0/12.4	2628±54	196±64	<sup>c)</sup>
DMPC/Chol	37	<sup>a)</sup>	332±106	332±106	332±106	<sup>a)</sup>	310±77	310±77	310±77
PhC	22	6.3/9.1	4424±1114	5057±235	865±226	8.5/12.4	3545±74	1480±122	<sup>c)</sup>
DPPC	22	<sup>a)</sup>	1680±233	1680±233	1680±233	<sup>a)</sup>	560±17	560±17	560±17
PhC/Phs	22	8.1/9.8	17001±294	1386±742	257±167	8.2/11.2	10758±148	2643±511	<sup>c)</sup>
DPPC/DPPG	22	7.1/9.0	1079±206	3879±446	631±176	7.0/11.2	786±180	2297±186	<sup>c)</sup>
DMPC/Chol/DMPG	37	8.6/9.6	427±44	108±147	171±150	8.2/8.3	1294±93	2567±526	315±2
PhC/DPPG	22	7.8/10.0	40456±1649	3527±1414	<sup>c)</sup>	8.2/ <sup>b)</sup>	36537±2602	2878±738	<sup>c)</sup>
SM	37	7.1/9.0	787±376	3104±576	719±275	<sup>a)</sup>	1389±426	4768±620	<sup>c)</sup>
SM/Chol	37	<sup>a)</sup>	1299±261	1299±261	1299±261	<sup>a)</sup>	1901±250	1901±250	1901±250
DOPC	37	8.3/10.1	21253±1453	5333±9280	3255±1026	8.2/ <sup>b)</sup>	19776±2682	5162±2281	<sup>c)</sup>
DOPC/Chol	37	8.6/ <sup>b)</sup>	7006±594	1839±6642	<sup>c)</sup>	8.2/ <sup>b)</sup>	9588±1092	2325±126	<sup>c)</sup>
BLES	37	8.1/8.5	11239±466	2789±4645	1608±106	8.1/8.5	11239±466	2789±4645	1608±106
Raft-like	37	<sup>a)</sup>	890±76	890±76	890±76	<sup>a)</sup>	809±86	809±86	809±86
Octanol	22	7.6/8.9	164±97	7720±528	15±101	8.9/11.3	152±34	1692±103	<sup>c)</sup>

Table 3.3: Membrane affinity parameters of indacaterol and salmeterol in different liposomal systems.  $P_A$ ,  $P_N$  and  $P_C$  are the partition coefficients for the cationic, net neutral and anionic species respectively. Fitted values ± estimated standard errors are shown. Lipid compositions according Tab. 1.4. <sup>a)</sup> no inflection points detectable; <sup>b)</sup> no second inflection point detectable; <sup>c)</sup> outside experimental pH range.

<i>Lipid composition</i>	$T_{exp}$ (°C)	<i>indacaterol</i>		<i>salmeterol</i>	
		$D^{pH7.4}$	$\log D^{pH7.4}$	$D^{pH7.4}$	$\log D^{pH7.4}$
DMPC	37	3306 ±605	3.52±0.64	4009 ±116	3.60±0.10
DMPC	4	1861 ±238	3.27±0.42	2109 ±89	3.32±0.14
DMPC/Chol	37	332±106	2.52±0.80	360±77	2.56±0.55
PhC	22	4924 ±166	3.69±0.12	3406 ±29	3.53±0.03
DPPC	22	1680 ±233	3.23±0.45	560±17	2.75±0.08
PhC/PhS	22	14648±1117	4.17±0.32	9681 ±212	3.99±0.09
DPPC/DPPG	22	2845 ±128	3.45±0.16	1818 ±228	3.26±0.41
DMPC/Chol/DMPG	37	409±63	2.61±0.40	1409 ±74	3.15±0.17
PhC/DPPG	22	30971± 4116	4.49±0.60	32122±1748	4.51±0.25
SM	37	2232 ±424	3.35±0.64	3324 ±222	3.52±0.24
SM/Chol	37	1299 ±261	3.11± 0.63	1901 ±250	3.28±0.43
DOPC	37	16156± 2387	4.21±0.62	17785±3516	4.25±0.84
DOPC/Chol	37	6686 ±675	3.83±0.39	8975 ±117	3.95±0.05
BLES	37	9887 ±185	4.00±0.07	9622 ±551	3.98±0.23
Raft-like	37	890±76	2.95±0.25	809±76	2.91±0.27
Rafts <sup>a)</sup>	37	10473±731	4.02±0.28	4527 ±1426	3.66±0.10
Octanol	22	3226 ±101	3.51±0.11	201±47	2.30±0.54

Table 3.4:  $D$  and  $\log D$  values of indacaterol and salmeterol with diverse liposomal systems, rafts and octanol at pH 7.4. Fitted values ± estimated standard errors are shown. Lipid compositions according Tab. 1.4. <sup>a)</sup> Rafts preparation according to sec. 2.2.

### 3 Results

---

Differences in the pH-partition profiles were highest for the DPPG/DPPG and SM liposomal systems. As already mentioned above, in such a systems the net neutral species revealed highest affinity for the membrane. Comparing their affinity values at physiological pH (Tab. 3.4), indacaterol showed a three folds higher affinity than salmeterol for the DPPC/DPPG partitioning systems. Contrarily salmeterol revealed a three folds higher affinity than indacaterol, at pH 7.4, for the DPPC/Chol/DPPG liposomal system. The experiments with rafts extract revealed a two folds higher affinity of indacaterol than of salmeterol. Interestingly, at pH 7.4, indacaterol revealed a 10 folds higher affinity than salmeterol in the octanol/buffer system.

## 3.4 Investigation of the drug/membrane interactions by SPR

### 3.4.1 Determination of drug/membrane affinity by SPR

The interaction of propranolol, salmeterol and indacaterol with PhC liposomes in SUBS pH 7.2 was investigated by SPR at different drug concentrations as described under Material and Methods. Representative sensograms are shown in Fig. 3.11.

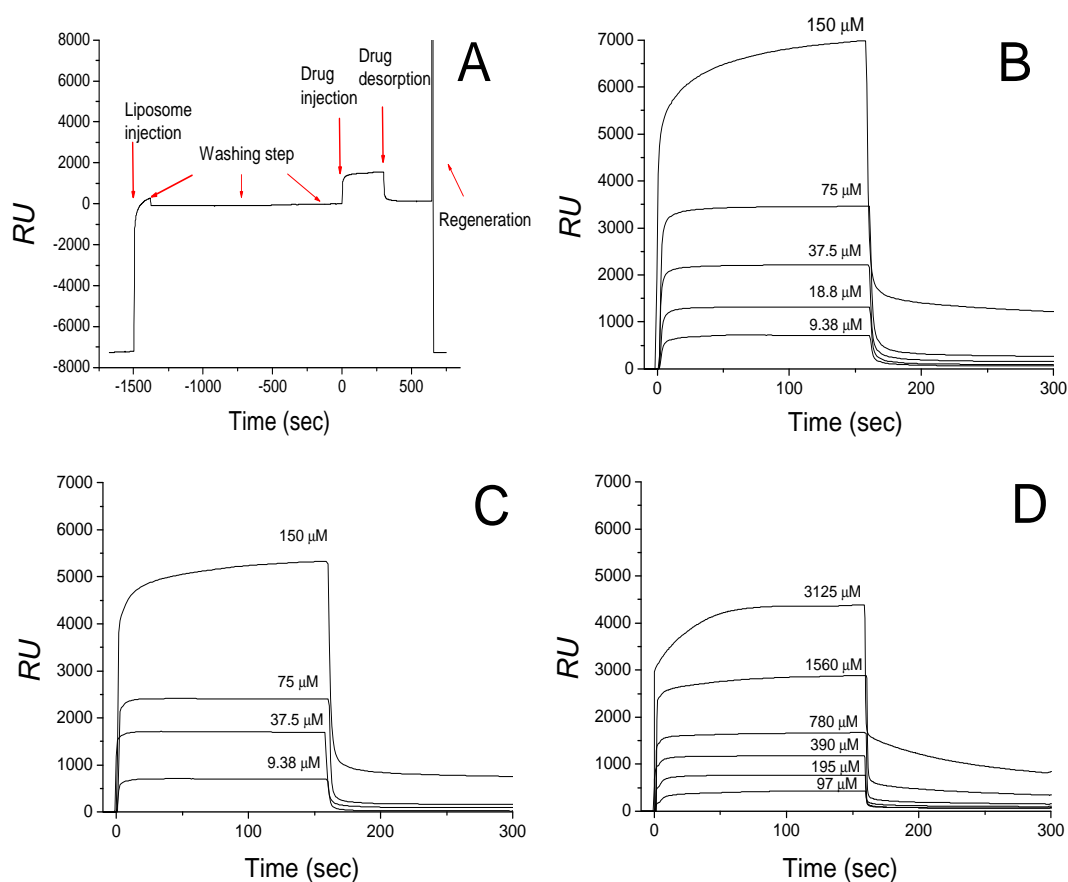


Fig. 3.11: SPR sensograms of the PhC liposomes adsorption on the L1 chip and of the interactions of indacaterol, salmeterol and propranolol with PhC liposomes at pH 7.2. Adsorption of PhC liposomes to the Biacore L1 chip and drug injection (A). Sensograms recorded with L1 chip covered with PhC liposomes ( $RU$  0) injecting indacaterol (B) salmeterol (C) propranolol (D) at different concentrations for 160 s in SUBS pH 7.2 containing 5 % DMSO. After 160 s drug-free buffer was flown through the cells.

The  $RU_{scaled}$  values, calculated according to eq. 2.6, were plotted against the drug concentrations as shown in Fig. 3.12. As expected, the data followed saturation functions and were

thus fitted with a single binding site isotherm. Including all investigated drug concentrations in the fit,  $K_D$  were  $(1.9 \pm 0.4) \cdot 10^{-3}$  M,  $(0.39 \pm 0.17) \cdot 10^{-3}$  M and  $(0.40 \pm 0.18) \cdot 10^{-3}$  M for propranolol, salmeterol and indacaterol, respectively. As high drug/lipid ratios within the bilayer may affect the membrane characteristics and therefore lead to erroneous results, the data were in addition fitted omitting the highest drug concentrations. The fitted  $K_D$  values decreased strikingly when the concentration range was reduced Fig. 3.12. Considering propranolol concentrations up to 500  $\mu$ M, the fitted  $K_D$  was  $(0.22 \pm 0.17) \cdot 10^{-3}$  M. Similar values, i.e.  $0.19 \cdot 10^{-3}$  M and  $0.31 \cdot 10^{-3}$  M, depending on the buffer system, have previously been determined by SPR for propranolol with di-oleoyl-phosphatidylcholine liposomes at the same pH and in the same concentration range [Abdiche and Myszkka, 2004].

At the highest concentrations of drugs, dissociation was not completed after within the measuring time (Fig. 3.12). A similar observation was made for compounds with relatively high membrane affinities, in particular cationic amphiphilic drugs, by [Abdiche and Myszkka, 2004]. Correction of the plateau values for the offset from zero after a 150 s dissociation phase resulted in a reduction of the fitted  $K_D$  values as shown in Fig. 3.12. The propranolol data were in addition fitted with a function considering two binding sites (sum of two binding isotherms, eq. 2.6) to take into account possible adsorption of the drug to the chip surface. As expected, the fit improved. The  $K_D$  values corresponding to the high affinity binding site were below those shown in Fig. 3.11 for the fits with the three lowest concentrations. However, they varied strikingly between the single experiments. The low affinity  $K_D$  values were even more variable, ranging from 4 mM to a few molar.

#### 3.4.2 Kinetic studies by SPR

To measure the kinetics of the interactions of the different ionic species of salmeterol and indacaterol with PhC bilayers, the liposomes were immobilized on a Biacore L1 sensor chip and binding kinetics were recorded between pH 5.0 and 10.0. As kinetic studies require an excess of lipids over solute to assure 1<sup>st</sup> order reactions, drug concentrations need to be at least 10 times lower than the estimated lipid amount per chamber volume, i.e. 1.0 to 1.5 mM (see Sec. 2.6). At concentrations  $<100 \mu$ M only salmeterol and indacaterol revealed analyzable sensograms. Kinetics were thus analysed at 60  $\mu$ M. The adsorption and desorption phases of indacaterol followed bi-exponential functions in the pH range under investigation, for salmeterol they were bi-exponential up to pH 8.6 and mono or bi-exponential functions at the higher pH values (Fig. 3.13).



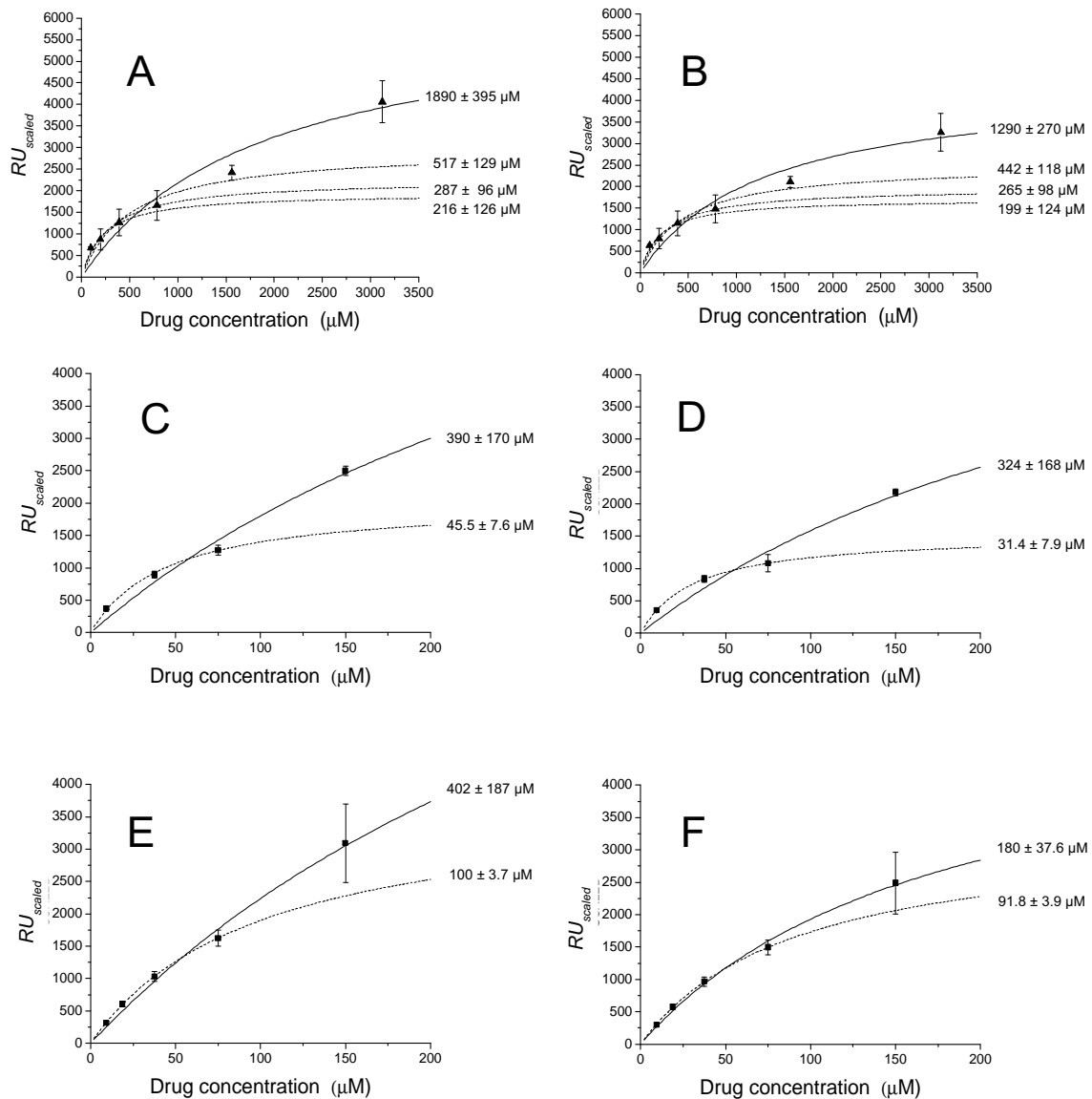


Fig. 3.12: **Binding isotherms of propranolol, salmeterol and indacaterol to PhC liposomes at pH 7.2.** The plotted values of  $RU_{scaled}$  were derived from the plateau values 150 s after the injection of propranolol (A) or salmeterol (C) or indacaterol (E) into PhC liposome-covered chips. In (B), (D) and (F) the respective plateau values were corrected for the residual  $RU$  values 150 s after starting the desorption phase. Mean values of 3 independent experiments with their standard deviations are shown. The continuous lines represent the fit according to a single binding site isotherm including all data points. The dashed lines show the fit functions after excluding the highest concentration (propranolol, salmeterol and indacaterol), and the two and three highest concentrations (propranolol). The fitted  $K_D$  values are shown next to the respective lines.

The apparent rate constants of the faster phases of the bi-exponential functions,  $k_1$ , were not reproducible and were beyond the time resolution of the instrument. Some kinetics

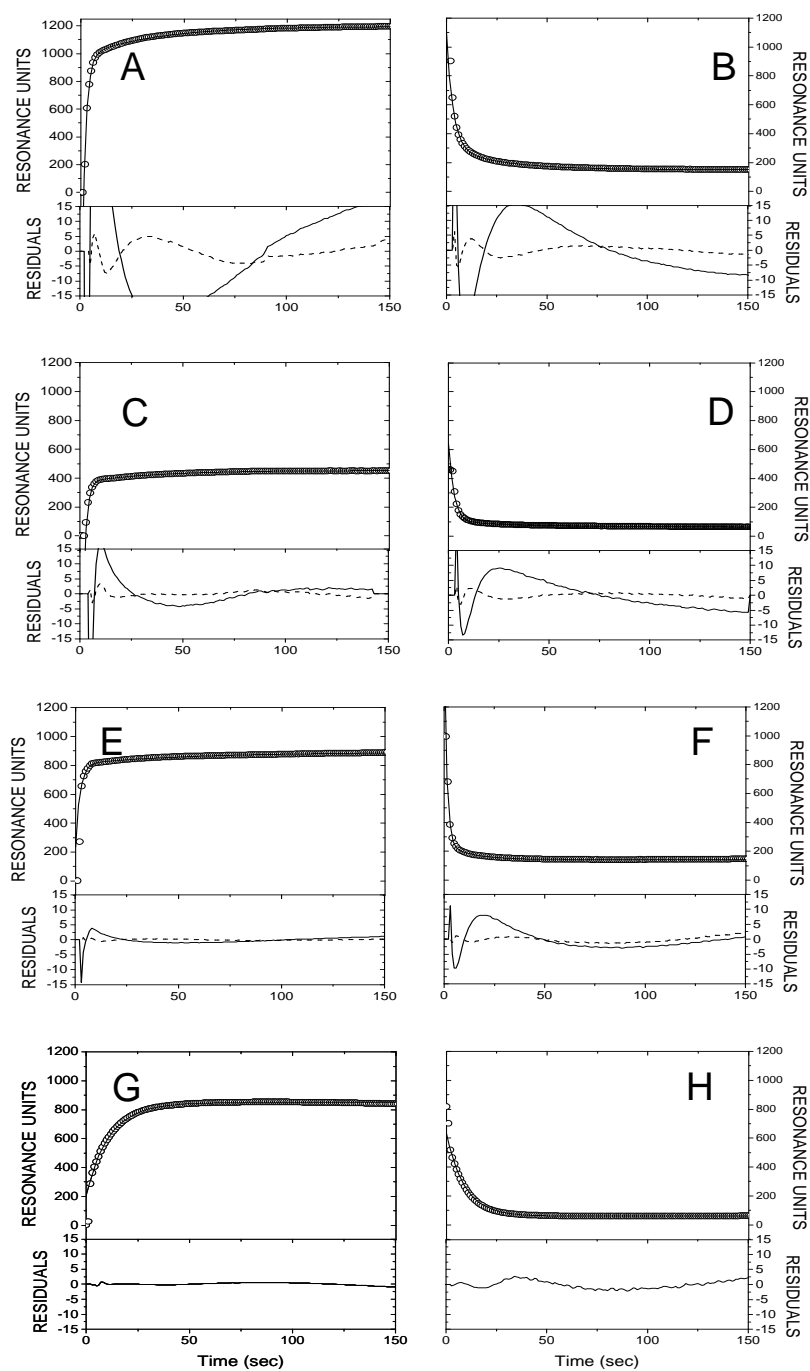


Fig. 3.13: Association and dissociation kinetics of indacaterol and salmeterol with PhC liposomes. Representative examples of the association phases (A,C, E, G) and the dissociation phases (B, D, F, H) of indacaterol ( $60 \mu\text{M}$ ) (A, B, C, D) and salmeterol ( $60 \mu\text{M}$ ) (E, F, G, H), collected with PhC liposomes-covered surfaces at pH 7.2 (A, B, E, F) and at pH 9.3 (C, D, G, H). Buffers contained 0.2% DMSO. The upper panels show the sensograms with the best fit function, the lower panels the residuals for the mono- (solid line) and bi-exponential (dashed line) fits.

were measured at lower concentrations down to  $9.4 \mu\text{M}$  salmeterol or indacaterol. These sensograms were also bi-exponential up to  $\text{pH} \sim 8$ . Representative sensograms at  $9.4 \mu\text{M}$  salmeterol and indacaterol are shown in Fig. 3.11. Figure 3.14 shows the fitted apparent rate constants  $k_2$  (slower phases of bi-exponential functions) and  $k$  (mono-exponential functions) of the association and dissociation phases for indacaterol and salmeterol.

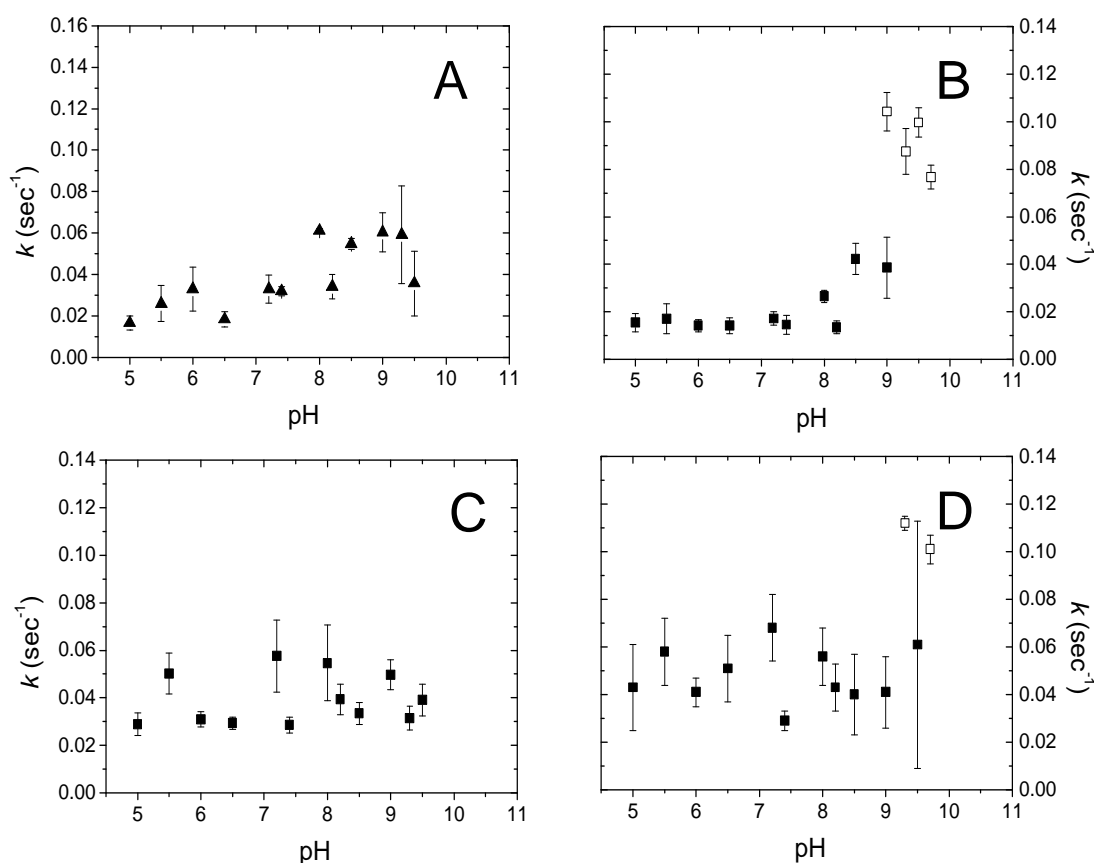


Fig. 3.14: **pH-Dependence of the fitted apparent rate constants  $k_2$  and  $k$  of the liposome association and dissociation phases of indacaterol and salmeterol.** The association (A, B) and dissociation (C, D) phases of indacaterol (A, C) and salmeterol (B, D), respectively, to and from PhC liposomes were recorded at various pH values and the apparent rate constants of the slow phases of the bi-exponential functions ( $k_2$ , closed symbols) and of the mono-exponential functions ( $k$ , open symbols) were estimated from non-linear curve fitting as shown in Fig. 3.13. Mean values of 6 independent experiments with standard deviations.

For indacaterol the  $k_2$  of the association phases were between  $0.02$  and  $0.06 \text{ s}^{-1}$  in the investigated pH range; the respective values of the apparent rate constant of the dissociation phases were between  $0.03$  and  $0.06 \text{ s}^{-1}$ . For salmeterol the  $k_2$  values were pH-independent from pH 5 to pH 8, ranged between  $0.01$  and  $0.03 \text{ s}^{-1}$  for the association phases and between  $0.03$  and  $0.07 \text{ s}^{-1}$  for the dissociation phases.

The kinetics of salmeterol changed from the bi-exponential to the mono-exponential behavior by increasing the pH above  $pK_{a1}$  value. The fittings of the mono-exponential kinetics give  $k$  values between 0.08 and 0.12  $s^{-1}$ . It should be noted that the determination of the rate constants was variable at pH close to the  $pK_{a1}$  value (Fig. 3.14 B and D): this could be indicative of the transitory behavior of the kinetics. To test whether the observed rate constants ( $k_2$ ,  $k$ ) were directly related to the partitioning of the drugs into the membrane, the ratios of the fitted apparent rate constants of the association and the dissociation phases were plotted against the pH and compared to the relative plateau values ( $RU_{eq}/RU_{Lipo}$ ) of the association phases at the respective pH values. If  $k_2$  or  $k$  are mainly determined by the partitioning rate constants, their ratio should directly be related to  $D$  at constant volume ratios of membrane to buffer. The profiles are shown in Fig. 3.15. The fact that they differ in their shapes excludes the possibility that  $k_2$  and  $k$  are directly related to the partitioning process over the investigated pH range.

#### 3.4.3 Concentration-dependence of salmeterol and indacaerol partitioning in the PhC liposome system

In order to investigate whether the discrepancies between the pH-partition profiles from SPR and equilibrium dialysis resulted from a concentration-dependent partitioning, the influence of the drugs concentration on the partitioning of salmeterol and indacaterol in PhC liposomes was investigated. Equilibrium dialysis experiments were carried out at different salmeterol concentrations between 0.24 and 600  $\mu\text{M}$  at pH 7.2 and pH 9.5. To solubilize salmeterol, 0.2% DMSO was added at concentrations  $\geq 20$   $\mu\text{M}$  and 2% at concentrations  $\geq 300$   $\mu\text{M}$ . The concentration-dependence of salmeterol partitioning is shown in Fig. 3.16. The distribution coefficient at pH 7.2 was strongly dependent on the drug concentration. It was  $\sim 4000$  at concentrations up to  $10^{-6}$  M and decreased to  $\sim 1000$  at concentrations between  $10^{-4}$  and  $10^{-3}$  M. The membrane affinity at pH 9.5 increased with increasing concentration. The distribution coefficient was  $\sim 1000$  in the concentration range between  $10^{-7}$  and  $10^{-4}$  M but increased to  $\sim 2000$  when the concentration of salmeterol was increased to  $10^{-3}$  M. This behaviour leads to completely different pH-distribution profiles at low and high concentrations. Under ideal conditions, i.e. salmeterol concentrations  $\leq 10^{-6}$  M, the cation has the highest affinity to PhC liposomes as shown in Fig. 3.4. However, at concentrations  $> 100$   $\mu\text{M}$ ,  $D$  was higher at pH 9.5 than at pH 7.2, where the cation predominates. For indacaterol equilibrium dialysis experiments were carried out at indacaterol up to 50  $\mu\text{M}$  0.2% DMSO in the pH range 6 to 10.5 with no evidence for any deviation from the partitioning at lower concentration, i.e. 1  $\mu\text{M}$ . The concentration-dependence of the pH-distribution profile could partially explain the discrepancies between the effects of pH on the SPR  $RU_{eq}$  results

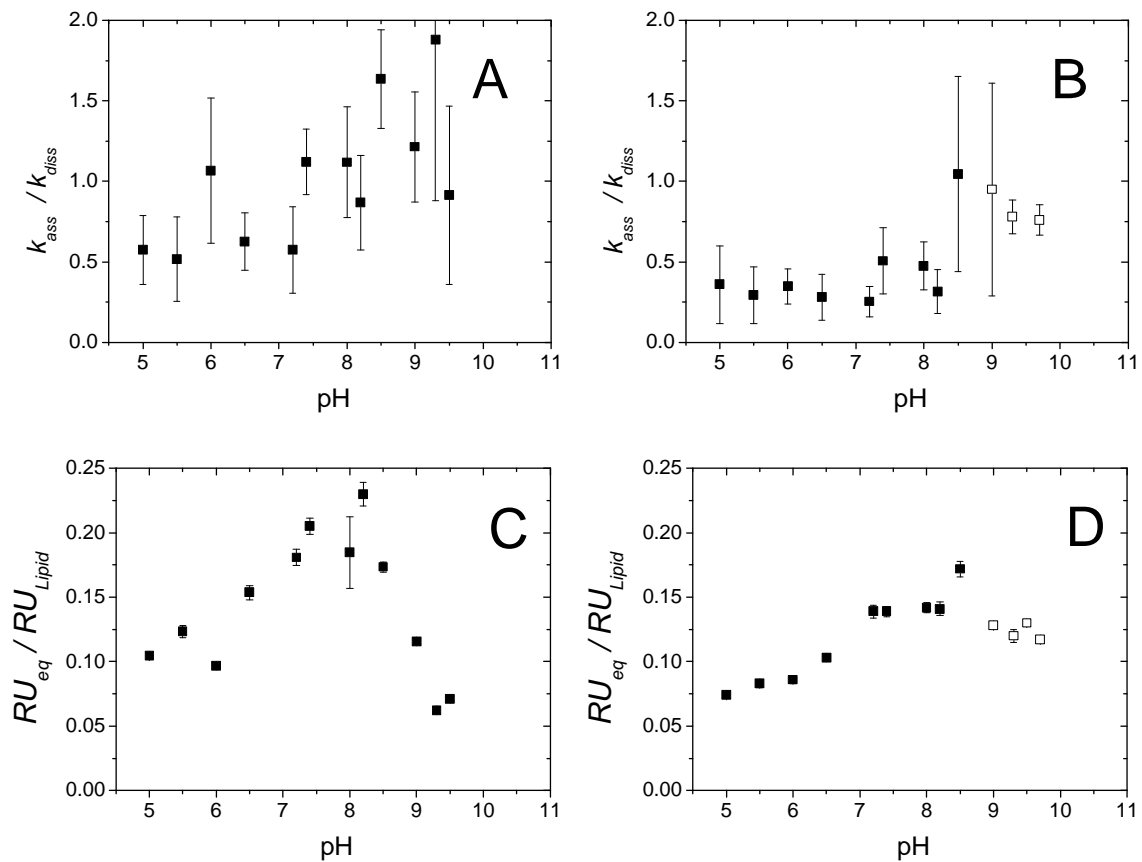


Fig. 3.15: **Comparison between the ratios of the fitted apparent rate constants of the association and the dissociation phases and the plateau values of the association phases.** The ratios of the observed association ( $k_{ass}$ ) and dissociation ( $k_{diss}$ ) rate constants ( $k_2$  and  $k$  from Fig. 3.14) were calculated for indacaterol (A) and salmeterol (B). The  $RU_{eq}$  values correspond to the  $RU_{drug}$  values extrapolated to the equilibrium of the corresponding association phases for indacaterol (C) and salmeterol (D). Open symbols indicate mono-exponential kinetics in the association phase or in both phases.

for salmeterol (Fig. 3.15) and on the partition results from equilibrium dialysis (Fig. 3.4). However additional control experiments with DMPC liposomes did not give evidence for any concentration-dependent partitioning profile in the investigated concentration range of pH 7.0 and 9.5, neither for salmeterol nor for indacaterol.

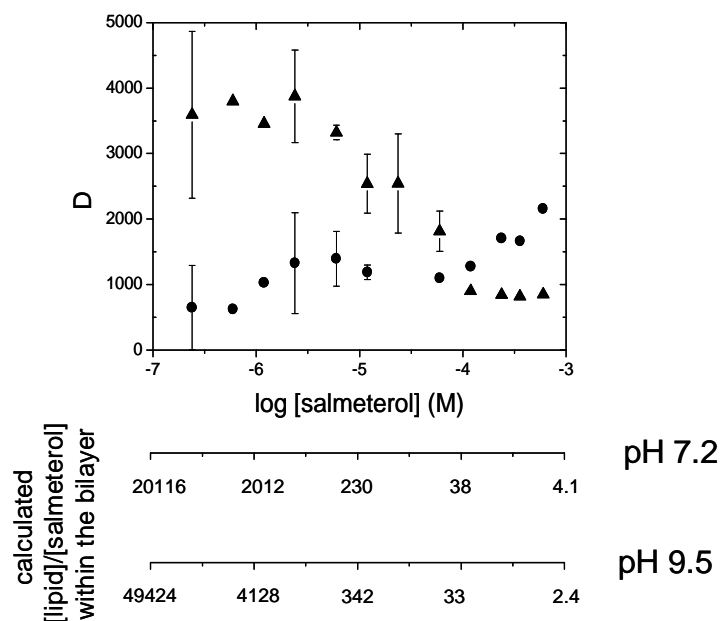


Fig. 3.16: **Concentration-dependent partitioning of salmeterol in PhC liposomes.**

Distribution of salmeterol in PhC liposomes at pH 7.2 (▲) and pH 9.5 (●). At concentrations  $\geq 20 \mu\text{M}$  ( $\log[\text{salmeterol}] \geq -4.7$ ) 0.2 % DMSO was added to the system, at concentrations  $> 300 \mu\text{M}$  ( $\log[\text{salmeterol}] \geq -3.5$ ) the DMSO content was 2 %. As seen from the data, DMSO had no significant effect on partitioning. The molar lipid/salmeterol ratios within the bilayers were estimated with eq. 2.5. The free concentrations in buffer were between  $\sim 3$  and  $\sim 5$  times lower than the indicated total salmeterol concentrations.

## 3.5 Permeation of lipid bilayers as determined by the terbium(III)-permeation assay

### 3.5.1 Complex formation between Tb(III) and 2-hydroxynicotinic acid (OHNA)

The equilibrium constants for the formation of a 1:1 complex between OHNA and Tb(III) at 25°C in different aqueous environments were determined by spectrofluorimetric titrations of OHNA with an excess of Tb(III). The  $K_A$  values were derived from the binding isotherms shown in Fig. 3.17 as described in sec. 2.7. They were  $1.17 \cdot 10^5 \text{ M}^{-1}$  in MOPS pH 6.5 and  $4.83 \cdot 10^4 \text{ M}^{-1}$  in TRIS pH 6.5. At pH 2.5, where the neutral OHNA species predominates,  $K_A$  was  $\sim 1 \text{ M}^{-1}$  in both buffer systems. As expected, the binding was significantly weaker in 0.2 M EDTA pH 6.5 than in MOPS and TRIS at the same pH. The respective apparent  $K_A$  was estimated as  $0.5 \text{ M}^{-1}$  from the binding isotherm Fig. 3.17. The data are summarized in Tab. 3.5.

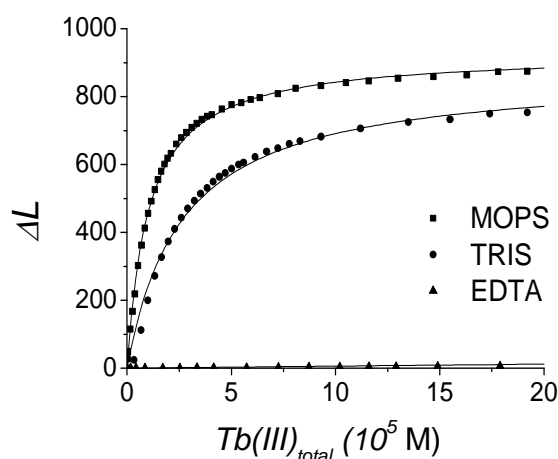


Fig. 3.17: **Binding isotherms for the 1:1 complex formation between Tb(III) and OHNA in various buffers at pH 6.5 and 25°C.** An OHNA solution was titrated with Tb(III) and the changes in luminescence ( $\Delta L$ ) were recorded. Squares, titration in MOPS; circles, TRIS; triangles, 0.2 M EDTA. The total OHNA concentration was  $\sim 2 \cdot 10^{-6} \text{ M}$ , total Tb(III) concentrations ranged from  $2 \cdot 10^{-7}$  to  $2 \cdot 10^{-4} \text{ M}$ .  $\lambda_{ex}$  was 305 nm,  $\lambda_{em}$  545 nm. The lines show the fitted binding isotherms. Omitting Tb(III) concentrations  $< 2 \cdot 10^{-5} \text{ M}$  did not significantly change the fit parameters.

To shed light on the influence of liposomes on the binding reaction between OHNA and Tb(III), the apparent equilibrium constants were also determined in a liposome suspension. Liposomes may reduce the concentration of free OHNA in the sample due to moderate

membrane partitioning of OHNA [Thomae et al., 2005]. Figure 3.18 shows the binding isotherms for the complex formation between OHNA and Tb(III) in the presence of 1 and 10 mg/ml liposomes in MOPS pH 6.5. The  $K_A$  values were significantly reduced in the presence of liposomes. The data are summarized in Tab. 3.5.

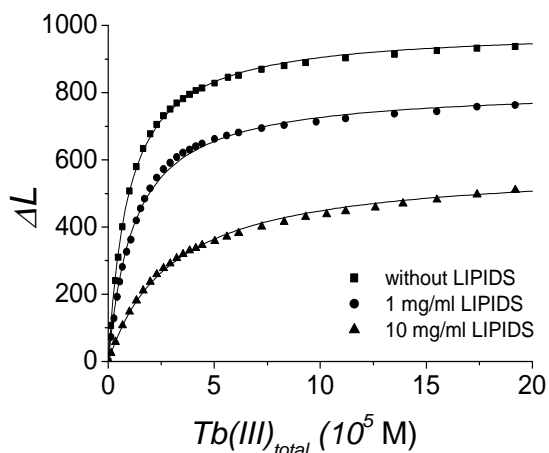


Fig. 3.18: **Influence of liposomes on the binding isotherms of the OHNA/Tb(III) complex formation.** Titrations were carried out in 0.2 M MOPS at pH 6.5. Squares, no addition of liposomes; circles, 1 mg/ml PhC; triangles, 10 mg/ml PhC. The lines show the fitted binding isotherms.

To estimate the thermodynamic parameters of the complex formation between Tb(III) and OHNA, titrations were performed at various temperatures between 10 and 37°C, and  $\ln(K_A)$  values were plotted against  $1/T$  Fig. 3.19. The Gibbs free energy variation ( $\Delta G^\circ$ ) was determined from the binding constants according to eq. 2.16. As no activity coefficients are known for the investigated reaction, a value of unity was assumed and the equilibrium concentrations were used instead of the activities. Under these conditions it is appropriate to adapt the terminology of apparent Gibbs free energy change,  $\Delta G^{\circ'}$ , enthalpy,  $\Delta H^{\circ'}$ , and entropy,  $\Delta S^{\circ'}$ .

The standard free energy change ( $\Delta G^{\circ'}$ ) for the interaction between OHNA and Tb(III) is relatively high in value and of negative sign. The reaction is exothermic ( $\Delta H^{\circ'} < 0$ ) in all investigated systems as judged from the Van't Hoff Plot shown in Fig. 3.19. However, the main contribution to  $\Delta G^{\circ'}$  comes from the positive change in entropy ( $\Delta S^{\circ'}$ ), resulting in high  $T \cdot \Delta S^{\circ'}$  values. It can be concluded that the positive entropy changes are the driving forces for the interactions between OHNA and Tb(III) in both buffer systems. The positive entropy change for the binding between OHNA and Tb(III) probably comes from the electrostatic attractions between the OHNA anions and the Tb(III) cations. Upon binding, water molecules bound to the reaction partners are released, which leads to positive entropy



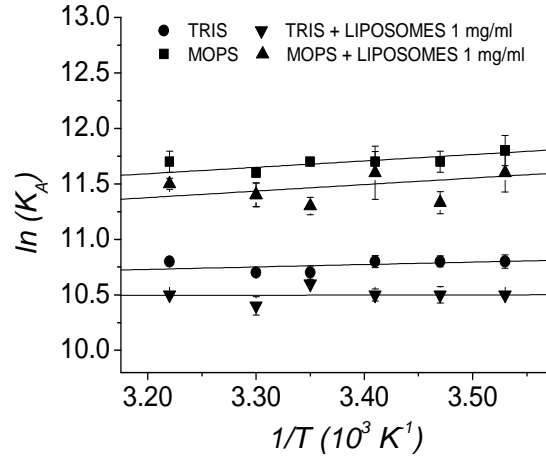


Fig. 3.19: **Van't Hoff Plots for the OHNA/Tb(III) complex formation.** Titrations were performed in MOPS 0.2M pH 6.5 and in TRIS 0.2 M pH 6.5 without added liposomes and after addition of liposomes (1 mg/ml; symbols see Figure). The lines represent the linear regressions of the experimental data.

	$K_A$ (mol <sup>-1</sup> )	$\Delta G^{o'}$ (KJ·mol <sup>-1</sup> )	$\Delta H^{o'}$ (KJ·mol <sup>-1</sup> )	$T \cdot \Delta S^{o'}$ (KJ·mol <sup>-1</sup> )
TRIS pH 6.5	$(4.83 \pm 0.15) \cdot 10^4$	$-26.7 \pm 0.1$	$-1.81 \pm 0.82$	$27.7 \pm 0.8$
TRIS pH 6.5 Liposomes 1 mg/ml	$(4.08 \pm 0.02) \cdot 10^4$	$-26.3 \pm 0.01$	$-0.152 \pm 1.76$	$25.7 \pm 0.9$
TRIS pH 2.5	$(0.1 \pm 1) \cdot 10^1$	$-5.7 \pm 7.4$		
MOPS pH 6.5	$(11.7 \pm 0.4) \cdot 10^4$	$-28.9 \pm 0.1$	$-4.77 \pm 1.56$	$24.1 \pm 0.8$
MOPS pH 6.5 Liposomes 1 mg/ml	$(8.24 \pm 0.48) \cdot 10^4$	$-28.0 \pm 0.2$	$-4.89 \pm 2.73$	$23.5 \pm 0.9$
MOPS pH 2.5	$(0.1 \pm 1) \cdot 10^1$	$-5.7 \pm 7.4$		

Table 3.5: **Overall equilibrium constants and thermodynamic parameters of the complex formation between OHNA and Tb(III) at 298 K.**

changes in the overall thermodynamic process. Based on our data shown in Fig. 3.19 we can not conclude whether the difference observed in  $K_A$  comparing the two buffer systems are due to differences in  $\Delta H^{o'}$ , in  $\Delta S^{o'}$  or both. The fit parameters (Tab.3.5) tend towards a change in  $\Delta H^{o'}$  while the liposomes appear to influence  $\Delta S^{o'}$  rather than  $\Delta H^{o'}$ .

### 3.5.2 Kinetics of the 1:1 complex formation between OHNA and Tb(III)

The kinetics of the OHNA/Tb(III) complex formation were investigated at 25°C with the same buffers employed for the static measurements. Experiments were carried out under pseudo-first order conditions in excess of Tb(III) over OHNA. Final Tb(III) concentrations varied between 20 and 200  $\mu\text{M}$ , the OHNA concentration was 1  $\mu\text{M}$ . When OHNA was rapidly mixed with Tb(III) in the stopped flow apparatus, a relaxation process was observed, characterized by an increase in luminescence. A representative stopped-flow curve for the OHNA/Tb(III) complex formation is shown in Fig. 3.20.

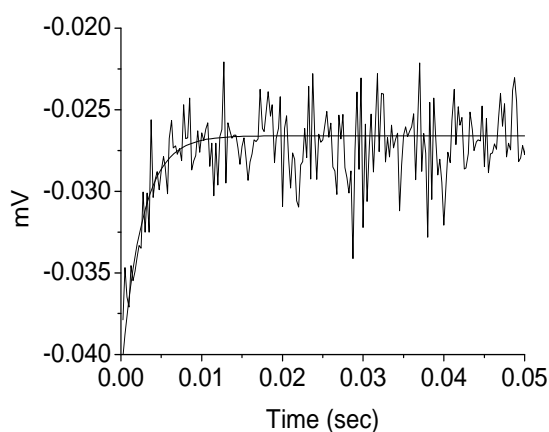


Fig. 3.20: Stopped flow trace of the OHNA/Tb(III) complex formation in TRIS 0.2M, pH 6.5 at 25°C. The final concentrations were  $1 \cdot 10^{-6}$  M OHNA and  $2 \cdot 10^{-5}$  M Tb(III).

At pH 6.5 the process occurs in the range of 20 milliseconds. The data were fitted with a mono-exponential function. The rate constants increased linearly with the concentration of Tb(III) and were between  $397 \text{ sec}^{-1}$  and  $998 \text{ sec}^{-1}$ . Stopped flow experiments at pH 2.5 revealed a similar relaxation process in the 20 milliseconds range.

### 3.5.3 Permeation kinetics of OHNA

Permeation kinetics of OHNA across lipid bilayers were studied between 5 and 50°C with Tb(III)-containing liposomes as described under Materials and Methods. The complex formation was followed in a luminescence spectrometer. The experiments were carried out in MOPS and TRIS at pH 2.5 and pH 6.5. In order to investigate the influence on the permeation kinetics of the complex formation between Tb(III) and OHNA in the liposomal lumen, control experiments were carried out with liposomes containing EDTA beside Tb(III) to decrease the apparent  $K_A$  of the complex. Additional control experiments with valinomycin and KCl (2.9) did not give evidence for any difference on the permeation kinetics. Permeation data were fitted according to eq. 2.18 and eq. 2.19. Permeation kinetics with Tb(III) liposomes (without EDTA) followed mono- or bi-exponential functions. Experiments in MOPS pH 6.5 were bi-exponential at all investigated temperatures. Kinetics in TRIS pH 6.5 followed mono-exponential functions between 10 and 25°C and were bi-exponential between 30 and 50°C. Representative examples with the fit functions and the respective residuals are shown in Fig. 3.21. The fast rate constants of the permeation kinetics of OHNA were temperature-dependent with highest  $Perm_{1app}$  values at 50°C and lowest values at 10°C.  $Perm_{1app}$  were similar in MOPS and TRIS Fig. 3.22. The slow rate constant of the bi-exponential permeation kinetics in MOPS was temperature-dependent in a similar manner. At pH 2.5, permeation kinetics were determined in MOPS and TRIS between 5 and 25°C. In both buffers the faster  $Perm_{app}$  value of the bi-exponential function was linearly increasing with increasing temperature. The slow  $Perm_{app}$  was similarly temperature-dependent in MOPS but was not significantly dependent on the temperature in TRIS Fig. 3.22.

The entry kinetics of OHNA into the aqueous lumen of EDTA/Tb(III)-containing liposomes were determined between 10°C and 50°C in MOPS and TRIS buffer at pH 6.5 Fig. 3.22. The permeation kinetics followed bi-exponential functions with the faster rate constant showing a clear temperature-dependence while the slow rate constant was temperature-independent. At temperatures  $\leq 30^\circ\text{C}$  the fast rate constants were  $\sim 4$  times higher in the presence of EDTA than in the absence. At higher temperatures EDTA-free liposomes produced slightly higher or equal rate constants. The slow rate constants in EDTA-containing liposomes were in the range of the slow rate-constant in EDTA-free liposomes at low temperatures. The temperature-dependence of the permeation kinetics was analyzed according to the Eyring's equation (eq. 2.22). The Eyring plots, i.e.  $\ln(Perm_{app}/T)$  vs.  $1/T$ , are shown in Fig. 3.23. The activation parameters of the fast and slow phases are reported in Tab. 3.6. As mentioned before, the activity coefficients are not known therefore it is appropriate to adopt the terminology of apparent Gibbs free energy of activation change,  $\Delta G^{\neq'}$ , enthalpy of activation,  $\Delta H^{\neq'}$ , and entropy of activation,  $\Delta S^{\neq'}$ .

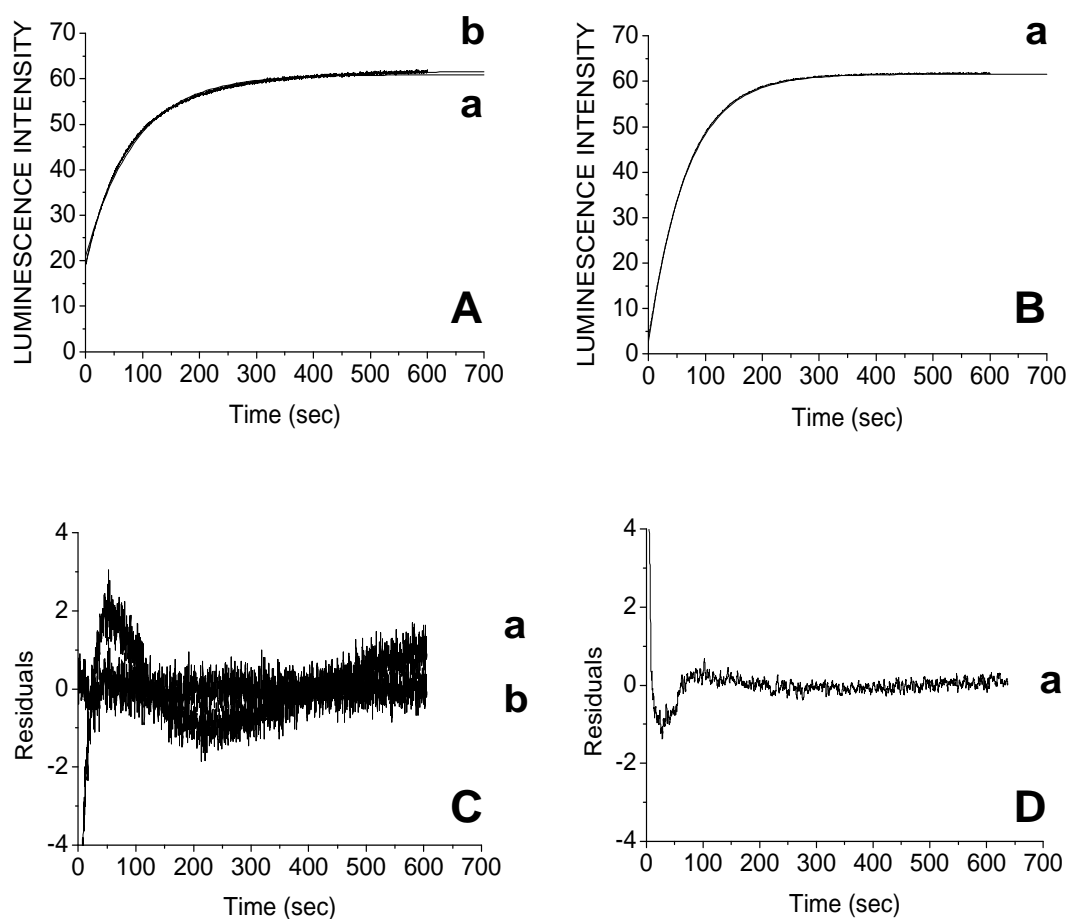


Fig. 3.21: Kinetics of OHNA entry into Tb(III)-containing egg PhC liposomes at pH 6.5, 25°C. A) 0.2 M MOPS; B) 0.2 M TRIS. Total OHNA concentrations were  $2 \cdot 10^{-6}$  M, lipid concentrations were 1 mg/ml;  $\lambda_{ex}$  was 305 nm,  $\lambda_{em}$  545 nm. The experimental data were fitted with a mono-exponential function (a) and a bi-exponential function (b), respectively. C and D show the residuals of the fits in A and B.

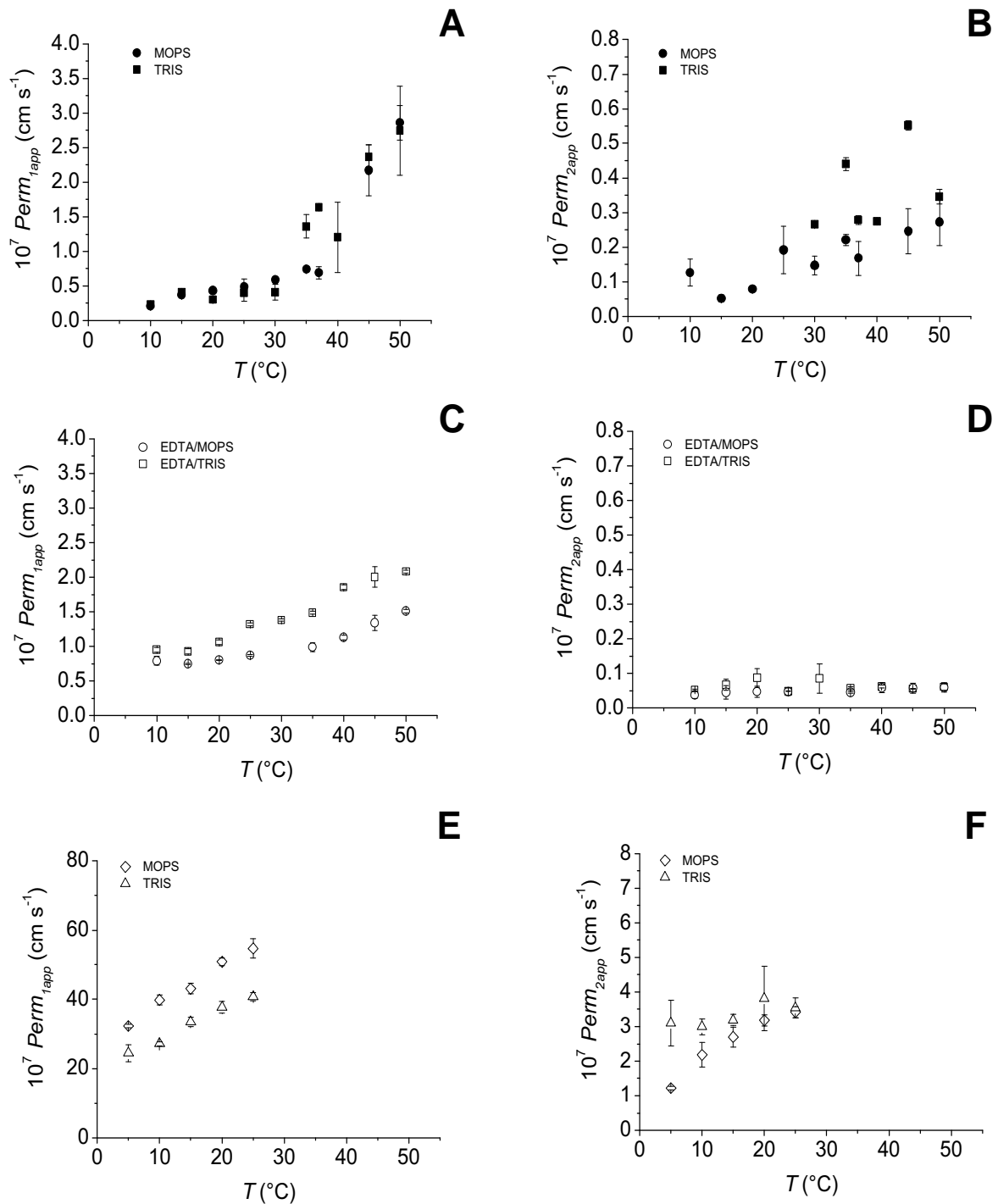


Fig. 3.22: **Apparent permeation coefficients of the entry of OHNA into Tb(III)-containing liposomes.** Liposomes contained either Tb(III) alone (A-D) or EDTA and Tb(III) (E and F). Kinetics were measured at pH 6.5 (A, B, E, F) and pH 2.5 (C, D). Circles, 0.2 M MOPS; squares, 0.2 M TRIS. Further experimental details as described in Fig. 3.21.

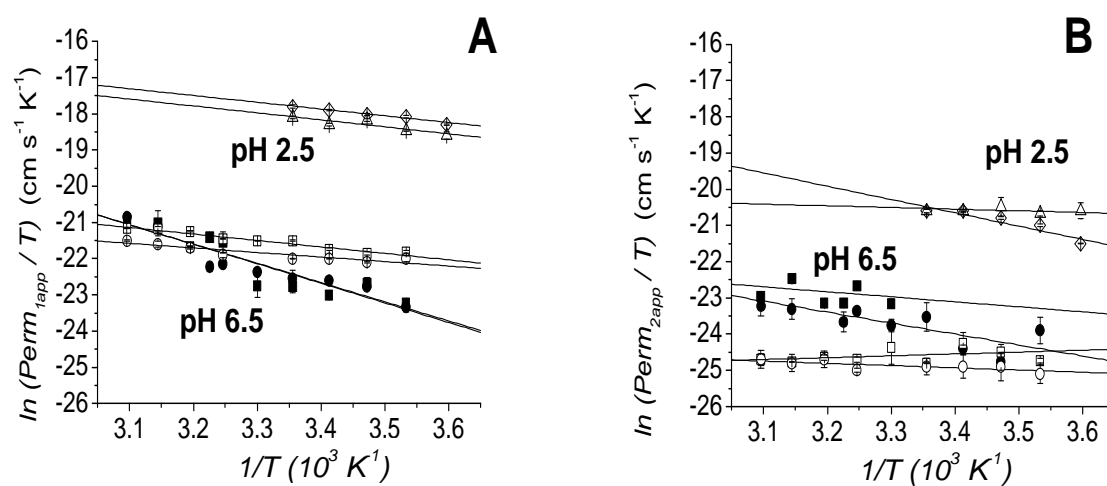


Fig. 3.23: Eyring's plot of the permeation kinetics of OHNA into Tb(III) and EDTA/Tb(III)-containing liposomes at pH 6.5 and 2.5. A)  $\text{Perm}_{1\text{app}}$ , B)  $\text{Perm}_{2\text{app}}$  from Fig. 3.22. Symbols, as in Fig. 3.22. Lines show linear regressions of the experimental data.

$Perm_{1app}$	$E_a$ (KJ·mol <sup>-1</sup> )	$\Delta G^{\neq'}$ (KJ·mol <sup>-1</sup> )	$\Delta H^{\neq'}$ (KJ·mol <sup>-1</sup> )	$T \cdot \Delta S^{\neq' a)}$ (KJ·mol <sup>-1</sup> )
TRIS pH 6.5	47.3 ± 3.2	145 ± 6	44.9 ± 3.2	-100 ± 2
TRIS/EDTA pH 6.5	17.3 ± 0.7	143 ± 2	14.8 ± 0.7	-128 ± 1
TRIS pH 2.5	18.5 ± 1.2	135 ± 2	16.0 ± 1.2	-119 ± 1
MOPS pH 6.5	46.6 ± 2.2	145 ± 6	44.1 ± 2.2	-101 ± 2
MOPS/EDTA pH 6.5	12.5 ± 0.9	144 ± 2	10.0 ± 0.9	-134 ± 1
MOPS pH 2.5	18.0 ± 1.1	135 ± 2	15.5 ± 1.1	-119 ± 1

$Perm_{2app}$	$E_a$ (KJ·mol <sup>-1</sup> )	$\Delta G^{\neq'}$ (KJ·mol <sup>-1</sup> )	$\Delta H^{\neq'}$ (KJ·mol <sup>-1</sup> )	$T \cdot \Delta S^{\neq' a)}$ (KJ·mol <sup>-1</sup> )
TRIS pH 6.5	14.0 ± 5.0	147 ± 6	11.5 ± 5.0	-135 ± 1
TRIS/EDTA pH 6.5	1.80 ± 2.79	159 ± 4	-4.28 ± 2.79	-155 ± 1
TRIS pH 2.5	6.32 ± 2.96	141 ± 4	3.84 ± 2.96	-137 ± 1
MOPS pH 6.5	27.6 ± 4.0	145 ± 9	25.1 ± 4.0	-120 ± 4
MOPS/EDTA pH 6.5	7.59 ± 2.2	132 ± 8	5.11 ± 2.53	-127 ± 5
MOPS pH 2.5	33.0 ± 4.0	141 ± 7	30.5 ± 4.0	-111 ± 3

Table 3.6: **Activation parameters of the permeation kinetics  $Perm_{1app}$  and  $Perm_{2app}$  of OHNA into Tb(III) and EDTA/Tb(III)-containing liposomes at 298K.** <sup>a)</sup> note that the entropy values represent the average of the back extrapolated values for each experimental point (sec. 2.9) and include the correction term for the liposome size  $\ln(r/3)$  as shown in eq. 2.22,  $\Delta S^{\neq'}$  was calculated for liposomes with a radius of 100 nm as described in sec. 2.9.





## 4 Discussion

The titrated  $pK_a$  values of the amine and phenolic hydroxyl of indacaterol were lower than the respective values of salmeterol, indicating that at physiological pH indacaterol is present mostly as zwitterionic and neutral species while the cation form is most abundant for salmeterol. Accordingly octanol-water partition experiments show maxima at different pH values. A maximum log D of 3.8 was found at pH 8.2 for indacaterol and a log D value of 3.2 was measured at pH 10.1 for salmeterol. At pH 7.4, i.e. the physiological pH, indacaterol had 15 fold higher partition coefficient than salmeterol. The partition into egg phosphatidyl choline (PhC) liposomes was found to be similar for both compounds and modestly pH dependent with a similar affinity for the cationic and the net neutral species and a weaker affinity for the anionic species, except for the DPPC/DPPG and SM liposomes.

Having a closer look at the lipid bilayer as a distribution system, the relatively high membrane affinity of charged species can be rationalized as follow: while charge neutralization within the zwitterion is favourable in octanol, leading to higher distribution coefficients for zwitterions than for net charged species [Avdeef et al., 1998, Betageri and Rogers, 1988, Hellwich and Schubert, 1995, Plember van Balen et al., 2001], charge neutralization can be achieved by interactions with the phosphate and the amine moieties, respectively, of the lipid headgroups independent of the presence of a counter-charge within the molecule. A similar behavior, as we observed with the  $\beta_2$ -agonists, was observed before with cetirizine, a H1 receptor antagonist with two basic and one acidic groups [Plember van Balen et al., 2001]. The mono-cation usually had a higher affinity to lipid bilayers than the zwitterionic and the anionic species, respectively.

Depending on the sterical arrangement of the hydrophobic moiety/moieties and the charged groups, less charges may be favourable for a good fit within the bilayer. The zwitterions of salmeterol and indacaterol, which are the main ionization species between the two  $pK_a$  values and which have the highest partition coefficient in the octanol/buffer system, may need more energy to partition into the bilayer than the corresponding cations. We expect that the hydrophobic tails of the compounds are buried in the acyl chain region, independently

## 4 Discussion

of the charge of the amine and phenol groups. The positive charge of the cation, which is localized at the amine group may interact with the negatively charged phosphate groups of the lipids while the neutral phenol could be located at the height of the carbonyl groups and the first C atoms of the acyl chains, forming hydrogen bonds with the carbonyl oxygens. Upon deprotonation of the phenolic hydroxyl group, the preferred location of the phenolate may change and tend towards the headgroup/buffer region where it can neutralize its charge with the quaternary amine of the choline or with electrolytes in the water phase. Due to the loss of the hydrophobic interaction between the aromatic ring and the acyl chains, the membrane affinity may decrease, although the charge distribution would fit with the charges of the headgroups (Fig. 4.1).

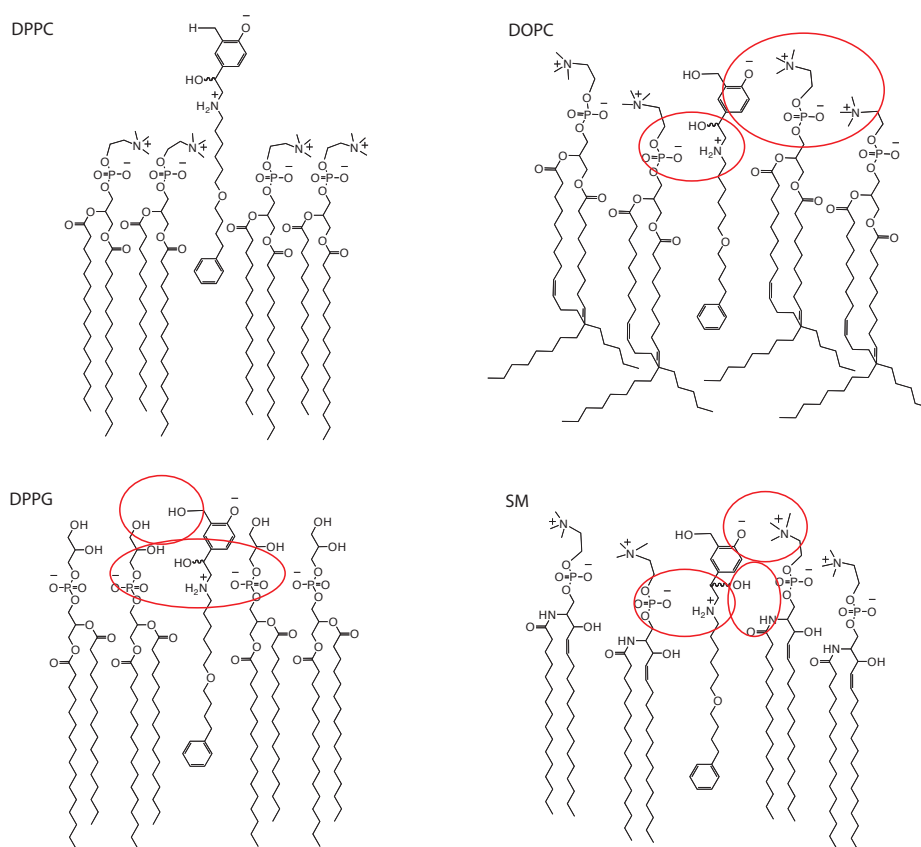


Fig. 4.1: Sterical arrangements of salmeterol with phospholipid membranes. See text for details.

The similarity in the pH-distribution profiles of indacaterol and salmeterol was observed for several liposome preparations with lipids of different acyl chain length, insaturations and headgroup charge, and for liposomes that included cholesterol and/or sphingomyelin. Hence neither the difference in the ionization pattern observed in aqueous solution nor the

---

difference in flexibility of the agonist tails seems to affect the interaction of salmeterol and indacaterol with lipid bilayers. The cations of propranolol [Kramer et al., 1997, 1998] and of desipramine [Marenchino et al., 2004] were the predominating partition species under the condition that the membranes contained negatively charged lipids. No free fatty acids or lysophosphatidylcholine, i.e. the negatively charged hydrolysis products of phospholipids, were detectable by HPLC in our PhC liposomes, we can thus exclude an attraction between negatively charged lipids and solute cations in PhC membranes.

In contrast to our own results, Austin et al. [2003] found that the net neutral species had a higher bilayer affinity in a system with saturated phospholipids (DMPC) while the cation and anion affinities were similar as in our system, resulting in a bell-shaped distribution profile. The high membrane affinity between the two  $pK_a$  values could either be due to a higher membrane affinity of the zwitterion than of the cation and the anion, or to a very high membrane affinity of the uncharged species. The lack of technical details and experimental conditions in the work of Austin et al. [2003] make impossible to elucidate the differences between their findings and our own results.

We found a bell-shaped distribution profile with highest membrane affinity in the pH range between the two inflection points with liposomes consisting of DPPC/DPPG 80/20 molar ratio and SM, though not for liposomes of DMPC which as saturated acyl chains, as DPPC and DPPG. DPPC/DPPG liposomes are characterized by their negative surface charge due to the phosphate moiety, moreover the glycerol group enhances the possibility of hydrogen bonding. Similarly the hydroxyl group of SM can act as a hydrogen bond donor but in this lipid the negative charge of the phosphate is neutralized by the quaternary amine. In addition the two membranes have a similar  $T_m$  that leads to *so* membranes at 37°C. The rigidity of the membrane could generate unfavourable conditions for the intercalation of the hydrophobic tail of the compounds resulting in an increased distance between the protonated amine of the solutes and the phosphate groups of adjacent phospholipids (Fig. 4.1). This results in a reduced charge neutralization between the solutes and the lipid headgroups together with the reduced hydrophobic interaction of the solute tail and the phospholipid acyl chains and therefore a disadvantageous energy balance. This model also explains the relatively low affinity of the drugs to the *so* membranes. The fact that the influence is highest for the cations underlines the above hypothesis that the hydrophobic moieties are buried deepest into the acyl chains if the compounds are in their cationic form, resulting in the best fit between acyl chains and charged headgroups. The higher affinity of the net neutral species to *so* membranes containing hydrogen bond donor groups could be assigned to the above described possible reduction of cation affinity in combination with a partial neutralization of the negative charge of the phenolate group by the hydrogen donor property of the lipids (Fig. 4.1).

The influence of cholesterol that is known to generate a stiffer membrane when present in percentages up to 30%, is evidenced by lower affinity of the compound for the cholesterol containing membranes.

The affinity of both indacaterol and salmeterol for DOPC bilayers was notably increased as compared to PhC bilayers. DOPC membranes have the same headgroups as PhC but differ in their acyl chain pattern. While PhC has a mix of unsaturated and saturated chains of differing length, all acyl chains of DOPC membranes carry one insaturation between C9 and C10 and are 18 C atoms in length. Surprisingly the fluidity estimated from the anisotropy of DPH was lower for DOPC membranes than for PhC membranes despite its very low  $T_m$ . The anisotropy measurements alone can thus not predict the true extent of the accessibility of the acyl chain region for a drug. It appears that a higher rigidity does not necessarily exclude a better intercalation of the solutes into DOPC than into PhC membranes.

The microdomain structure of biological membranes has attracted significant attention in the past decade [Jacobson et al., 2007] and function of the  $\beta_2$ -adrenoceptor has been linked with the presence of membrane rafts and calveolae in airway smooth muscle [Halayko et al., 2008]. Interestingly we found that when raft vesicles prepared by the cold TritonX-100 method (sec. 2.2) were used as the partition phase, indacaterol partition, i.e.  $10473 \pm 731$ , was 2 fold greater than that of salmeterol, i.e.  $4527 \pm 1426$ . As the rafts contain significant amounts of protein and can form highly ordered microdomains that might not be reproduced by pure lipid mixtures, further investigations will be required to explore the partition and concentration of hydrophobic agonists near the  $\beta_2$ -adrenoceptor membrane architecture and the potential effect it might have on their pharmacological profile.

The overall pharmacological profiles of the  $\beta_2$  agonists are likely to be the sum of several parameters and we propose a model that integrates the results discussed above (Fig. 4.2). After inhalation, the drug moves through the lung tissue to reach the  $\beta_2$ -adrenoceptor on smooth muscles before being distributed towards the systemic circulation. For a hydrophilic compound such as salbutamol the fraction of the drug partitioned in the membranes or rafts is negligible, the compound diffuses rapidly to activate the  $\beta_2$ -adrenoceptor with a weak affinity before being rapidly eliminated from the lung resulting in a fast onset and short duration of action. For highly lipophilic compounds, the drug partitions significantly into the membrane and raft domains whilst diffusing into the lung tissues. The proximal free drug concentration is sustained over-time by the local release from the lipid compartments long after the initial inhaled bulk free fraction has been eliminated (Fig. 4.2). For indacaterol this is likely to be one of the main mechanisms that provides extended duration of action, and its 2 fold higher affinity for raft microdomains compared to salmeterol might contribute to this difference in duration of action.

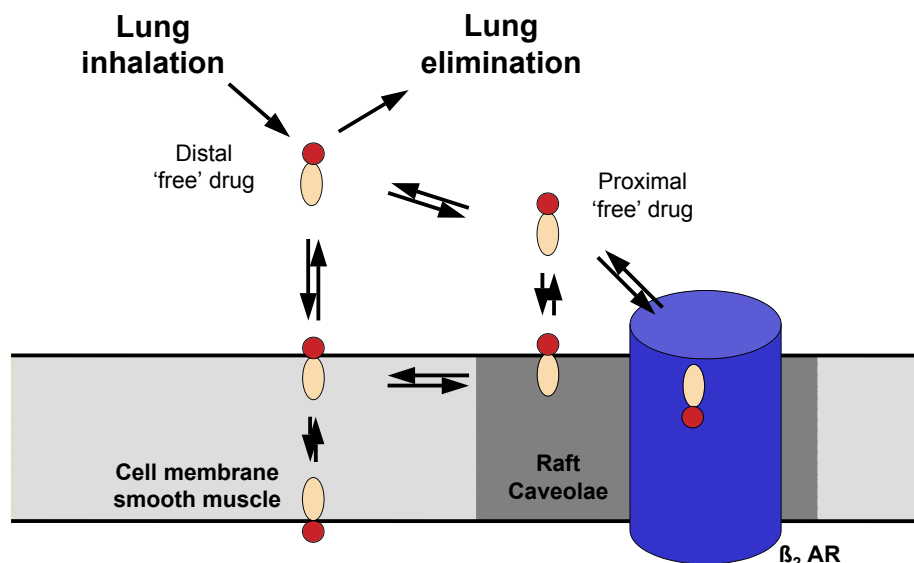


Fig. 4.2: **Model to explain pharmacology differences between beta-2 adrenoceptor agonists.** See text for details.

The shorter duration of action of salmeterol compared to indacaterol could also be the result of the partial agonist properties of salmeterol, implying that occupancy of a higher number of receptors is needed for sustaining a pharmacologically relevant efficacy level, which might be more difficult to achieve for an extended time period. Supporting this view, Battram et al. [2006] have shown that higher than expected doses of salmeterol are also required in in vivo pharmacological models to achieve a significant level of efficacy over time which might lead to a decrease in therapeutic index. The fast onset of indacaterol effect can be explained by two complementary properties. The higher efficacy of indacaterol implies that at equi-effective doses, a smaller number of  $\beta_2$ -adrenoceptor need to be reached compared to a partial agonist with similar hydrophobicity such as salmeterol. It is also possible that zwitterionic lipophilic compounds might have a faster diffusion rate across tissues than the cations or anions. At physiological pH the fast acting indacaterol is mostly present as a zwitterion species while the slow onset of action salmeterol is mostly present in its cationic form in aqueous solution. Finally for compounds with intermediate lipophilicity the high potency and efficacy at the receptor is likely to play a determinant role in providing a sustained duration of action, reaching 24 h in the case of the highly potent and efficacious carmoterol [Voss et al., 1992].

The kinetics of drug-membrane interactions investigated by SPR were pH-dependent according to the ionization state of the solutes. Under our experimental conditions, the apparent rate constant of salmeterol and indacaterol partitioning into the membrane at physiological pH was too fast for a quantitative analysis. The observed slower rate constants were assigned to the translocation process (flip-flop) at physiological pH. The translocation of indacaterol was 2 fold faster at pH values  $< 8.8$  supporting the view of a faster diffusion rate across tissues leading to a faster onset of action. Further experiments to test this model such as interaction kinetics with the  $\beta_2$ -adrenoceptor will likely provide a more detailed understanding of the various parameters responsible for the pharmacological properties of long acting  $\beta_2$ -adrenoceptor agonists.

The SPR results are analyzed in details in the following paragraphs. The dissociation constants  $K_D$  of salmeterol, indacaterol and propranolol at pH 7.2, estimated by SPR varied strikingly depending on the concentration range used for the fit. Excluding the highest concentrations resulted in a decrease of the fitted  $K_D$  values. Lipid bilayers are dynamic systems in that they change their characteristics upon partitioning of solutes. The Langmuir isotherm may not be the ideal function to describe concentration-dependent interactions between drugs and membranes and to determine membrane affinities. This is also obvious from the concentration dependence of  $D$  in the equilibrium dialysis experiments for salmeterol. While  $D$  decreases with increasing salmeterol concentrations at pH 7.2 the opposite was observed at pH 9.5.

It is interesting to note that the higher affinity of the salmeterol cation as compared to the net neutral and the anionic species is only observed at salmeterol concentrations  $< 100 \mu\text{M}$ . This may explain the difference between the pH-distribution profile determined by equilibrium dialysis and the shape of the RU values on the absorption plateaux at  $60 \mu\text{M}$  plotted against the pH.

As mentined above, the kinetics of lipid bilayer association and dissociation determined with SPR were bi-phasic for salmeterol at pH values  $\leq$  pH 8.8 and mono- or bi-phasic at higher pH values while they were bi-phasic at all investigated pH-values for indacaterol. This was not only seen at  $60 \mu\text{M}$ , where partitioning is concentration-dependent, but also at  $9.4 \mu\text{M}$ , where the partitioning is concentration-independent. The mono- and bi-exponential kinetics are in agreement with the model of partitioning and translocation presented in the Introduction (sec. 1.3): depending on the single rate constants the concentrations within the lipid leaflets follow mono- bi- or tri-exponential functions of time [Thomae et al., 2005]. In order to assign the observed rate constants to the processes of partitioning and translocation, the partition coefficients and the volume ratios of the aqueous and the bilayer compartments have to be taken into account [Penniston et al., 1969, Thomae et al., 2005]. This is shown

---

in Fig. 4.3.

More information on the kinetics and the single rate constants could be obtained by varying the lipid amount on the chip and working under conditions where the apparent partitioning rate constant (buffer to lipid bilayer) on the outer side of the liposomes ( $k_a$ ) is lipid concentration-dependent. In theory, lowering the lipid amount should decrease the apparent rate constant of partitioning into the membrane. If there is a range where the rate constant is low enough to be resolved by SPR and the signal is still high enough for monitoring the kinetics, the partition rate constant from the outer buffer into the lipid bilayer should be accessible. This could be achieved with a chip which displays no affinity for the studied compound and on which the liposomes would be attached by covalent binding, e.g. via a streptavidin-biotin system.

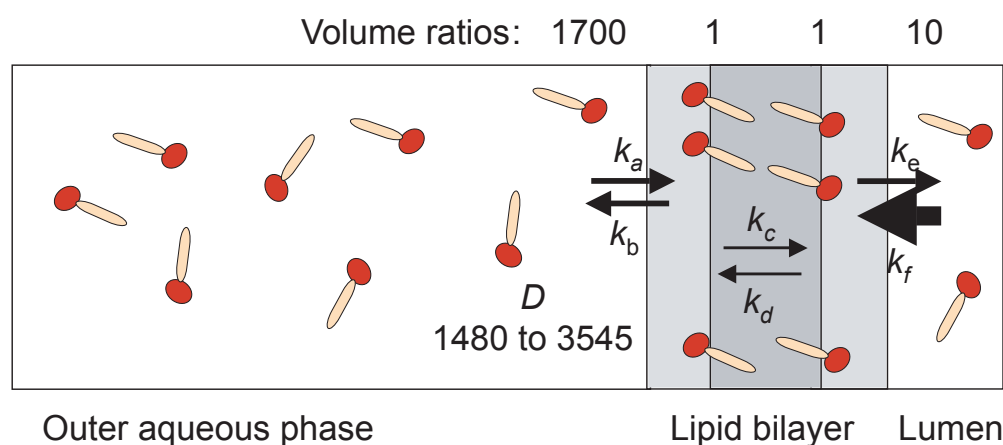


Fig. 4.3: **Apparent partition and translocation rate constants as a function of the partition coefficient and the volume ratios between the aqueous phases and the lipid leaflets.** Light grey denotes the lipid head group region of the lipid bilayer as well as the more hydrophilic part of salmeterol (ellipses), dark grey indicates the acyl chain region of the lipid bilayer as well as the more hydrophobic part of salmeterol. The aqueous phases outside the liposomes and inside (lumen) are shown in white. The volume ratios in the chip chamber are estimated as follows: the outer aqueous phase to the outer lipid leaflet volume ratio is about 1700/1 as calculated from the lipid amount on the chip and the chamber volume (see Methods). The volume ratio between the inner aqueous phase and the inner lipid leaflet is about 10/1, as estimated from the average liposome diameter, i.e. 100 nm, and a bilayer thickness of 7 nm. Considering the partition coefficients (for salmeterol between  $P_N$  1480 and  $P_C$  3545) and the above volume ratios, the apparent rate constants for the partitioning from the outer buffer phase into the outer lipid leaflet ( $k_a$ ) and the rate constants for the partitioning from the lipid leaflets to the respective aqueous phases ( $k_b$  and  $k_e$ ) must be in the same range at the lower partition coefficients. This is indicated in by the similar thickness of the arrows representing the respective apparent rate constants. At the higher  $D$  values, i.e. in the pH range  $< \text{pH } 8.8$ , the expected  $k_a$  is about two times higher than  $k_b$  and  $k_e$  ( $3545/1700$ ). The partition rate constant from the inner aqueous phase into the inner lipid leaflet ( $k_f$ ) is negligible since it is about 170 times higher than  $k_a$ , as estimated from the volume ratios ( $k_a \times 1700/10$ ). Simulating the situation with PermSim [Thomae et al., 2007] [www.biopharmacy.ethz.ch/simulations], assuming that the SPR signal follows the sum of the concentrations in the two lipid leaflets (sum of  $A_{lo}$  and  $A_{li}$  in the simulation tool) and taking into account the above discussed relationships between  $k_a$ ,  $k_b$ ,  $k_e$  and  $k_f$ , reveals a bi-phasic function (sum of  $A_{lo}$  and  $A_{li}$ ) if the translocation rate constants are one or more magnitudes lower than  $k_a$ . In this case the experimentally determined slow phase ( $k_2$ ) is mainly determined by the flip-flop rate constant ( $k_{c,d}$ ) and the fast phase ( $k_1$ ) by the apparent partition rate constant  $k_a$ . The simulated kinetics followed a mono-exponential function, if the flip-flop rate constants ( $k_c=k_d$ ) are similar or faster than  $k_a$ . Monoexponential kinetics were observed in our experiments for salmeterol at  $\text{pH} > 8.8$  while at  $\text{pH} < 8.8$ , the experimentally derived functions were bi-phasic. The membrane affinity of the net neutral salmeterol ( $P_N$ ) determined by equilibrium dialysis was between two and three times lower than that of the cation ( $P_C$ ), which predominates in the pH range  $< \text{pH } 8.8$ . Either  $k_a$  is reduced as compared to the cation or  $k_b$  is increased, or both. As discussed above kinetics were mono-exponential in the pH range where the net neutral form predominates. A reduction in  $k_a$  and/or an increase in the translocation rate constant ( $k_{c,d}$ ) compared to the lower pH range, resulting in similar rate constants for partitioning and translocation ( $k_a \sim k_{c,d}$ ) or in  $k_a < k_{c,d}$  would be in agreement with the mono-exponential kinetics.



## 4.1 Permeation kinetics

The results of the permeation experiments are discussed in this separate section of the thesis because they do not directly investigate the agonist/membrane interactions, however, they lay a basis for further investigations of the membrane interactions of  $\beta_2$ -adrenoceptor agonists. In this work we investigated the influence of  $\text{Tb}^{3+}$  on the permeation kinetics of the model compound OHNA in its anionic form and elucidated the thermodynamics of ion and neutral species permeation of this ACA. To explore the possibility that the kinetics and thermodynamics could be affected by the luminal complex formation between ACA and  $\text{Tb}^{3+}$ , we weakened the interaction between the OHNA anion and the lanthanide cation by prior complexation of  $\text{Tb}^{3+}$  with an excess of EDTA. In the presence of EDTA the apparent  $K_A$  of OHNA at pH 6.5 was reduced by about five orders of magnitude. The resulting  $K_A$  of the ternary complex was similar to that observed for the 1:1 complex of  $\text{Tb}^{3+}$  and neutral OHNA at pH 2.5. The influence of EDTA on the permeation rate was minor and even negligible for the fast phase of the permeation kinetic at 37°C, while the effects on the activation parameters of the process were striking. This fact indicates that the complex formation, which is used for the detection of permeant in the liposomal lumen, is not rate-determining in the permeation assay, however, it has an influence on the permeation process.

Comparison of the thermodynamic parameters of the fast phase of permeation kinetics in the presence and absence of EDTA at pH 6.5, unravels the significant influence of the complex formation on the activation energy of the observed process. While  $\Delta G^{\ddagger'}$  was unaffected (rate constants of the fast phase were hardly affected, see above),  $\Delta H^{\ddagger'}$  was strikingly higher in the  $\text{Tb}^{3+}$  than in the  $\text{Tb}^{3+}/\text{EDTA}$  system. The difference in  $\Delta H^{\ddagger'}$  was compensated by the corresponding change in  $-T \cdot \Delta S^{\ddagger'}$ . The high  $\Delta H^{\ddagger'}$  values in the  $\text{Tb}^{3+}$  system at pH 6.5 reflect the activation energy for the complex formation between OHNA anion and  $\text{Tb}^{3+}$ . The reduction of  $\Delta H^{\ddagger'}$  in the presence of EDTA indicates, that the activated state for the formation of the ternary complex of OHNA anion with  $\text{Tb}^{3+}/\text{EDTA}$  is significantly different from that between OHNA anion and  $\text{Tb}^{3+}$  in the absence of EDTA. The reduction in  $\Delta H^{\ddagger'}$  is presumably due to the charge neutralization by EDTA and the weaker hydration of the resulting  $\text{Tb}^{3+}/\text{EDTA}$  complex as compared to  $\text{Tb}^{3+}$  alone.

The permeation processes at pH 6.5 in presence of EDTA and at pH 2.5 in absence of EDTA, i.e. for the ACA anion and the neutral species, respectively, revealed similar  $\Delta H^{\ddagger'}$  values. They were maximally  $16.0 \pm 1.2$  kJ/mol for the fast phase and  $5.1 \pm 2.5$  kJ/mol for the slow phase (except pH 2.5 containing MOPS) and were similar or even lower at pH 6.5 than at pH 2.5. The charge of OHNA had thus no significant influence on  $\Delta H^{\ddagger'}$  of the observed

permeation kinetics. The main difference of anion and neutral species permeation in both the fast and the slow phases was the contribution of  $-T \cdot \Delta S^{\neq}$ .

This was not true for the slow phase in MOPS (see bracket above), where  $\Delta H^{\neq}$  was relatively high at pH 2.5 and the value for  $-T \cdot \Delta S^{\neq}$  accordingly lower. As the temperature-dependence of the latter system did not reveal a linear function in the Eyring plot, it is excluded from further interpretations.

From our data we can not extract how the interaction of OHNA anion and neutral form with  $\text{Tb}^{3+}/\text{EDTA}$  and with  $\text{Tb}^{3+}$ , respectively, contributes to  $\Delta H^{\neq}$  and  $\Delta S^{\neq}$ . However, the total contribution of  $\Delta H^{\neq}$  to the observed permeation process was relatively low for both ionization species.

We did not find any study in the literature that directly compared the permeation kinetics and thermodynamics of the permeation process of an acid or a base and its corresponding ion. This is the first time that we directly analyzed the two in parallel and found that the charge had no significant influence on  $\Delta H^{\neq}$  and a relatively small influence on  $\Delta G^{\neq}$  and  $\Delta S^{\neq}$ . This could be related to the exceptional possibilities for charge delocalization of OHNA [Dogra, 2005] but is in contrast to the expectations based on the Born energy, which is needed to partition a charge into an environment with a dielectric constant of two, as estimated for the membrane core [Lauger et al., 1981]. Assuming the charge can delocalize over the complete OHNA anion, the estimated Born energy would amount to  $\sim 27$  kJ/mol. In our experiments we found that the maximum difference between the free activation energy of the neutral and the anionic species was 9 kJ/mol considering the fast phase of the permeation kinetics. It should be added here that the Born energy was defined for electrolytes. The extrapolation to the size of organic ions may be erroneous.

According to the “flip-flop” model [Thomae et al., 2005, Lauger et al., 1981], the overall permeation process in our assay consists of four single equilibria: partitioning between the outer aqueous phase and the outer lipid leaflet, flip-flop between the two lipid leaflets, partitioning between the inner lipid leaflet and the aqueous inner space and finally, complex formation with  $\text{Tb}^{3+}$  or interaction with  $\text{Tb}^{3+}/\text{EDTA}$ . In the case of the biphasic permeation kinetics, more than one rate constant contribute to the observed kinetics. The apparent rate constants of the faster and slower phases at 25°C differed by at least a factor of ten between the systems in presence of EDTA at pH 6.5 and those in absence of EDTA at pH 2.5. This indicates, that none of the single rate constants had a significant influence on both phases, meaning that the two observed phases reflect different processes and are independent of each other. The apparent rate constants for the anion are lower than for the neutral form for both phases, indicating that at least two rate constants of the processes described above are slower for the anion than for the neutral species. The slow phases of both neutral and an-

ionic ( $\text{Tb}^{3+}/\text{EDTA}$  system) species are characterized by negligible  $\Delta H^{\neq'}$  values and appear to be determined by  $T \cdot \Delta S^{\neq'}$  alone (MOPS pH 2.5 is excepted, see above). Considering the low membrane affinities of both ionization species ( $\log P < 1$ ) [Thomae et al., 2005] and the relatively high ratios of aqueous volumes to barrier volume on both sides of the membrane, the partitioning rate constants may be lower than the flip-flop rate constants.

In conclusion, comparing the permeation of anionic and neutral OHNA the main differences lie in  $T \cdot \Delta S^{\neq'}$  rather than in  $\Delta H^{\neq'}$ . The rate-limiting step for ion permeation is probably the dehydration, the charge contribution to permeation is in  $T \cdot \Delta S^{\neq'}$  rather than in  $\Delta H^{\neq'}$ . The difference in the permeation kinetics of anion and neutral species is temperature-independent, as directly seen from the parallel lines in the Eyring plots.

In our model,  $\Delta S^{\neq'}$  is not only influenced by the degree of freedom of the activated system, but also by the size of the liposomes, i.e. by the ratio between the smaller aqueous volume and the barrier area. An increase of this ratio should lead to lower apparent rate constants and a corresponding increase in  $\Delta S^{\neq'}$ , as seen from Eq. 2.22. The activation energy and  $\Delta H^{\neq'}$  should remain unaffected by a change in the volume/area ratio.

This study provides the basis for further developing the Tb(III)-permeation assay as a method for studying membrane permeation of  $\beta_2$ -agonists. The Tb(III) liposome permeation assay allows to explore lipid bilayer permeation kinetics of ACAs over a broad pH range. The  $\beta_2$ -agonists and any other compound may be covalently linked to an ACA to shed light on their permeation behavior. A similar approach was used to study peptide permeation [Kramer, 2001, Shimanouchi et al., 2007].



## 5 Conclusions and Outlook

The main question we address in this work is how the differences of the time to onset and duration of the therapeutical effect of indacaterol and salmeterol are related to their interactions with lipid membranes.

We suggest a new model that is a further development of the "micro-kinetic model" suggested by Anderson et al. [1994]; we consider an additional step of reaction with the drug in a proximal position to the receptor. The proximal free drug concentration is sustained over-time by the local release from the lipid compartments long after the initial inhaled bulk free fraction has been eliminated. For indacaterol this is likely to be one of the main mechanisms that provides extended duration of action, and its two fold higher affinity for raft microdomains compared to salmeterol might contribute to this difference in duration of action.

According to our model the fast onset of indacaterol can be explained by two complementary properties. The higher efficacy of indacaterol implies that at equi-effective doses, a smaller number of  $\beta_2$ -adrenoceptor need to be reached compared to a partial agonist with similar hydrophobicity such as salmeterol. It is also possible that zwitterionic lipophilic compounds might have a faster diffusion rate across tissues. Indacaterol is mainly zwitterionic at physiological pH while salmeterol is mainly cationic.

SPR experiments revealed biphasic kinetics of interactions of indacaterol and salmeterol with immobilized membranes at pH 7.4. The slower phase was assigned to membrane translocation and it was two fold faster, at pH values  $< 8.8$ , for indacaterol than for salmeterol, supporting the view of a faster diffusion rate across tissues leading to a faster onset of action.

The permeation experiments with OHNA lay a basis for further investigations of the membrane interaction of  $\beta_2$  agonists. Compounds of interest could be conjugated to an ACA and studied in the lanthanide liposomal assay to disclose the kinetics and thermodynamics of membrane permeation. There are no informations available on the permeation of

$\beta_2$ -adrenoceptor agonists across lipid bilayers, the possibility of investigating the thermodynamics of their permeation process could open new interpretations for a detailed understanding of the differences in the biological effect of the agonists.

The present study can be extended to explore further details of drug/membrane interactions. Even though the SPR experiments give an idea of the kinetics of drug-membrane interaction more detailed investigations are desirable. It would be highly interesting to follow the interactions with relaxation methods or stopped flow techniques in order to define the micro-kinetics of drug-membrane interactions. Certainly, insight into the kinetics of drug-membrane interaction would contribute to the understanding of the mechanism of the *in vivo* effects. However, to definitively disclose the intriguing properties of  $\beta_2$  agonists, it would be helpful to perform experiments including the  $\beta_2$  adrenoceptor in the model membrane. The investigation of the rate constants defining the drug/receptor interaction may be resolute for a more detailed understanding of the various parameters responsible for the pharmacological properties of long acting  $\beta_2$ -adrenoceptor agonist.

# Bibliography

- Y. N. Abdiche and D. G. Myszka. Probing the mechanism of drug/lipid membrane interactions using biacore. *Anal Biochem*, 328(2):233–43, 2004.
- Chadha H. S. Abraham M. H. Applications of a solvation equation to drug transport properties. In Pliska V. Testa B. and Waterbeemd H. editors, editors, *Lipophilicity in drug action and toxicology.*, volume 4, pages 311–337. VHC Verlagsgesellschaft mbH., Weinheim, 1996.
- V. Alikhani, D. Beer, D. Bentley, I. Bruce, B. M. Cuenoud, R. A. Fairhurst, P. Gedeck, S. Haberthuer, C. Hayden, D. Janus, L. Jordan, C. Lewis, K. Smithies, and E. Wissler. Long-chain formoterol analogues: an investigation into the effect of increasing amino-substituent chain length on the beta2-adrenoceptor activity. *Bioorg Med Chem Lett*, 14(18):4705–10, 2004.
- D. Allan. Mapping the lipid distribution in the membranes of bhk cells (mini-review). *Mol Membr Biol*, 13(2):81–4, 1996.
- J. A. Allen, J. Z. Yu, R. J. Donati, and M. M. Rasenick. Beta-adrenergic receptor stimulation promotes g alpha s internalization through lipid rafts: a study in living cells. *Mol Pharmacol*, 67(5):1493–504, 2005.
- G. Anderluh, M. Besenicar, A. Kladnik, J. H. Lakey, and P. Macek. Properties of nonfused liposomes immobilized on an l1 biacore chip and their permeabilization by a eukaryotic pore-forming toxin. *Anal Biochem*, 344(1):43–52, 2005.
- G. P. Anderson, A. Linden, and K. F. Rabe. Why are long-acting beta-adrenoceptor agonists long-acting? *Eur Respir J*, 7(3):569–78, 1994.
- R. P. Austin, P. Barton, R. V. Bonnert, R. C. Brown, P. A. Cage, D. R. Cheshire, A. M. Davis, I. G. Dougall, F. Ince, G. Pairaudeau, and A. Young. Qsar and the rational design of long-acting dual d2-receptor/beta 2-adrenoceptor agonists. *J Med Chem*, 46(15):3210–20, 2003.

- A. Avdeef, K. J. Box, J. E. Comer, C. Hibbert, and K. Y. Tam. pH-metric log<sub>p</sub> 10. determination of liposomal membrane-water partition coefficients of ionizable drugs. *Pharm Res*, 15(2):209–15, 1998.
- C. L. Baird, E. S. Courtenay, and D. G. Myszka. Surface plasmon resonance characterization of drug/liposome interactions. *Anal Biochem*, 310(1):93–9, 2002.
- A. D. Bangham, M. M. Standish, and J. C. Watkins. Diffusion of univalent ions across the lamellae of swollen phospholipids. *Journal of Molecular Biology*, 13(1):238–252, 1965.
- B. Barnes, P. Effect of beta-agonists in asthma treatment. In M. Powels R., O Byrne P., editor, *Beta2-agonists in asthma treatment.*, volume 1, pages 35–64. Marcel Decker, New York, U.S., 1977.
- C. Battram, S. J. Charlton, B. Cuenoud, M. R. Dowling, R. A. Fairhurst, D. Farr, J. R. Fozard, J. R. Leighton-Davies, C. A. Lewis, L. McEvoy, R. J. Turner, and A. Trifileff. In vitro and in vivo pharmacological characterization of 5-[(r)-2-(5,6-diethyl-indan-2-ylamino)-1-hydroxy-ethyl]-8-hydroxy-1h-quinolin-2-one (indacaterol), a novel inhaled beta(2) adrenoceptor agonist with a 24-h duration of action. *J Pharmacol Exp Ther*, 317(2):762–70, 2006.
- K. M. Beeh, E. Derom, F. Kannies, R. Cameron, M. Higgins, and A. van As. Indacaterol, a novel inhaled beta2-agonist, provides sustained 24-h bronchodilation in asthma. *Eur Respir J*, 29(5):871–8, 2007.
- J. Beier, P. Chanez, J. B. Martinot, A. J. Schreurs, R. Tkacova, W. Bao, D. Jack, and M. Higgins. Safety, tolerability and efficacy of indacaterol, a novel once-daily beta(2)-agonist, in patients with copd: a 28-day randomised, placebo controlled clinical trial. *Pulm Pharmacol Ther*, 20(6):740–9, 2007.
- S. Belli, P. M. Elsener, H. Wunderli-Allenspach, and D. Kraemer, S. Cholesterol-mediated activation of p-glycoprotein: Distinct effects on basal and drug-induced atpase activities. *J Pharm Sci*, accepted July 2008, 2008.
- A. Bergendal, A. Linden, B. E. Skoogh, M. Gerspacher, G. P. Anderson, and C. G. Lofdahl. Extent of salmeterol-mediated reassertion of relaxation in guinea-pig trachea pretreated with aliphatic side chain structural analogues. *Br J Pharmacol*, 117(6):1009–15, 1996.
- G. V. Betageri and J. A. Rogers. Thermodynamic of partitioning of beta-blockers in the n-octanol-buffer and liposome systems. *Int. J. Pharm.*, 46:95–102, 1988.
- G. Bouchard, A. Pagliara, P. A. Carrupt, B. Testa, V. Gobry, and H. H. Girault. The-



- oretical and experimental exploration of the lipophilicity of zwitterionic drugs in the 1,2-dichloroethane/water system. *Pharm Res*, 19(8):1150–9, 2002.
- R. T. Brittain. Approaches to a long-acting, selective beta 2-adrenoceptor stimulant. *Lung*, 168 Suppl:111–4, 1990.
- B. B. Brodie and C. A. Hogben. Some physico-chemical factors in drug action. *J Pharm Pharmacol*, 9(6):345–80, 1957.
- D. A. Brown and J. K. Rose. Sorting of gpi-anchored proteins to glycolipid-enriched membrane subdomains during transport to the apical cell surface. *Cell*, 68(3):533–44, 1992. 0092-8674 (Print) Journal Article Research Support, Non-U.S. Gov't Research Support, U.S. Gov't, P.H.S.
- M. F. Brown and G. D. Williams. Membrane nmr: a dynamic research area. *J Biochem Biophys Methods*, 11(2-3):71–81, 1985. 0165-022X (Print) Journal Article Research Support, Non-U.S. Gov't Research Support, U.S. Gov't, P.H.S. Review.
- K. Bucher, C. A. Besse, S. W. Kamau, H. Wunderli-Allenspach, and S. D. Kramer. Isolated rafts from adriamycin-resistant p388 cells contain functional atpases and provide an easy test system for p-glycoprotein-related activities. *Pharm Res*, 22(3):449–57, 2005. 0724-8741 (Print) Journal Article.
- G. Camenisch, J. Alsenz, H. van de Waterbeemd, and G. Folkers. Estimation of permeability by passive diffusion through caco-2 cell monolayers using the drugs' lipophilicity and molecular weight. *Eur J Pharm Sci*, 6(4):317–24, 1998.
- G. Cevc. Membrane electrostatics. *Biochim Biophys Acta*, 1031(3):311–82, 1990.
- V. Cherezov, D. M. Rosenbaum, M. A. Hanson, S. G. Rasmussen, F. S. Thian, T. S. Kobilka, H. J. Choi, P. Kuhn, W. I. Weis, B. K. Kobilka, and R. C. Stevens. High-resolution crystal structure of an engineered human beta2-adrenergic g protein-coupled receptor. *Science*, 318(5854):1258–65, 2007.
- A. G. Chuchalin, A. N. Tsoi, K. Richter, N. Krug, R. Dahl, P. B. Luursema, R. Cameron, W. Bao, M. Higgins, R. Woessner, and A. van As. Safety and tolerability of indacaterol in asthma: a randomized, placebo-controlled 28-day study. *Respir Med*, 101(10):2065–75, 2007.
- R. B. Clark, C. Allal, J. Friedman, M. Johnson, and R. Barber. Stable activation and desensitization of beta 2-adrenergic receptor stimulation of adenylyl cyclase by salmeterol: evidence for quasi-irreversible binding to an exosite. *Mol Pharmacol*, 49(1):182–9, 1996.

- R. J. Clarke. Binding and diffusion kinetics of the interaction of a hydrophobic potential-sensitive dye with lipid vesicles. *Biophys Chem*, 39(1):91–106, 1991.
- E. Danelian, A. Karlen, R. Karlsson, S. Winiwarter, A. Hansson, S. Lofas, H. Lennernas, and M. D. Hamalainen. Spr biosensor studies of the direct interaction between 27 drugs and a liposome surface: correlation with fraction absorbed in humans. *J Med Chem*, 43(11):2083–6, 2000.
- J. M. Diamond and Y. Katz. Interpretation of nonelectrolyte partition coefficients between dimyristoyl lecithin and water. *J Membr Biol*, 17(2):121–54, 1974.
- A. Disalvo, E. and S. Simon. *Permeability and stability of lipid bilayers*. CRC Press, Florida U.S., 1995.
- S.K. Dogra. Spectral characteristics of 2-hydroxynicotinic acid: effects of solvent and acid or base concentrations. *J. Mol. Struct.*, 737:189–199, 2005.
- C. Dordas and P. H. Brown. Permeability of boric acid across lipid bilayers and factors affecting it. *J Membr Biol*, 175(2):95–105, 2000.
- G. D. Eytan. Mechanism of multidrug resistance in relation to passive membrane permeation. *Biomed Pharmacother*, 59(3):90–7, 2005.
- G. D. Eytan and P. W. Kuchel. Mechanism of action of p-glycoprotein in relation to passive membrane permeation. *Int Rev Cytol*, 190:175–250, 1999.
- F. Frezard and A. Garnier-Suillerot. Permeability of lipid bilayer to anthracycline derivatives. role of the bilayer composition and of the temperature. *Biochimica et Biophysica Acta*, 1389(1):13–22, 1998.
- A. Frostell-Karlsson, H. Widegren, C. E. Green, M. D. Hamalainen, L. Westerlund, R. Karlsson, K. Fenner, and H. van de Waterbeemd. Biosensor analysis of the interaction between drug compounds and liposomes of different properties; a two-dimensional characterization tool for estimation of membrane absorption. *J Pharm Sci*, 94(1):25–37, 2005.
- Robrt B. Gennis. *Biomembranes*. CRC Press, Boston, 1989.
- S. A. Green, D. A. Rathz, A. J. Schuster, and S. B. Liggett. The ile164 beta(2)-adrenoceptor polymorphism alters salmeterol exosite binding and conventional agonist coupling to g(s). *Eur J Pharmacol*, 421(3):141–7, 2001.
- J. Gutknecht and D. C. Tosteson. Diffusion of weak acids across lipid bilayer membranes: effects of chemical reactions in the unstirred layers. *Science*, 182(118):1258–61, 1973.

- A. J. Halayko, T. Tran, and R. Gosens. Phenotype and functional plasticity of airway smooth muscle: role of caveolae and caveolins. *Proc Am Thorac Soc*, 5(1):80–8, 2008.
- K. K. Halling, B. Ramstedt, and J. P. Slotte. Glycosylation induces shifts in the lateral distribution of cholesterol from ordered towards less ordered domains. *Biochim Biophys Acta*, 2008. 0006-3002 (Print) Journal article.
- K. Hashizaki, H. Taguchi, C. Itoh, H. Sakai, M. Abe, Y. Saito, and N. Ogawa. Effects of poly(ethylene glycol) (peg) chain length of peg-lipid on the permeability of liposomal bilayer membranes. *Chemical and Pharmaceutical Bulletin*, 51(7):815–820, 2003.
- U. Hellwich and R. Schubert. Concentration-dependent binding of the chiral beta-blocker oxprenolol to isoelectric or negatively charged unilamellar vesicles. *Biochem Pharmacol*, 49(4):511–7, 1995.
- C. A. Hogben, D. J. Tocco, B. B. Brodie, and L. S. Schanker. On the mechanism of intestinal absorption of drugs. *J Pharmacol Exp Ther*, 125(4):275–82, 1959.
- C. Huang and J. T. Mason. Geometric packing constraints in egg phosphatidylcholine vesicles. *Proc Natl Acad Sci U S A*, 75(1):308–10, 1978.
- J. H. Ipsen, G. Karlstrom, O. G. Mouritsen, H. Wennerstrom, and M. J. Zuckermann. Phase equilibria in the phosphatidylcholine-cholesterol system. *Biochim Biophys Acta*, 905(1):162–172, 1987.
- K. Jacobson, O. G. Mouritsen, and R. G. Anderson. Lipid rafts: at a crossroad between cell biology and physics. *Nat Cell Biol*, 9(1):7–14, 2007.
- A. B. Jeppsson, C. G. Lofdahl, B. Waldeck, and E. Widmark. On the predictive value of experiments in vitro in the evaluation of the effect duration of bronchodilator drugs for local administration. *Pulm Pharmacol*, 2(2):81–5, 1989.
- A. B. Jeppsson, C. Roos, B. Waldeck, and E. Widmark. Pharmacodynamic and pharmacokinetic aspects on the transport of bronchodilator drugs through the tracheal epithelium of the guinea-pig. *Pharmacol Toxicol*, 64(1):58–63, 1989b.
- M. Johnson. Pharmacology of long-acting beta-agonists. *Ann Allergy Asthma Immunol*, 75(2):177–9, 1995.
- M. Johnson. The beta-adrenoceptor. *Am J Respir Crit Care Med*, 158(5 Pt 3):S146–53, 1998.
- N. Kahya, D. Scherfeld, K. Bacia, and P. Schwille. Lipid domain formation and dynamics

- in giant unilamellar vesicles explored by fluorescence correlation spectroscopy. *Journal of Structural Biology*, 147(1):77–89, 2004.
- R. D. Kaiser and E. London. Location of diphenylhexatriene (dph) and its derivatives within membranes: comparison of different fluorescence quenching analyses of membrane depth. *Biochemistry*, 37(22):8180–90, 1998. 0006-2960 (Print) Comparative Study Journal Article Research Support, U.S. Gov't, P.H.S.
- S. W. Kamau, S. D. Kramer, M. Gunthert, and H. Wunderli-Allenspach. Effect of the modulation of the membrane lipid composition on the localization and function of p-glycoprotein in *mdr1-mdck* cells. *In Vitro Cell Dev Biol Anim*, 41(7):207–16, 2005.
- F. Kannies, R. A. Jorres, and H. Magnussen. Effect of reproterol either alone or combined with disodium cromoglycate on airway responsiveness to methacholine. *Pulm Pharmacol Ther*, 18(5):315–20, 2005.
- E. H. Kerns. High throughput physicochemical profiling for drug discovery. *J Pharm Sci*, 90(11):1838–58, 2001.
- A. M. Kleinfeld and J. Storch. Transfer of long-chain fluorescent fatty acids between small and large unilamellar vesicles. *Biochemistry*, 32(8):2053–61, 1993.
- A. M. Kleinfeld, P. Chu, and J. Storch. Flip-flop is slow and rate limiting for the movement of long chain anthroyloxy fatty acids across lipid vesicles. *Biochemistry*, 36(19):5702–11, 1997.
- K. A. Konnors, editor. *Binding Constants. The measurement of molecular complex stability*. John Wiley and Sons, Inc., New York, 1987.
- S. D. Kramer. Liposomes/wather partitioning: theory, techniques and applications. In B. Testa, H. van de Waterbeemd, G. Folkers, and R. Guy, editors, *Pharmacokinetic optimization in drug research*, volume 1, pages 401–428. VHCA Wiley-VHC Zurich, Zurich Weinheim, 2001.
- S. D. Kramer. Lipid bilayers in adme: permeation barriers and distribution compartments. In B. Testa, S. D. Kramer, H. Wunderli-Allenspach, and G. Folkers, editors, *Pharmacokinetic profiling in drug research: biological, physiochemical and computational strategies*, volume 1. Wiley-VHC, Weinheim, 2005.
- S. D. Kramer and H. Wunderli-Allenspach. No entry for tat(44-57) into liposomes and intact *mdck* cells: novel approach to study membrane permeation of cell-penetrating peptides. *Biochim Biophys Acta*, 1609(2):161–9, 2003.

- S. D. Kramer, C. Jakits-Deiser, and H. Wunderli-Allenspach. Free fatty acids cause pH-dependent changes in drug-lipid membrane interactions around physiological pH. *Pharm Res*, 14(6):827–32, 1997.
- S. D. Kramer, A. Braun, C. Jakits-Deiser, and H. Wunderli-Allenspach. Towards the predictability of drug-lipid membrane interactions: the pH-dependent affinity of propranolol to phosphatidylinositol containing liposomes. *Pharm Res*, 15(5):739–44, 1998. 0724-8741 (Print) Journal Article.
- M. Kurschner, K. Nielsen, J. R. von Langen, W. A. Schenk, U. Zimmermann, and V. L. Sukhorukov. Effect of fluorine substitution on the interaction of lipophilic ions with the plasma membrane of mammalian cells. *Biophys J*, 79(3):1490–7, 2000.
- D. D. Lasic. *Liposomes: from physics to applications*. Elsevier Science Publishers B.V., Amsterdam, 1993.
- P. Lauger, R. Benz, G. Stark, E. Bamberg, P. C. Jordan, A. Fahr, and W. Brock. Relaxation studies of ion transport systems in lipid bilayer membranes. *Q Rev Biophys*, 14(4):513–98, 1981.
- B. R. Lentz. Use of fluorescent probes to monitor molecular order and motions within liposome bilayers. *Chem Phys Lipids*, 64(1-3):99–116, 1993.
- A. Lindberg, Z. Szalai, T. Pullerits, and E. Radezky. Fast onset of effect of budesonide/formoterol versus salmeterol/fluticasone and salbutamol in patients with chronic obstructive pulmonary disease and reversible airway obstruction. *Respirology*, 12(5):732–9, 2007.
- A. Linden, K. F. Rabe, and C. G. Lofdahl. Pharmacological basis for duration of effect: formoterol and salmeterol versus short-acting beta 2-adrenoceptor agonists. *Lung*, 174(1):1–22, 1996.
- C. A. Lipinski, F. Lombardo, B. W. Dominy, and P. J. Feeney. Experimental and computational approaches to estimate solubility and permeability in drug discovery and development settings. *Adv Drug Deliv Rev*, 46(1-3):3–26, 2001.
- C. G. Lofdahl. Basic pharmacology of new long-acting sympathomimetics. *Lung*, 168 Suppl: 18–21, 1990.
- R. G. Males and F. G. Herring. A 1h-nmr study of the permeation of glycolic acid through phospholipid membranes. *Biochim Biophys Acta*, 1416(1-2):333–8, 1999.
- A. Malkia, L. Murtomaki, A. Urtti, and K. Kontturi. Drug permeation in biomembranes: in

- vitro and in silico prediction and influence of physicochemical properties. *Eur J Pharm Sci*, 23(1):13–47, 2004.
- M. Marenchino, A. L. Alpstag-Wohrle, B. Christen, H. Wunderli-Allenspach, and S. D. Kramer. Alpha-tocopherol influences the lipid membrane affinity of desipramine in a ph-dependent manner. *Eur J Pharm Sci*, 21(2-3):313–21, 2004. 0928-0987 (Print) Comparative Study Journal Article Research Support, Non-U.S. Gov't.
- D. Marsh, A. M., and D. Phil. *Handbook of lipid bilayers*. CRC Press, Boston, 1990.
- R. C. Mashru, V. B. Sutariya, M. G. Sankalia, and J. M. Sankalia. Effect of ph on in vitro permeation of ondansetron hydrochloride across porcine buccal mucosa. *Pharm Dev Technol*, 10(2):241–7, 2005.
- R. P. Mason, D. G. Rhodes, and L. G. Herbette. Reevaluating equilibrium and kinetic binding parameters for lipophilic drugs based on a structural model for drug interaction with biological membranes. *J Med Chem*, 34(3):869–77, 1991.
- L. D. Mayer, M. J. Hope, and P. R. Cullis. Vesicles of variable sizes produced by a rapid extrusion procedure. *Biochim Biophys Acta*, 858(1):161–8, 1986. 0006-3002 (Print) Journal Article Research Support, Non-U.S. Gov't.
- S. McLaughlin. The electrostatic properties of membranes. *Annual Review of Biophysics and Biophysical Chemistry*, 18:113–136, 1989. 0883-9182 (Print) Journal Article Review.
- O. G. Mouritsen and K. Jorgensen. Small-scale lipid-membrane structure: simulation versus experiment. *Current Opinion in Structural Biology*, 7(4):518–527, 1997.
- S. Munro. Lipid rafts: elusive or illusive? *Cell*, 115(4):377–88, 2003.
- R. Neubert. Ion pair transport across membranes. *Pharm Res*, 6(9):743–7, 1989.
- K. Ochsner, M., M. Jaekel, M. Mutz, P. Anderson, G., and E. John. Comparative biophysical analysis of the interaction of bronchodilating beta(2)-adrenoceptor agonists with lipid membranes. *Eur J Pharm Sci*, 34:451–462, 1999.
- A. Pagliara, M. Reist, S. Geinoz, P. A. Carrupt, and B. Testa. Evaluation and prediction of drug permeation. *Journal of Pharmacy and Pharmacology*, 51(12):1339–1357, 1999.
- M. Palmqvist, G. Persson, L. Lazer, J. Rosenborg, P. Larsson, and J. Lotvall. Inhaled dry-powder formoterol and salmeterol in asthmatic patients: onset of action, duration of effect and potency. *Eur Respir J*, 10(11):2484–9, 1997.
- W. M. Pardridge. Transport of small molecules through the blood-brain barrier: biology and methodology. *Advanced Drug Delivery Reviews*, 15(1-3):5–36, 1995.

- S. Paula, A. G. Volkov, and D. W. Deamer. Permeation of halide anions through phospholipid bilayers occurs by the solubility-diffusion mechanism. *Biophys J*, 74(1):319–27, 1998.
- G.M. Pauletti and H. Wunderli-Allenspach. Partition coefficient in vitro: artificial membranes as a standardized distribution model. *Eur J Pharm Sci*, 1:273–82, 1994.
- J. T. Penniston, L. Beckett, D. L. Bentley, and C. Hansch. Passive permeation of organic compounds through biological tissue: a non-steady-state theory. *Mol Pharmacol*, 5(4):333–41, 1969.
- G. Plember van Balen, G. Caron, G. Ermondi, A. Pagliara, T. Grandi, G. Bouchard, R. Fruttero, P. A. Carrupt, and B. Testa. Lipophilicity behaviour of the zwitterionic antihistamine cetirizine in phosphatidylcholine liposomes/water systems. *Pharm Res*, 18(5):694–701, 2001.
- A. Pokorny, P. F. Almeida, E. C. Melo, and W. L. Vaz. Kinetics of amphiphile association with two-phase lipid bilayer vesicles. *Biophys J*, 78(1):267–80, 2000.
- K. Rebolj, N. P. Ulrih, P. Macek, and K. Sepcic. Steroid structural requirements for interaction of ostreolysin, a lipid-raft binding cytolysin, with lipid monolayers and bilayers. *Biochim Biophys Acta*, 1758(10):1662–70, 2006.
- T. Rodgers, D. Leahy, and M. Rowland. Tissue distribution of basic drugs: accounting for enantiomeric, compound and regional differences amongst beta-blocking drugs in rat. *J Pharm Sci*, 94(6):1237–48, 2005.
- D. M. Rosenbaum, V. Cherezov, M. A. Hanson, S. G. Rasmussen, F. S. Thian, T. S. Kobilka, H. J. Choi, X. J. Yao, W. I. Weis, R. C. Stevens, and B. K. Kobilka. GPCR engineering yields high-resolution structural insights into beta2-adrenergic receptor function. *Science*, 318(5854):1266–73, 2007.
- M. M. Sacre and J. F. Tocanne. Importance of glycerol and fatty acid residues on the ionic properties of phosphatidylglycerols at the air-water interface. *Chem Phys Lipids*, 18(3-4):334–54, 1977.
- Z. Salamon, H. A. Macleod, and G. Tollin. Surface plasmon resonance spectroscopy as a tool for investigating the biochemical and biophysical properties of membrane protein systems. i: Theoretical principles. *Biochim Biophys Acta*, 1331(2):117–29, 1997a.
- Z. Salamon, H. A. Macleod, and G. Tollin. Surface plasmon resonance spectroscopy as a tool for investigating the biochemical and biophysical properties of membrane protein systems. ii: Applications to biological systems. *Biochim Biophys Acta*, 1331(2):131–52, 1997b.

- S. M. Saparov, Y. N. Antonenko, and P. Pohl. A new model of weak acid permeation through membranes revisited: does overton still rule? *Biophys J*, 90(11):L86–8, 2006.
- P. Sengupta, B. Baird, and D. Holowka. Lipid rafts, fluid/fluid phase separation, and their relevance to plasma membrane structure and function. *Semin Cell Dev Biol*, 18(5):583–90, 2007.
- P. R. Seo, Z. S. Teksin, J. P. Kao, and J. E. Polli. Lipid composition effect on permeability across pampa. *Eur J Pharm Sci*, 29(3-4):259–68, 2006. 0928-0987 (Print) Journal Article Research Support, Non-U.S. Gov't.
- T. Shimanouchi, P. Walde, J. Gardiner, Y. R. Mahajan, D. Seebach, A. Thomae, S. D. Kramer, M. Voser, and R. Kuboi. Permeation of a beta-heptapeptide derivative across phospholipid bilayers. *Biochim Biophys Acta*, 1768(11):2726–36, 2007.
- P. A. Shore, B. B. Brodie, and C. A. Hogben. The gastric secretion of drugs: a ph partition hypothesis. *J Pharmacol Exp Ther*, 119(3):361–9, 1957.
- H. Simonin, L. Beney, and P. Gervais. Controlling the membrane fluidity of yeasts during coupled thermal and osmotic treatments. *Biotechnol Bioeng*, 2007. 0006-3592 (Print) Journal article.
- K. Simons and E. Ikonen. Functional rafts in cell membranes. *Nature*, 387(6633):569–72, 1997.
- S. J. Singer and Garth L. Nicolson. The fluid mosaic model of the structure of cell membranes. *Science*, 175(4023):720–731, 1972. TY - JOUR M1 - Article type: Full Length Article / Full publication date: Feb. 18, 1972 (19720218). / Copyright 1972 American Association for the Advancement of Science.
- W. D. Stein. Kinetics of the multidrug transporter (p-glycoprotein) and its reversal. *Physiol Rev*, 77(2):545–90, 1997.
- K. Takacs-Novak and G. Szasz. Ion-pair partition of quaternary ammonium drugs: the influence of counter ions of different lipophilicity, size, and flexibility. *Pharm Res*, 16(10):1633–8, 1999.
- H. Takanaga, I. Tamai, and A. Tsuji. pH-dependent and carrier-mediated transport of salicylic acid across caco-2 cells. *J Pharm Pharmacol*, 46(7):567–70, 1994.
- A. Teschemacher and H. Lemoine. Kinetic analysis of drug-receptor interactions of long-acting beta2 sympathomimetics in isolated receptor membranes: evidence against prolonged effects of salmeterol and formoterol on receptor-coupled adenylyl cyclase. *J Pharmacol Exp Ther*, 288(3):1084–92, 1999.



- B. Testa, P. A. Carrupt, P. Gaillard, F. Billois, and P. Weber. Lipophilicity in molecular modeling. *Pharm Res*, 13(3):335–43, 1996.
- B. Testa, H. van de Waterbeemd, G. Folkers, and R. Guy. *Pharmacokinetic Optimization in Drug Research*. Verlag Helvetica Chimica Acta Wiley-VCH, Zürich, 1. edition, 2001.
- A. V. Thomae, H. Wunderli-Allenspach, and S. D. Kramer. Permeation of aromatic carboxylic acids across lipid bilayers: the ph-partition hypothesis revisited. *Biophys J*, 89(3):1802–11, 2005.
- A. V. Thomae, T. Koch, C. Panse, H. Wunderli-Allenspach, and S. D. Kramer. Comparing the lipid membrane affinity and permeation of drug-like acids: the intriguing effects of cholesterol and charged lipids. *Pharm Res*, 24(8):1457–72, 2007.
- A. Ullman, A. Bergendal, A. Linden, B. Waldeck, B. E. Skoogh, and C. G. Lofdahl. Onset of action and duration of effect of formoterol and salmeterol compared to salbutamol in isolated guinea pig trachea with or without epithelium. *Allergy*, 47(4 Pt 2):384–7, 1992.
- J. A. van Noord, J. J. Smeets, J. A. Raaijmakers, A. M. Bommer, and F. P. Maesen. Salmeterol versus formoterol in patients with moderately severe asthma: onset and duration of action. *Eur Respir J*, 9(8):1684–8, 1996.
- D. F. Veber, S. R. Johnson, H. Y. Cheng, B. R. Smith, K. W. Ward, and K. D. Kopple. Molecular properties that influence the oral bioavailability of drug candidates. *J Med Chem*, 45(12):2615–23, 2002.
- H. P. Voss, D. Donnell, and A. Bast. Atypical molecular pharmacology of a new long-acting beta 2-adrenoceptor agonist, ta 2005. *Eur J Pharmacol*, 227(4):403–9, 1992.
- B. Waldeck. Beta-adrenoceptor agonists and asthma—100 years of development. *Eur J Pharmacol*, 445(1-2):1–12, 2002.
- T. Wegener, H. Hedenstrom, and B. Melander. Rapid onset of action of inhaled formoterol in asthmatic patients. *Chest*, 102(2):535–8, 1992.
- J. Wilschut, N. Duzgunes, R. Fraley, and D. Papahadjopoulos. Studies on the mechanism of membrane fusion: kinetics of calcium ion induced fusion of phosphatidylserine vesicles followed by a new assay for mixing of aqueous vesicle contents. *Biochemistry*, 19(26):6011–6021, 1980.
- W. Yamanaka and R. Ostwald. Lipid composition of heart, kidney and lung in guinea pigs made anemic by dietary cholesterol. *J Nutr*, 95(3):381–7, 1968.

B. J. Zwolinski, H. Eyring, and Reese C. E. Diffusion and membrane permeability. i. *J. Physiol. Colloid. Chem.*, 53:1426–1453, 1949.

# List of Publications

## Journal Articles

T. Biver, D. Lombardi, F. Secco, M.R. Tine', and M. Venturini, A. Bianchi, B. Valtancoli, *Kinetic and equilibrium studies on the polyazamacrocyclic neotetren: metal-complex formation and DNA interaction*. Dalton Trans. 2006 (12) 1524-33.

D. Lombardi, Bernard Cuenoud, Heidi Wunderli-Allenspach, Stefanie D. Krämer, *Characterization of the Interactions between Salmeterol and Lipid Bilayers by Surface Plasmon Resonance and Equilibrium Dialysis with Liposomes*. Submitted.

## Posters

6th EBSA and British Biophysical Society Congress, July 14-18 2007, Imperial College London, U.K.

Poster: D. Lombardi, H. Wunderli-Hallenspach, S. D. Kraemer, *Lipid bilayer permeation studies using terbium (III) complexes as a probe: thermodynamic and kinetic characterization*

Biophysical Society 51st Annual Meeting, March 3-7, 2007 Baltimore, MD, USA

Poster: D. Lombardi, B. Cuenoud, S. D. Kraemer, *Kinetic Study of Drug/Lipid Membrane Interactions with Surface Plasmon Resonance Spectroscopy (SPR)*.

EUFEPS conference on Optimization of Drug-Like Properties of Leads in Discovery: Fine-Tuning the Physchem-Biopharmaceutical-ADME-Tox Profile. March 2-3, 2006 ETH Zurich, Switzerland.

Poster: D. Lombardi, H. Wunderli-Hallenspach, S. D. Kraemer, *Terbium(III) complexes as a probe in lipid bilayer permeation studies: thermodynamic and kinetic characterization of the complex formation between terbium(III) and aromatic carboxylic acids*.



# Curriculum Vitae

## Biological data

*Name* Dario Lombardi  
*Date of birth* 09.04.1979  
*Place of birth* Piombino, LI, Italy

## Education

*04/2005-09/2008* Ph. D. Studies in Biopharmacy at the Department of Chemistry and Applied Biosciences, ETH Zurich, Switzerland under the supervision of Prof. Dr. Heidi Wunderli-Allespach and Dr. Stefanie D. Kraemer.

*11/2004* Chemist's habitation, University of Pisa (Pisa, Italy).

*10/2004* Master degree in chemistry at the University of Pisa (Pisa, Italy).  
Master thesis: "Thermodynamic and kinetic study of new metal intercalator formation and their interaction with DNA."  
Supervision of Prof. Dr. F. Secco and Prof. Dr. M. R. Tine.

*07/1998* Final secondary school exam (58/60), Industrial Technical Institute (I.T.I.).  
Chemical and biological specialization.  
I.T.I. G. Galilei, Livorno, Italy.



# Acknowledgements

First of all, I would like to express my thanks to my supervisor Prof. Dr. Heidi Wunderli-Allenspach for offering me a Ph.D. position in the Biopharmacy group and for motivating me to explore and develop my ideas. I am grateful for her encouraging and critical advises.

My co-referee Dr. Stefanie D. Krämer was a solid support through all the years, she was always ready for discussing projects and solving daily problems. Her enthusiasm for science was always a big motivation. Many thanks.

Many thanks to Dr. Bernard Cuenoud for the extremely interesting discussions concerning  $\beta$ -2 agonists. I am glad for his encouraging support and for offering the opportunity to collaborate with Novartis.

I am very grateful to Prof. Dr. Karl-Heinz Altmann for his friendly acceptance to be my co-referee and for his valuable advices.

My time at the ETH Zurich will be unforgettable thanks to the special colleagues and friends I met here.

A special thank to all former and current group members for the nice atmosphere in the lab and the scientific discussions. I am also grateful to whom introduced me to L<sup>A</sup>T<sub>E</sub>X.

Many thanks to themembers of the group of Prof. Dario Neri: they always treated me as part of the group and I found there very good friends.

I am grateful to everyone that was involved in the *permchem* project, I hope it will be a durable adventure!

Finally I would like to thank my family that never stops to encourage me during the last years. I am highly grateful to Valeria that always supported me through the storms, low tides and downwind.